Evaluation of Simplified Methods of Analysis for Timber Bridges

by

Riley N. Nader

Submitted in partial fulfilment of the requirements
for the degree of Master of Applied Science

at

Dalhousie University
Halifax, Nova Scotia
April 2022

TABLE OF CONTENTS

Table of Contents ii
List of Tables v
List of Figures vii
Abstract ix
Abbreviations and Symbols x
Acknowledgments xiv
Chapter 1: Introduction 1
1.1. Timber Bridges 1
1.1.1. Types of Timber Bridges 1
1.2. Bridge Evaluation According to CSA S6 2
1.2.1. Methods of Evaluation 2
1.2.2. Methods of Analysis 4
1.3. Summary of Limitations 4
1.4. Thesis Overview 5
Chapter 2: Relevant Research and Evaluation Criteria 6
2.1. Evaluation Criteria for Bridges 6
2.1.1. General Method 6
2.1.2. Mean Load Method 7
2.1.3. Advantages of the Mean Load Method 8
2.2. Analysis Methods 8
2.2.1. Rigorous Methods of Analysis 9
2.2.2. Simplified Method of Analysis 12
2.2.3. Recent Research on SMAs for Timber Bridges 22
2.3. Properties of Structural Wood 26
2.4. Summary 27
Chapter 3: Finite Element Modelling of Timber Bridges 28
3.1. Introduction and Finite Element Modelling Overview 28
3.2. Finite Element Modeling 28
3.2.1. Bridge Geometry Modelling 29
3.2.2. Model Sensitivity Study 30
3.3. Finite Element Models Evaluated Against Experimental Results 39

3.4. Summary and Recommendations 40
Chapter 4: Parametric Study of Load Distribution in Timber Bridges 42
4.1. Scope 42
4.2. General Analysis Method for Numerical FE Parametric Study 42
Chapter 5: Evaluation of SMAs 47
5.1. Scope 47
5.2. Effect of Span 47
5.3. Effect of Girder Spacing 48
5.4. Effect of Girder Depth 49
5.5. Inherent Bias Factors, COVs, and Summary 49
Chapter 6: Experimental Testing of Timber Girders 51
6.1. Introduction and Experimental Program Overview 51
6.2. Experimental Specimen Description 51
6.3. Experimental Specimen Geometric Properties and Moisture Content 52
6.3.1. Geometric Properties 52
6.3.2. Moisture Content 54
6.4. Instrumentation and Testing Procedure 55
6.5. Nominal Bending Strength Calculations 56
6.6. Experimental Results 57
6.7. Inherent Bias Factor, COVs and Discussion 59
Chapter 7: Recommendations for Improvement to the SMA and the Evaluation of Timber Bridges in CSA S6:19 60
7.1. Scope 60
7.2. Alternative 1: Update Statistical Parameters 60
7.3. Alternative 2: Revise SMA Equations 61
7.3.1. Generating The Equations 61
7.4. Alternative 3: Sophisticated Analysis 62
7.5. Comparison of Proposed Methods 62
Chapter 8: Summary, Conclusions and Recommendations 65
8.1. Summary 65
8.2. Conclusions 66
8.3. Recommendations for Evaluation of Timber Bridges in Canada 67
8.4. Recommendations for Future Work & Research 67
References 68
Appendix A: Finite Element Modelling Sensitivity Study Graphs 70
A.1. Effect of Deck Thickness on Deflection & LDF Values 70
A.2. Deck Material Properties Comparison 70

A.3. Effect of Modulus of Elasticity 71
Appendix B: Parametric Study Bridge Parameters 75
B.1. Parametric Study Parameter Distribution 75
B.2. Parametric Study Model Parameters and FE Results 77
Appendix C: Calculation Procedure/Example using The Mean Load Method 82
C.1. Starting off and Calculating D_T 82
C.2. Calculate the Truck Load Fraction (F_T) and the Girder Moment (M_L) 83
C.3. Calculate Timber Resistance per Mean Load Method 84
C.4. Calculate Loads per Mean Load Method 85
C.5. Calculate the Std. Dev. and COVs 86
C.6. Determine the Target Reliability Index 87
C.7. Determine the Value of The Live Load Capacity Factor 89
C.8. Clauses and Tables to Calculate Timber Resistance 90
C.9. Tables with Statistical Parameters 93

LIST OF TABLES

Table 2.1. Moment *D* values, in meters, corresponding to ULS and SLS II 18
Table 2.2. Moment *F* and C_f values, corresponding to ULS and SLS II [recreated from CSA S6-00] 20
Table 2.3. D_T for wood deck on wood girder bridges for class A and B highways [recreated from CSA S6-14] 21
Table 2.4. γ_c values for exterior girders of slab on girder bridges for moment 22
Table 3.1. Deck model material properties 31
Table 3.2. Initial FE sensitivity study results 32
Table 3.3. Final FE sensitivity study results 32
Table 3.4. Values of *E* for girders used in T1 & T2 [Smith (2018)] 32
Table 3.5. Maximum predicted LDF values 40
Table 4.1. Parameters and ranges included in parametric study 42
Table 4.2. Number of design lanes by deck width 45
Table 5.1. SMA evaluation results 50
Table 6.1. Test specimen geometric properties 52
Table 6.2. Measured geometric properties of test specimens 53
Table 6.3. Test specimen moisture content readings 54
Table 6.4. Test specimen section modulus and theoretical bending strength 57
Table 6.5. Test specimen experimental results 58
Table 7.1. Statistical parameters for use in the Mean Load Method 60
Table 7.2. Maximum anticipated girder moment comparison 63
Table 7.3. Live load capacity factor (*F*) comparison 63
Table 7.4. Live load capacity factor (*F*) comparison using experimental test results 64

Table B.1. Model parameters and FE results 77
Table B.2. Model parameters (continued) 78
Table B.3. Model parameters (continued) 79
Table B.5. Model parameters (continued) 81
Table C.1. Bridge parameters for HFX061 as measured by SHM Canada (2021) 82
Table C.2.. D_T equations for *n* lanes 83
Table C.3. Target reliability index β, for normal and permit traffic [recreated from CSA S6:19] 88

Table C.4. Variable values used in the Mean Load Method for HFX 061 89

Table C.5. Treatment factor (K_T) for lumber [recreated from CSA S6:19] 90

Table C.6. Load-sharing factor for bending, shear, and tension for all species and grades [recreated from CSA S6:19] 91

Table C.7. Values of D_e [recreated from CSA S6:19] 91

Table C.8. Effective length (L_e) for bending members [partly recreated from CSA S6:19] 92

Table C.9. Modification factor for lateral stability (K_L) [recreated from CSA S6:19] 93

Table C.10. Statistical parameters for various dead loads [recreated from CSA S6.1:19] 93

Table C.11. Statistical parameters for traffic loads [recreated from CSA S6.1:19] 93

Table C.12. Statistical parameters for lateral distribution categories for live load [recreated from CSA S6.1:19] 93

Table C.13. Statistical parameters for dynamic load allowance [recreated from CSA S6.1:19] 93

LIST OF FIGURES

Fig. 1.1. Different timber bridge decks 2
Fig. 2.1. Bridge idealization by orthotropic plate theory 9
Fig. 2.2. Slab idealization by grillage [partly reproduced from (Jaeger & Bakht, 1982)] 10
Fig. 2.3. Longitudinal moment distribution across a transverse section of a bridge 13
Fig. 2.4. Principle directions in wood specimens 16
Fig. 2.5. Values of the torsional coefficient, *K* [reproduced from Bakht & Jager (1985)] 16
Fig. 2.6. Constructed third scale bridge tested by Smith 2018 23
Fig. 2.7. Instrumentation of third scale bridge model (Smith 2018) 23
Fig. 2.8. Instrumentation and wearing surface examples from SHM bridge load testing 25
Fig. 3.1. Different connection modelling procedures 29
Fig. 3.2. Different girder element models for sensitivity study 33
Fig. 3.3. Element type sensitivity study results 34
Fig. 3.4. Effect of using individual values for *E* on deflection and LDF 35
Fig. 3.5. Effect of changing *E* uniformly on deflection and LDF (HFX 322) 36
Fig. 3.6. Mesh sensitivity models 37
Fig. 3.7. Effect of mesh density on *LDF* 38
Fig. 3.8. Comparison of LDFs between FE models and lab and field test data 39
Fig. 4.1. CSA S6:19 loading (CSA 2019a) 43
Fig. 4.2. Design truck clearance envelope 44
Fig. 4.3. Comparisons of actual and predicted truck fractions using CSA S6-06 and CSA S6:19 46
Fig. 5.1. Plots of F_{Ta}/F_{Tp} vs. span 48
Fig. 5.2. Plots of F_{Ta}/F_{Tp} vs. girder spacing 48
Fig. 5.3. Plots of F_{Ta}/F_{Tp} vs. girder depth 49
Fig. 6.1. Decommissioned timber girders 51
Fig. 6.2. Testing measurement definitions 53
Fig. 6.3. LVDT at support 55
Fig. 6.4. Testing set up 56
Fig. 6.5. Total load vs. mid-span deflection plots for experimental tests 57

Fig. A.1. Effect of deck thickness 70
Fig. A.2. Effect of material properties models on LDF 70
Fig. A.3. HFX061 Lane 1 71
Fig. A.4. HFX061 Lane 2 71
Fig. A.5. HFX061 Lane 3 72
Fig. A.6. HFX322 Lane 1 72
Fig. A.7. HFX322 Lane 2 73
Fig. A.8. HFX322 Lane 3 73
Fig. A.9. HFX322 Lane 4 74
Fig. A.10. HFX322 Lane 5 74
Fig. B.1. Parametric study parameter distributions 76

ABSTRACT

The design of timber bridges in Canada is carried out in conjunction with the Canadian Highway Bridge Design Code (CHBDC) (CSA S6:19). A key feature of this code is the ability to employ a Simplified Method of Analysis (SMA) (CSA S6:19 Clause 5.6) to determine the forces acting on a bridge and in its various members (i.e., beams/girders). Since it was first introduced in the early 1980s, the SMA's development has been largely governed by its application to steel/concrete bridges (e.g., prestressed-concrete-girder and composite steel-girder bridges) – rather than short-span timber bridges. As a result, for short-span timber bridges, the SMA is markedly over-conservative (i.e., it gives design loads that are much larger than those calculated by rigorous analysis).

In the province of Nova Scotia, Nova Scotia Public Works (NSPW) manages over 2000 short-span timber bridges, many of which (44%) were constructed in the 1950s and 1980s and lack complete design information. NSPW hence relies upon the SMA to assess this bridge inventory in a timely manner, to determine the need for repair/maintenance, or replacement. Due to the SMAs inherent conservatism when applied to such bridges, it identifies (often incorrectly) that many of Nova Scotia's timber bridges do not satisfy code requirements, which prompts the need for large, unnecessary, capital expenditures. This thesis presents a research study to (a) evaluate the effect of key parameters (including bridge span, girder spacing, number of girders, and girder material properties) on the overall bridge and bridge-member force distributions (herein called "load distributions"), and (b) develop a new method for the accurate (yet, still safe) evaluation of short-span timber bridges that can consider these factors.

ABBREVIATIONS AND SYMBOLS

AASHTO	=	American Association of State Highway and Transportation Officials
ASTM	=	American Society for Testing and Materials
COV	=	Coefficient of Variation
CSA	=	Canadian Standards Association
DOF	=	Degree of Freedom
FE	=	Finite Element
FEM	=	Finite Element Method
FLS	=	Fatigue Limit State
LDF	=	Load Distribution Factor
LRFD	=	Load and Resistance Factor Design
LSD	=	Limit States Design
LVDT	=	Linear Variable Displacement Transducer
NSPW	=	Nova Scotia Public Works
OHBDC	=	Ontario Highway Bridge Design Code
PDE	=	Partial Differential Equation
SMA	=	Simplified Method of Analysis
SLS	=	Serviceability Limit State
SS	=	Select Structural
ULS	=	Ultimate Limit State
VED	=	Vehicle Edge Distance

A	=	nominal unfactored loads other than dead and live
C_f	=	correction factor for load distribution
D	=	dead load effect (in CSA S6-14/19 Clause14.15.2.2); nominal unfactored dead load (in CSA S6-14/19 Clause14.15.2.1); load distribution parameter (in CSA S6-83); load distribution parameter containing the appropriate multi-lane reduction factors (in CSA S6-88)
$\overline{D}$	=	mean dead load effect
D_1	=	coupling rigidity per unit width

D_2	=	coupling rigidity per unit length
D_C	=	curb width, taken as 0.3 m
D_d	=	design load distribution parameter
D_T	=	truck load distribution width, CSA S6-14, S6:19
D_{VE}	=	vehicle edge distance, CSA S6-14, S6:19
D_x	=	longitudinal flexural rigidity per unit width
D_{xy}	=	longitudinal torsional rigidity per unit width
D_y	=	transverse flexural rigidity per unit length
D_{yx}	=	transverse torsional rigidity per unit length
E	=	modulus of elasticity
E_{app}	=	the apparent modulus of elasticity of a test specimen
E_L	=	modulus of elasticity in the *L* direction
E_R	=	modulus of elasticity of in the *R* direction
E_T	=	modulus of elasticity in the *T* direction
F	=	live load capacity factor (in CSA S6-14/19 Clause14.15.2.1/2); width dimension characterizing load distribution for a bridge, CSA S6-00, S6-06
F_S	=	skew factor
F_T	=	truck load fraction
F_b	=	bending strength parallel to grain
F_m	=	amplification factor to account for transverse variation in maximum longitudinal moment intensity, CSA S6-00, S6-06
G_{LR}	=	modulus of rigidity in the longitudinal-radial plane
G_{LT}	=	modulus of rigidity in the longitudinal-tangential plane
G_{TR}	=	modulus of rigidity in the radial-tangential plane
I_D	=	dynamic load allowance
K	=	torsional coefficient
K_D	=	load duration factor
K_H	=	system factor
K_L	=	lateral stability factor for bending members
K_m	=	modification factor for load sharing
K_{Sb}	=	service condition factor for bending
K_T	=	treatment factor
K_{Zb}	=	size factor for bending for sawn lumber
L	=	nominal live load effect (in CSA S6-14/19 Clause14.15.2.2); nominal unfactored live load (in CSA S6-14/19 Clause14.15.2.1); span length

$\bar{L}$	=	mean live load effect
M	=	moment caused by one line of wheels or one-half lane loading, CSA S6-88
M_a	=	actual bending moment resistance of test specimen
M_L	=	longitudinal moment per girder due to CL-W loading, CSA S6-14, S6:19
M_n	=	theoretical bending moment resistance of test specimen
M_S	=	maximum longitudinal moment per girder due to live load, CSA S6-88, S6-00, S6-06
$M_{S\,avg}$	=	average moment per girder due to live load
M_T	=	longitudinal moment generated by one lane of CL-W loading, CSA S6-14, S6:19
M_t	=	maximum longitudinal moment for one lane-width of truck or lane loading, CSA S6 00, S6-06
N	=	number of girders
P	=	increment of applied load on the flexural specimen below the proportional limit
P_{max}	=	the maximum load borne by the specimen, loaded to failure
R	=	nominal resistance
$\overline{R}$	=	mean resistance of girder
R_L	=	modification factor for multi-lane loading
R_r	=	factored resistance of girder
S	=	centre-to-centre spacing of longitudinal girders; section modulus
S_C	=	transverse distance from free edge of cantilever overhang to centerline of exterior girder
S_D	=	standard deviation for dead-load effect
S_L	=	standard deviation for live-load effect
S_R	=	modulus of rupture
U	=	resistance adjustment factor
V	=	coefficient of variation
V_{AD}	=	coefficient of variation for dead-load analysis method
V_{AL}	=	coefficient of variation for live-load analysis method
V_D	=	coefficient of variation for dead-load effect
V_I	=	coefficient of variation for dynamic load allowance
V_L	=	coefficient of variation for live-load effect
V_R	=	coefficient of variation for resistance
V_S	=	coefficient of variation for load effects
W_b	=	total bridge width
W_c	=	bridge deck width
W_e	=	design lane width

a	=	distance from a support to the closest load point
b	=	half width of bridge deck
b_g	=	width of girder
f_{bb}	=	specified strength in bending, MPa
i	=	subscript used to denote girders
n	=	number of design lanes
t	=	thickness of deck
t_g	=	depth of girder
α	=	first characteristic parameter for orthotropic plates
α_A	=	load factor for all other loads
α_D	=	load factor for dead load
α_L	=	load factor for live load
β	=	reliability index
Δ	=	deflection at mid span
Δ_i	=	deflection of girder i
Δ_{avg}	=	average girder deflection
δ	=	bias coefficient
δ_{AD}	=	bias coefficient for dead-load analysis method
δ_{AL}	=	bias coefficient for live-load analysis method
δ_D	=	bias coefficient for dead-load effect
δ_I	=	bias coefficient for dynamic load allowance
δ_L	=	bias coefficient for live-load effect
δ_R	=	bias coefficient for resistance
θ	=	second characteristic parameter for orthotropic plates
λ	=	lane width parameter, CSA S6-14, S6:19
μ	=	lane width modification factor
γ_C	=	truck load modification factor, CSA S6-14, S6:19

ACKNOWLEDGMENTS

Firstly, I cannot thank my supervisors, Dr. Kyle Tousignant and Dr. John Newhook, enough for all their support and guidance over these last two years – not just in research, but also in my journey to become a young professional. These past two years, dealing with COVID-19 has made education difficult due to constant uncertainty in many aspects, but Dr. Kyle Tousignant was always optimistic and helped me see the light when I was struggling. I can't say enough good things about the wonderful research group I've spent the last year sharing an office with. Thank you for the endless laughs and for allowing me to bounce ideas and problems off you. I would also like to thank Mr. Jordan Maerz, and Mr. Jesse Keane, the incredibly knowledgeable and helpful technicians in Dalhousie's Heavy Structures Lab, (Sorry for making your lab smell like creosote for a few weeks during my testing.).

Many thanks are given to everyone at SHM Consulting Canada, especially, Dr. Vidya Limaye, Phil Vickers, and Cyrus Hoseinpour, for allowing me to attend field bridge testing and supplying me with data and guidance. To all the wonderful people at Nova Scotia Public Works (NSPW), namely Justin Clarke, Will Crocker, Amjad Memon, and Raymond Daniels: thank you for all your input and for providing me with technical documents and test specimens. This research would not have happened without you.

I would also have been unable to conduct this research without the funding and financial aid from NSPW, the Nova Scotia Graduate Scholarship (NSGS) program, and Dr. Robert Gillespie. Nor would much of this work have been possible without the generosity of MIDAS I.T. for providing me free access to their software and technical support help.

Finally, on a personal level, I would like to extend my sincerest thanks to all my wonderful friends and family members for all their support and encouragement throughout my education. Thank you for never allowing me to think I was unable to accomplish my goals and dreams. I couldn't ask for a better group of people to surround myself with.

Chapter 1: INTRODUCTION

1.1. TIMBER BRIDGES

In metropolitan areas of Nova Scotia (and other Canadian provinces), concrete and steel bridge construction is the mainstream; however, on secondary routes, and in more rural areas, there are approximately 2000 timber bridges being maintained and in-service in Nova Scotia and thousands more across Canada.

1.1.1. TYPES OF TIMBER BRIDGES

Concerning timber bridges, the Canadian Highway Bridge Design Code (CHBDC) (CSA S6) recognizes many different forms, including wood decks supported by steel girders, composite decks supported by timber girders, and cast-in-place or precast concrete decks supported by timber girders; however, the focus of this research is on all-wood construction (i.e., timber decks supported on timber girders). CSA S6:19 (CSA 2019a) makes a distinction between different all-wood timber bridges for both design and evaluation to account for differences in their mechanical properties and behaviour. The first two distinctions are the direction of the decking (transverse or longitudinal, relative to the bridge span/direction of travel), and the type of wood deck.

For longitudinal decking (which can be stress laminated, nail laminated, or plank), the deck is supported on transverse beams that distribute the load to girders. Stress laminated decks are built by placing glulam beams (or planks) side by side on their narrow face(s) and holding them together by using prestressed steel bars. Stress lamination creates a plate-like assemblage, which allows the deck to exhibit (close to) orthotropic properties (Ekholm, Ekevad, & Kliger, 2014). Nail laminated decks are similar to stress laminated decks – the only difference being that instead of using prestressed steel bars that run through the entirety of the deck, individual beams are connected to their neighbour(s) by nails or spikes. A longitudinal stress/nail laminated deck is illustrated in Fig. 1.1(a). Plank decks are laid with their wide face down and attached only to the girders, often through joists, by nails [see Fig 1.1(b)].

For transverse deck spans (which can, again, be stress laminated, nail laminated, or plank), the deck is supported directly on girders. A transverse stress/laminated deck is illustrated in Fig. 1.1(c), and a transverse wood plank deck is illustrated in Fig. 1.1(d).

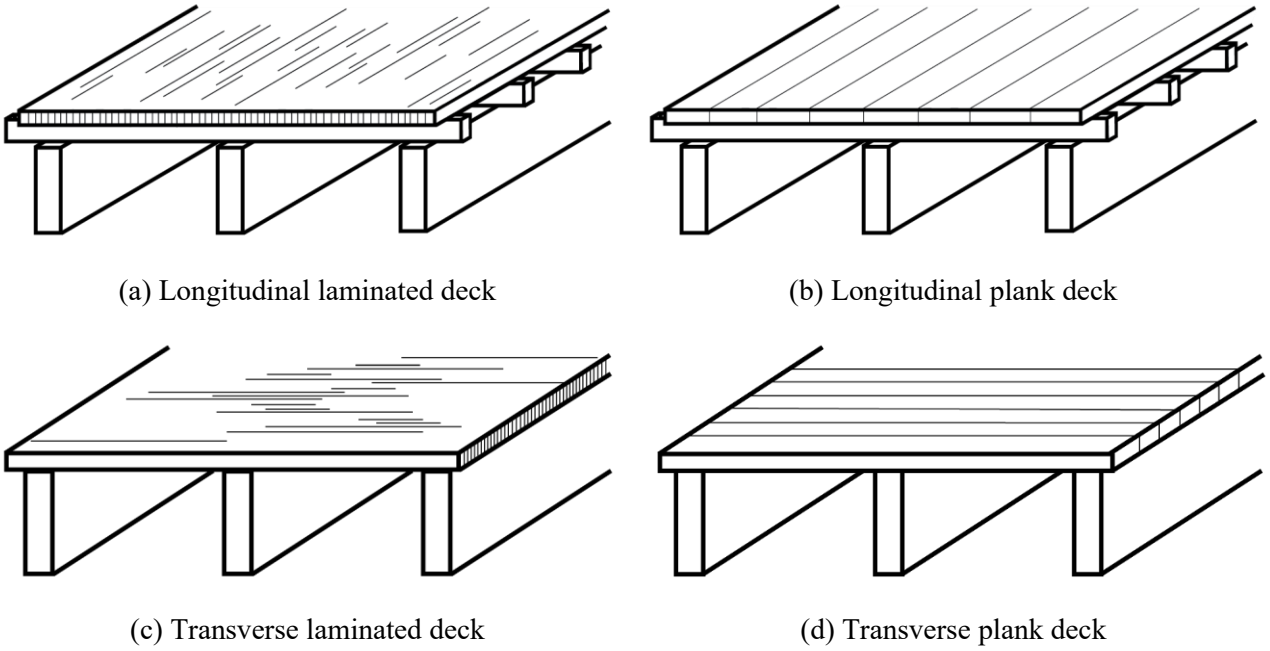

(a) Longitudinal laminated deck (b) Longitudinal plank deck

(c) Transverse laminated deck (d) Transverse plank deck

Fig. 1.1. Different timber bridge decks

The third distinction (which was alluded to previously) is the type of timber product(s) used for the girders. There are several options, but the two main types (again, for girders): are glulam or sawn timber. Glulam girders are comprised of multiple smaller pieces of timber held together by an adhesive; sawn-timber girders are created from a single tree. While the latter is usually more economical, it has the following downsides: uncertainty in mechanical properties, and difficulty detecting imperfections.

The primary focus of this research is on all-wood (timber) bridges with transverse plank decks and sawn-timber girders.

1.2. Bridge Evaluation According to CSA S6

The evaluation of bridges (be it steel, concrete, or timber) is completed per Section 14 of the CHBDC (CSA, 2019a). Section 14 specifies the methods for evaluating existing bridge structures in Canada for load limit restrictions, serviceability, or fatigue loadings. Acceptable methods of evaluation are outlined in Section 1.2.1 of this thesis, and further explained in Chapter 2.

1.2.1. Methods of Evaluation

According to Clause 14.5.1 of CSA S6:19 (CSA, 2019a), a bridge can be evaluated using one or more of the following methods:

a) Ultimate limit state (ULS) method(s), including:
   i. Clauses 14.15.2.1 and 14.15.2.2 with the load and resistance adjustment factors in Clauses 14.13 and 14.14 (herein, called the General Method)
   ii. The Mean Load Method, as specified in Clause 14.15.2.3
   iii. The Load Testing Method, as specified in Clause 14.16
b) Serviceability limit state (SLS) methods and/or fatigue limit state (FLS) methods; and
c) Other methods approved by the owner

This Chapter (and this thesis) primarily focuses on the evaluation of bridges at ULS [using the Methods list in a), above]. Concerning ULS, the focus of Clause 14.5.1 of the CHBDC (CSA, 2019a) is the calculation of the Live Load Capacity Factor (F) for a given bridge. The factor F is a way of measuring the ratio of capacity-to-demand, where a value less than 1.0 is considered unsafe and values greater than 1.0 are considered safe, not dissimilar to a factor of safety.

1.2.1.1. The General Method

The General Method [given in CSA S6:19 Clause 14.5.1a) i)] provides a relatively simple, standardized approach for calculating F. It takes into account nominal (unfactored) load effects and factored resistances, modified by load and resistance adjustment factors that are specified based on a target reliability index (β) and a resistance category. Limitations arise when using the General Method for timber bridges due to: (i) the lack of ability to account for accuracy in the analysis method(s), and (ii) the paucity of an adjustment factor for resistances (U). Moreover, resistance adjustment factors (U) are given for both steel and concrete in CSA S6 Clause 14.14.2 (CSA, 2019a), as well as for composite construction; however, none exist for timber. Clause 14.14.2 states "…where no value for U is specified … and in lieu of better information … a value of $U = 1.0$ may be used." (CSA, 2019a). Taking the value of $U = 1.0$ for timber girders likely under predicts the strength.

1.2.1.2. The Mean Load Method

The Mean Load Method [given in CSA S6:19 Clause 14.5.1a)ii)] is believed to be a more accurate and in-depth approach for calculating F (compared to the General Method). The increased accuracy is due to the Mean Load Method's ability to account precisely for β, and the accuracy of not only the analysis method(s) but also the resistance(s) of elements through the use of statistical parameters. The Mean Load Method considers the nominal/specified values of loads and resistance, as well as corresponding bias coefficients (δ) and coefficient of variations (COV) (V), as explained in Section 2.1.2. The current limitation for using the Mean Load Method for timber bridges is grounded in the proper quantification of these statistical parameters (δ and V) [primarily, for the analysis method(s) and resistance]. While some values are provided in CSA S6 and the Commentary (CSA S6.1) (CSA, 2019b), they are likely to not be in line with the true values – particularly for analysis done using the CHBDC Simplified Method of Analysis Clause 5.6 in CSA S6:19.

Moreover, the resistance bias coefficient (δ_R) and COV (V_R) are not well known for flexure of new or in-situ timber girders. In the late 1970s, Madsen and Nielsen developed a large database for various grades and sizes of new sawn lumber specimens, summarised in "Load and Resistance Factor Calibration for Wood Bridges" (Nowak & Eamon, 2005); however, since then, there have been no other large-scale studies performed to discern these parameters.

1.2.2. METHODS OF ANALYSIS

There are many different methods of analysis available for bridges, but they are generally split into two categories, rigorous and simplified methods. Before the adoption of the simplified method of analysis (SMA), the only methods of analysis were rigorous methods, these include methods such as plate theory, grillage analogy, semi continuum analysis, and finite element method (FEM). These rigorous methods of analysis are considered to be the most accurate way to analyze a bridge when correctly employed, but they can be complex and time-consuming. With the adoption of the SMA, analyzing bridges became relatively easy. An important part of the SMA is knowing that because it's a "simplified" method the results may lack accuracy. To compensate for this possible loss of accuracy, statistical parameters for the analysis method used were introduced into the code (δ_{AL} and V_{AL}). For all bridge types, SMAs are used in codes to efficiently predict bridge behaviour. Yet, despite substantial changes that occurred between the 2006 and 2014 editions of CSA S6 to the SMA for transverse wood deck on wood girder bridges ("timber bridges"), the statistical parameters for lateral live-load distribution in Table C14.4 of CSA S6.1 (CSA, 2019b) have remained the same. Moreover, the SMA has become increasingly conservative, leading to increased expenditure for bridge rehabilitation or replacement.

1.3. SUMMARY OF LIMITATIONS

As discussed, both the General Method and the Mean Load Method are limited when it comes to the evaluation of timber bridges. For the General Method, resistance adjustment factors are given for both steel and concrete, as well as composite construction, but none are presented for Timber. Clause 14.14.2 States "…Where no value for [the resistance adjustment factor] U is specified… and in lieu of better information, a value of U=1.0 may be used." (CSA, 2019a). Similarly, looking at the Statistical parameters used for resistance in the Mean Load Method, the resistance bias coefficient (δ_R) and COV (V_R) are not well known for flexure of new or in-situ timber girders. In the late 1970s, Madsen and Nielsen developed a large database for various grades and sizes of new sawn lumber specimens, summarised in Nowak et al.'s 2005 work entitled "Load and Resistance Factor Calibration for Wood Bridges" (Nowak & Eamon, 2005), though since then no large-scale study has been undertaken. Furthermore, when it comes to bridge analysis methods, the preferred method (the SMA) tends to over-predict the design moment, due to the oversimplification of the load distributions for timber bridges, leading to a very conservative design.

1.4. THESIS OVERVIEW

This thesis aims to address the above-noted limitations concerning statistical parameters and analysis methods for the evaluation of timber bridges.

Chapter 2 presents an extensive literature review on bridge evaluation and analysis methods, bridge modelling, design, and recent work conducted on these topics. The Chapter summarizes the historical development of the SMA in the CHBDC, reviews (in detail) the work of Smith (2018) related to the topic, and summarizes the results of field-load tests conducted on six timber bridges in Nova Scotia (SHM Canada 2021) (herein, called the test bridges) used in Chapter 3.

Chapter 3 discusses finite-element (FE) modelling of timber bridges and presents a series of sensitivity studies to determine the best-suited girder/deck element and mesh density combination(s). The models are validated by comparison of the results (i.e., girder deflections, strains, and bending moments) to the test bridges reviewed in Chapter 2 [i.e., two laboratory tests by Smith (2018) and two field load tests (on HFX 061 and HFX 322) conducted by SHM Canada (SHM Canada 2021)].

Chapter 4 presents a parametric study, performed using the validated FE models to determine load-distribution factors (LDFs) for (all-wood) timber bridges with transverse plank decks and sawn-timber girders across a range of typical parameters [i.e., 2m ≤ clear span (L) ≤ 16m, 4m ≤ overall width (W_b) ≤ 12m, 0.25m ≤ girder depth (t_g) ≤ 0.6m, 0.1m ≤ girder width (b_g) ≤ 0.25m, 0.15m ≤ girder spacing (S) ≤ 0.8m]. These parameters reflect the larger of the "practical range" of dimensions given by Nowak and Lind (2005), Smith (2018), and SHM Canada (2021). Results from Chapter 4 are used in subsequent chapters to obtain statistical parameters for live load analysis (δ_{AL} and V_{AL}, for various versions of the SMA for timber bridges) and develop more accurate SMA, for use in CSA S6.

Chapter 5 evaluates the accuracy of past and current versions of the SMAs using the results from Chapter 4 and determines δ_{AL} and V_{AL} for different versions of the SMA in CSA S6.

Chapter 6 discusses the selection and testing of decommissioned timber girders undertaken at Dalhousie's Heavy Structures Laboratory. The tests performed were done to characterize the typical in-situ properties [e.g. the elastic modulus (E) and bending strength parallel to the grain (f_{bb})] of the girders, and to determine corresponding bias coefficients and COVs for the resistance (δ_{AL} and V_{AL}).

Chapter 7 introduces recommendations to improve the SMA and the accuracy of timber bridge evaluation using CSA S6, from the findings in Chapters 3-6. The recommendations are compared to each other using two case study bridges and demonstrates the impact of the recommendations (i.e., the evaluation of two timber bridges in Nova Scotia by using various analysis and evaluation methods).

Conclusions of this research program are presented in Chapter 8.

Chapter 2: RELEVANT RESEARCH AND EVALUATION CRITERIA

2.1. EVALUATION CRITERIA FOR BRIDGES

The evaluation of bridges for ULS is typically done by calculating the live load capacity factor (F) using one of two methods: the General Method, or the Mean Load Method. These methods are outlined in CSA S6:19 Clauses 14.15.2.1 and 14.15.2.3, respectively. As mentioned in Section 1.2.1, F is a way of measuring the ratio of capacity-to-demand, where a value less than 1.0 is considered unsafe and values greater than 1.0 are considered safe.

2.1.1. GENERAL METHOD

Due to its relative simplicity, the General Method is the most commonly used approach for timber bridge evaluation, whereby F is calculated as follows:

$$F = \frac{UR_r - \Sigma\alpha_D D - \Sigma\alpha_A A}{\alpha_L L(1+I_D)} \tag{2.1}$$

where U is the resistance adjustment factor; R_r is the factored resistance of an element; α_D, α_A, and α_L are load factors for dead, other, and live loads, respectively; D, A, and L are the nominal (un-factored) dead, other, and live load effects, respectively; and I_D is the dynamic load allowance.

For the analysis of timber bridges for moment, R_r can be taken as the factored bending resistance of a girder. The purpose of U is to "fine-tune" R_r by considering the inherent bias in resistance factor(s) used in the code. On that note, Clause C14.14.2 of CSA S6.1:19 states that "… while approximations made to the resistance factors in the interests of simplicity are appropriate for the design of new bridges, in the evaluation of existing bridges their use may lead to unnecessary bridge postings or strengthenings." (CSA, 2019b). The factor U is important to account for this. However, the list of U values given in CSA S6:19 is not exhaustive, and it only covers certain resistance categories for steel and concrete. Furthermore, no U values are given for timber. This knowledge gap adds to the inaccuracy of the General Method.

When no U value is given, and in lieu of better information, CSA S6 specifies that a value of 1.0 can be used.

For bridge evaluation in accordance with Chapter 14 of CSA S6:19, the level of safety is measured by using the reliability index (β) which is inversely related to the probability of failure (CSA, 2019b). For new bridges, a target β of 3.5 is required for a 75-year design life. For evaluation (of existing bridges), it is beneficial if the β value used is consistent with that used in design. For evaluation, β is determined based on different levels of system and element behaviour, as well as inspection level. The target β (which can range from 2.75 to 4.00) is then used to choose load factors (α_D, α_A, and α_L) that are input into the General Method expression, Eq. (2.1).

CSA S6.1 (CSA 2019b) notes, in Clause 14.12.1, that "…[the General Method] may produce a live load rating factor [F] that does not achieve the exact value of the reliability index [β] chosen…." and that "…when using [the General Method], elements with very high or very low dead-to-live load ratios tend to achieve a reliability index slightly lower than the target value". The Commentary further states that "…the Mean Load Method… will produce live load rating factors consistent with the target reliability index regardless of the dead-to-live load ratio". Hence, while the General Method is simpler, the Mean Load Method is preferable.

2.1.2. MEAN LOAD METHOD

Instead of using resistance and load factors, as is done in the General Method, the uncertainty in loads, resistances, and analysis methods are taken into account in the Mean Load Method through statistical parameters [i.e., bias coefficients (δ) and COVs (V)]. According to the Mean Load Method, F is calculated as follows:

$$F = \frac{\overline{R}\exp\left[-\beta(V_R^2 + V_S^2)^{0.5}\right] - \sum\overline{D}}{\overline{L}} \tag{2.2}$$

where $\overline{R}$ is the mean resistance, defined in Eq. (2.3); V_R is the COV of the resistance; V_S is the COV of the total load effects, defined in Eq. (2.4); $\sum\overline{D}$ the sum of the mean dead load effects, defined in Eq. (2.7); and $\overline{L}$ is the mean static and dynamic live load effect, defined in Eq. (2.8):

$$\overline{R} = \delta_R R \tag{2.3}$$

$$V_S = \frac{(S_D^2 + S_L^2)^{0.5}}{\left(\sum\overline{D} + \overline{L}\right)} \tag{2.4}$$

where:

$$S_D = \left[\sum\left[\left(V_D^2 + V_{AD}^2\right)\left(\delta_D\delta_{AD}D\right)^2\right]\right]^{0.5} \tag{2.5}$$

$$S_L = \left[V_{AL}^2 + V_L^2 + \frac{(V_I\delta_I I_D)^2}{(1+\delta_I I_D)^2}\right]^{0.5}\overline{L} \tag{2.6}$$

$$\sum\overline{D} = \sum\left(\delta_D\delta_{AD}D\right) \tag{2.7}$$

and:

$$\overline{L} = \delta_L \delta_{AL} L(1 + \delta_I I_D) \tag{2.8}$$

where δ_R is the resistance bias factor; R is the nominal resistance; S_D is the standard deviation of the dead load effect; S_L is the standard deviation of the live load effect; V_D and V_{AD} are the COVs for the dead load effect and dead load analysis method, respectively; δ_D and δ_{AD} are the bias coefficients for the dead load effect and dead load analysis method, respectively; D is the nominal (unfactored) dead load effect; V_{AL} and V_L are the COVs of the live load analysis method and live load effect, respectively; δ_I and V_I are the bias coefficient and COV for dynamic load allowance; δ_L and δ_{AL} are the bias coefficients of the live load and the analysis methods, respectively; and L is the nominal live load effect.

While more daunting than the General Method, the Mean Load Method is greatly simplified by the provision of some values for statistical parameters in CSA S6.1.

2.1.3. Advantages of the Mean Load Method

There are many situations in which the Mean Load Method may be beneficial to use over the General Method (some of which are noted in CSA S6.1:19, and are mentioned here):

a) If the uncertainty in the load analysis method or resistance is significantly different than that assumed by the code;
b) If the purpose of the evaluation is to assess the risk associated with permitting passage of a load over a structure, β is a variable in the Mean Load Method equation, Eq. (2.2), so a direct solution for β may be obtained (to achieve the same result using the General Method, an iterative process would be required);
c) When greater accuracy is required than can be obtained using single-valued load resistance factors that are approximations to cover various situations.

Although the Mean Load Method is more accurate than the General Method, in theory, the actual accuracy depends on the validity of the statistical parameter values used in Eq. (2.2), and for timber bridges, very little information is given in the CSA S6 Commentary (CSA 2019b) in that regard. This lack of knowledge hence poses a problem when attempting to evaluate existing timber bridges with any degree of accuracy.

2.2. Analysis Methods

Both the General Method and the Mean Load Method for bridge evaluation rely on an accurate prediction of the maximum longitudinal moment (M_L) any one girder is likely to experience. CSA S6:19 allows the use of several different analysis methods to accurately determine this moment, which can be split into two categories: rigorous methods of analysis, and the Simplified Method of Analysis (SMA).

There are multiple acceptable rigorous methods of analysis such as plate theories, grillage analogy, semi-continuum analysis, and the finite element method (FEM), which are outlined below (in Section 2.2.1); however, there is only one SMA. The SMA in CSA S6:19 (CSA 2019a) has undergone multiple revisions since it was first introduced into the Ontario Highway Bridge Design Code (OHBDC) in the early 1980s. These are reviewed in Section 2.2.2.

2.2.1. Rigorous Methods of Analysis

2.2.1.1. Plate Theories

There are multiple different plate theories available for use in the analysis of bridge behaviour, the primary one being the orthotropic plate method, where the bridge is idealized as an orthotropic plate, as shown in Fig. 2.1(a) and 2.1(b).

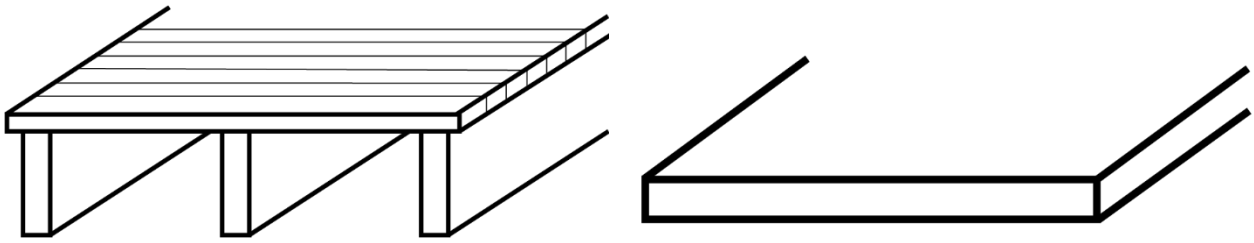

(a) Original bridge (b) Equivalent orthotropic plate

Fig. 2.1. Bridge idealization by orthotropic plate theory

The idealized orthotropic plate has two different sets of flexural rigidities in the two perpendicular directions (Cusens & Pama, 1975). The equilibrium of an orthotropic plate leads to a 4th order partial differential equation (PDE) (assuming elastic properties and small deflections). While most designers are already not comfortable solving 4th order PDEs, this analysis method is further complicated by the idealization of loads as a sum of harmonics. Unlike the semi-continuum method explained in Section 2.2.1.3, there is no technique to achieve quick convergence of results. This leads to some more complicated structures occasionally requiring up to 41 harmonics for analysis under specified loading (Bakht & Mufti, 2015).

2.2.1.2. Grillage Analogy

Prior to the popularization of FEM, and the use of FE programs in bridge design and evaluation, the grillage analogy was one of the most popular rigorous methods of analysis. The grillage analogy is a 2-D model that comprises of interconnecting beams, with longitudinal beams representing the girders and associated/tributary slab/deck section(s), and transverse beams representing solely the slab/deck and its corresponding mechanical properties. The grillage method idealization is shown in Fig. 2.2.

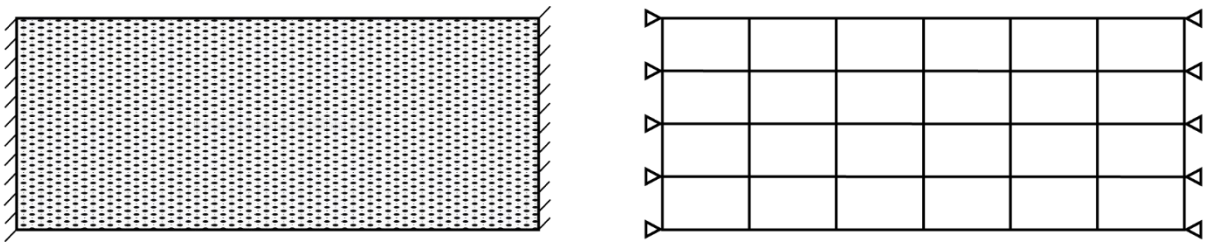

(a) Slab bridge (b) Idealized grillage

Fig. 2.2. Slab idealization by grillage [partly reproduced from (Jaeger & Bakht, 1982)]

Three main reasons led to the popularity of the grillage analogy for rigorous analysis (Jager & Bakht, 1982):

a) The ability for it to be used in cases where complicating features are present (e.g., heavy skew, isolated supports, edge stiffening, etc.);
b) Its suitability for completing necessary calculations associated with analysis and design on a computer; and
c) Its ability to provide the designer with a feel for the structural behaviour of the bridge (i.e., how the various loadings are distributed and taken to the supports).

Although grillage analogy was widely used due to its robust nature, it has several pitfalls. Typically, grillages only use nodes at the intersection of longitudinal and transverse beams, which introduces errors when the loading positions don't coincide with these nodes. To overcome this, non-coincident loads are usually distributed to surrounding nodes without accounting for the associated moments. This usually has little effect in the longitudinal direction but can introduce significant errors in the transverse direction – particularly when the load is on a cantilevered portion of the bridge deck (Jager & Bakht, 1982).

2.2.1.3. Semi-Continuum

The semi-continuum method is a hybrid of the orthotropic plate method and the grillage analogy. The semi-continuum method represents the girders as discrete longitudinal members and the slab as a continuous transverse medium (Hambly, 1991). This tends to better represent slab-on-girder bridges when compared to either of the methods that it draws from. This can be explained using simple beam-type mathematical models (Bakht & Mufti, 2015). The most notable advantages of the semi-continuum method are its accuracy and speed of convergence, as shown by Bakht et al. (1997) – even more so than the grillage analogy.

2.2.1.4. Finite Element Methods: General

FE methods have gained large amounts of popularity with the advancement of computers, allowing for very complex structures to be analyzed with relative ease compared to more primitive methods. While it is difficult to say when the FE method (FEM) was invented, its use in engineering in its modern form can be traced back to a Russian-Canadian structural engineer by the name of Alexander Hrennikoff, and his paper entitled Solutions of problems of elasticity by the framework method (Hrennikoff, 1941). Due to the increasing complexity of structural engineering problems causing the differential equations used in elasticity to be, in many cases, impossible to solve, another method of approach was needed (Hrennikoff, 1941). The FE method consists of subdividing the complex system into small individual components or "elements", whose behaviour is readily understood, then rebuilding the original system from those components to study its behaviour (Zienkiewicz et al. 2013).

While FE methods allow engineers to analyze complex problems with relative ease, they don't come without their difficulties. To conduct a proper FE analysis, many parameters need to be well known for one to be confident in the solution.

In Section 5.9 of CSA S6:19 (CSA, 2019a), requirements are outlined for refined methods of analysis, such as the FE modelling. These requirements include:

a) That the model be representative of the expected structural system behaviour;
b) That all members contain an adequate number of nodes to avoid any concentrated effects due to modelling;
c) That aspect ratio of all elements be at most 2;
d) That linear elastic properties be used for determining structural and component responses at all limit states; and
e) That the completed model be validated to ensure they reproduce the expected behaviour.

When modelling, a key parameter that needs to be carefully considered/optimized is the mesh density. While a finer mesh should yield a more accurate solution to most problems, calculation time increases exponentially.

2.2.1.5. Finite Element Methods: Timber Bridges

Modelling timber bridges using FE methods comes with its own set of complexities due to uncertainties in material properties (due to the orthotropic nature of and non-homogeneity of timber), time-dependant effects, and non-uniformity (i.e., different mechanical properties/dimensions from one girder to another within the same structure).

Another issue arises when looking at the possible composite action between the deck and girders. Unlike concrete or steel construction, where one can discern (with relative ease) the amount of composite action, timber decks (which are typically connected to girders through simple mechanical fasteners, such as spikes, screws, or nails), or connections thereto, can quickly degrade due to movement (e.g., expansion and shrinkage of the timber). This makes it difficult to accurately determine the amount of composite action between the deck and girders without field tests. Even if this can be determined, the question is raised: how does one model these connections, and what properties should be used?

One method for modelling composite action in timber bridges was demonstrated by Choi & Crews (2012). Choi & Crews (2012) modelled girders as solid elements and used semi-rigid links (on the top two "corner" nodes of each girder) to represent a screwed connection, which transferred rotational degrees of freedom (DOF) from the plate or shell element of the deck to the solid element of the girder. The level of composite action between the deck and the girder was indirectly controlled by changing the stiffness of the semi-rigid links (Choi & Crews, 2012).

Although the FE analyses can be much more involved and time-consuming than primitive methods, they often provide the best representations of real-world effects. Because of this, the results retrieved from the FE modelling in research – provided that the FE models are properly validated – are often taken to be "real" results (rather than approximations). This is the approach used herein to evaluate the accuracy of previous and current versions of the SMA (discussed in the following sections) in Chapters 4 and 5.

2.2.2. Simplified Method of Analysis

To overcome the complexities of the more rigorous methods of analysis, the simplified method of analysis (SMA) was introduced. The SMA in CSA S6:19 (CSA, 2019a) has evolved over the decades from the first adoption into the 1983 Ontario Highway Bridge Design Code (OHBDC) from the 1977 American Association of State Highway and Transportation Officials (AASHTO) code. The SMA, in general, aims to simplify the complex load distribution analysis problem of a bridge superstructure by idealizing the cross-section as an orthotropic plate, as shown in Figs. 2.3(a),(b). While this Section covers nearly the complete history of the SMA's use and evolution in Canada, the key versions discussed later in this thesis pertain to CSA S6-06, CSA S6-14, and CSA S6:19 (as this is the time where the discrepancy and conservatism in the evaluations are most prominent) (Smith 2018).

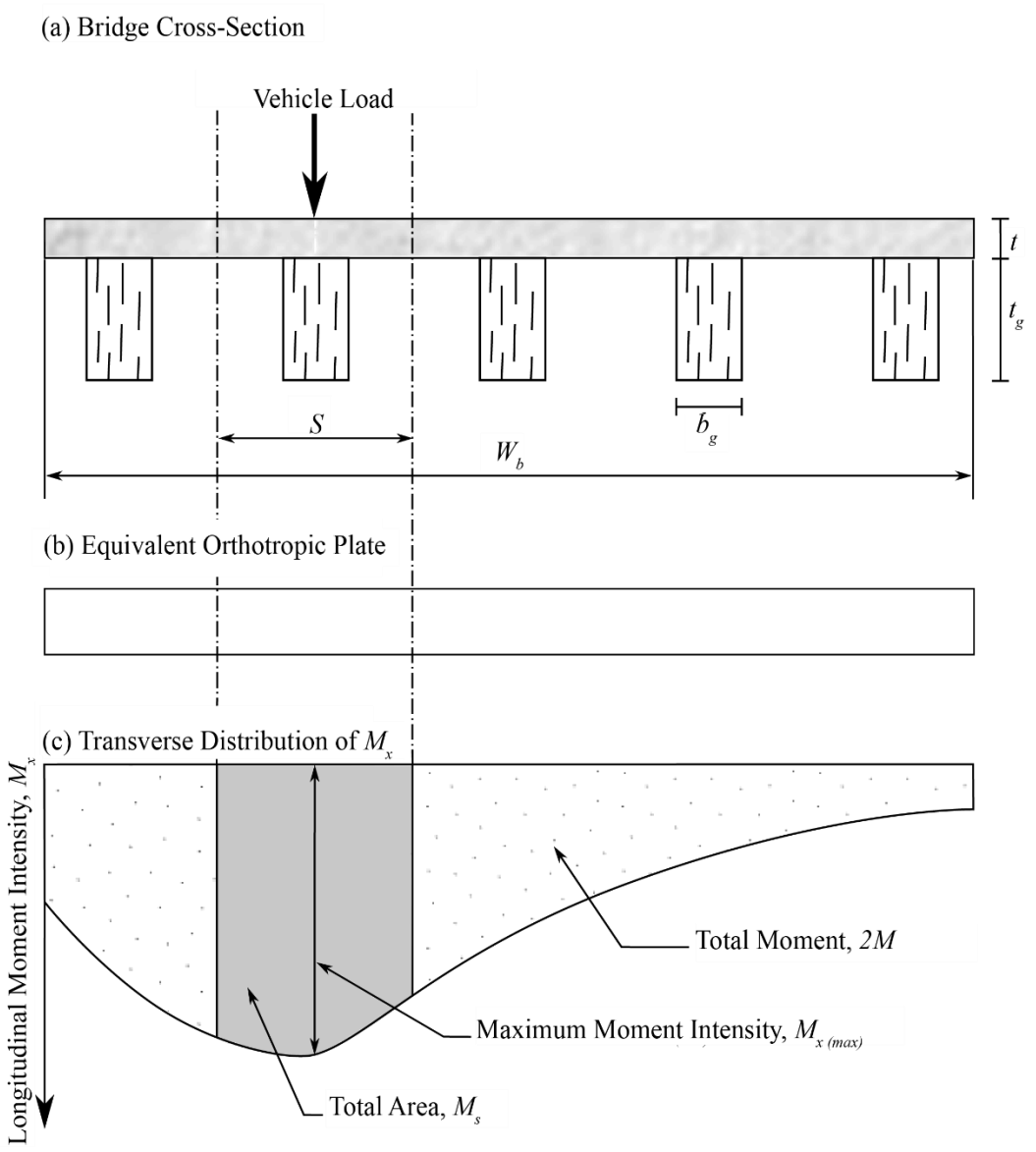

Fig. 2.3. Longitudinal moment distribution across a transverse section of a bridge

The distribution of longitudinal bending moment intensity (M_x) due to the typical vehicle load in Fig. 2.3(a) is shown, through a transverse section of the bridge, in Fig. 2.3(c). From the plot in Fig. 2.3(c), it can be seen that the maximum moment sustained by any of the girders (M_s) (which is shared with the associated portion of the bridge deck) is approximately:

$$M_s = SM_{x(\max)} \tag{2.9}$$

where S is the girder spacing; and $M_{x(max)}$ is the maximum longitudinal moment intensity [see Fig. 2.3(c)]. $M_{x(max)}$ depends on both the load applied and the load-sharing characteristics of the bridge.

According to the SMA used by AASHTO, the OHBDC and CSA, which is known as the "D-Type Method", M_s can be calculated as follows:

$$M_s = \frac{S}{D} M \tag{2.10}$$

where M is the total moment at the section under consideration due to the prescribed loading (see Fig. 2.3(c)); and D is the load-distribution parameter (with units of length). Hence, by equating the right-hand side of Eq. (2.9) to the right-hand side of Eq. (2.10), it is evident that:

$$D = \frac{M}{M_{x(\max)}} \tag{2.11}$$

The load-distribution parameter D is historically obtained by analyzing a bridge as a simply supported orthotropic plate or semi-continuum (Chan et al. 1995). (These analysis methods are discussed in previous sections.) Once D is known, M_s – for the bridge that was analyzed to obtain D or for another bridge with similar load-distribution characteristics – can be determined by multiplying the maximum load effect (at the section under consideration due to the prescribed loading) determined by simple beam analysis by the "load fraction" S/D [i.e., by using Eq. (2.10)].

The value of D can be specified in terms of load effects due to different prescribed loadings, e.g., due to either one or two longitudinal lines of wheels of a design vehicle (depending on the version of the code). In the former case, M_s is obtained from Eq. (2.10); in the latter case, M_s is obtained by replacing M [on the right-hand side of Eq. (2.10)] with $2M$. However, in both cases, the value of D will be different.

2.2.2.1. Conditions Required for Use of the SMA

Certain conditions are necessary for use of the SMA to ensure that the superstructure of a bridge can be accurately idealized as a simply supported orthotropic plate. As noted in Section C5.6.2 of the CSA S6:19 Commentary, CSA S6.1:19 (CSA, 2019b) (and in more detail in Section C5.7.1.1 of the CSA S6-06 Commentary, CSA S6.1-06) (CSA, 2006a), these conditions have been unchanged for over 30 years (with the exception of CSA '83) [dating to the 1980s when they were outlined in Bakht & Jaeger (1985)]. For straight, timber girder bridges, they include the following (CSA S6:19 Clause 5.6.2):

a) The width of the bridge is constant;
b) The deck is continuous along the entire bridge width;
c) The span between centreline of supports or bearing units is constant throughout the width of the bridge (i.e., all bridge girders, or girders, must have the same span);
d) The support conditions (at two opposite ends of the bridge) are closely equivalent to line supports;
e) Diaphragms and bracing systems comply with the applicable requirements of the code Sections relevant to the design material;
f) There are at least three longitudinal girders supporting the deck;

g) The girders have approximately the same flexural rigidity (with an allowed variation from the mean of not more than 10%);
h) The girders are approximately equally spaced (again, with an allowed variation from the mean of not more than 10%);
i) The minimum girder spacing is 0.6 m;
j) The maximum girder spacing is 4 m; and
k) The overhang length (S_c) on both sides of the bridge is not more than 1.0 m and does not exceed 50% of the mean spacing between longitudinal girders.

Note that i) specifies that the minimum girder spacing is 0.6 m, though typically the spacing of timber girders in Nova Scotia is between 0.5 m and 0.6 m (Smith, 2018).

2.2.2.2. SMA in OHBDC '83

In the 1983 edition of the OHBDC the load distribution parameter, D, was determined by using "characteristic parameters", α and θ, based on orthotropic plate theory (see Section 2.2.1.1), where:

$$\alpha = \frac{D_{xy} + D_{yx} + D_1 + D_2}{2(D_x D_y)^{0.5}} \tag{2.12}$$

$$\theta = \frac{b}{L} \bullet \left(\frac{D_x}{D_y} \right)^{0.25} \tag{2.13}$$

where D_x is the longitudinal flexural rigidity; D_y is the transverse flexural rigidity; D_{xy} is the longitudinal torsional rigidity; D_{yx} is the transverse torsional rigidity; D_1 is the longitudinal coupling rigidity (i.e., the contribution of transverse flexural rigidity to the opposite torsional rigidity); D_2 is the transverse coupling rigidity (i.e., the contribution of longitudinal flexural rigidity to the opposite torsional rigidity); b is the half-width of the deck, and L is the span length.

The rigidities denoted by D with subscripts above (i.e., D_x, D_y, D_{xy}, D_{yx}, D_1, and D_2) are in units of Nm. These can be calculated for straight, timber bridges, according to the following equations (Bakht & Jaeger, 1985):

$$D_x = \frac{E_L}{S} \bullet \frac{b_g t_g^{\,3}}{12} \tag{2.14}$$

$$D_y = E_L \bullet \frac{t^3}{12} \tag{2.15}$$

$$D_{xy} = \frac{G_{LT} K t_g b_g^{\,3}}{S} \tag{2.16}$$

$$D_{yx} = 0 \tag{2.17}$$

$$D_1 = 0 \tag{2.18}$$

$$D_2 = 0 \tag{2.19}$$

where E_L is the modulus of elasticity of timber in direction of L shown in Fig. 2.4; G_{LT} is the shear modulus of timber along axis L; t_g is the depth of the girder; b_g is the width of the girder; t is the thickness of the deck; S is the centre-to-centre spacing of the girders; K is the torsional coefficient (determined from Fig. 2.5), and W_b is the total bridge width [see Fig 2.3(a)].

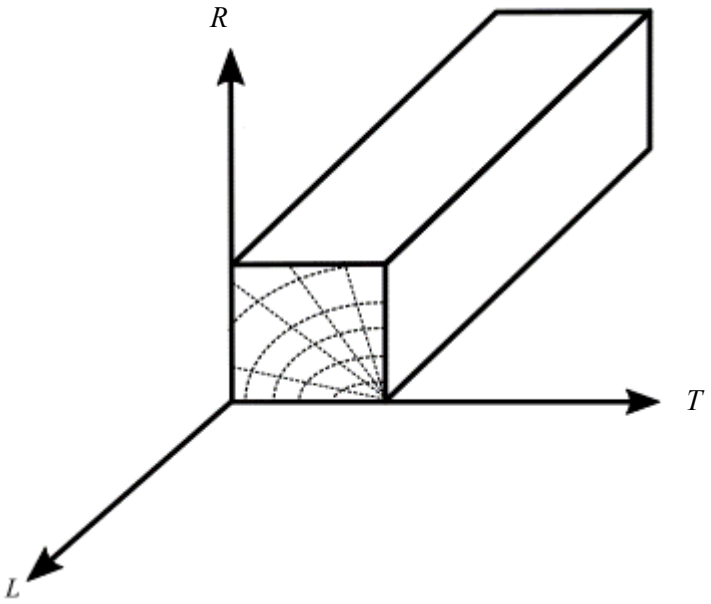

Fig. 2.4. Principle directions in wood specimens

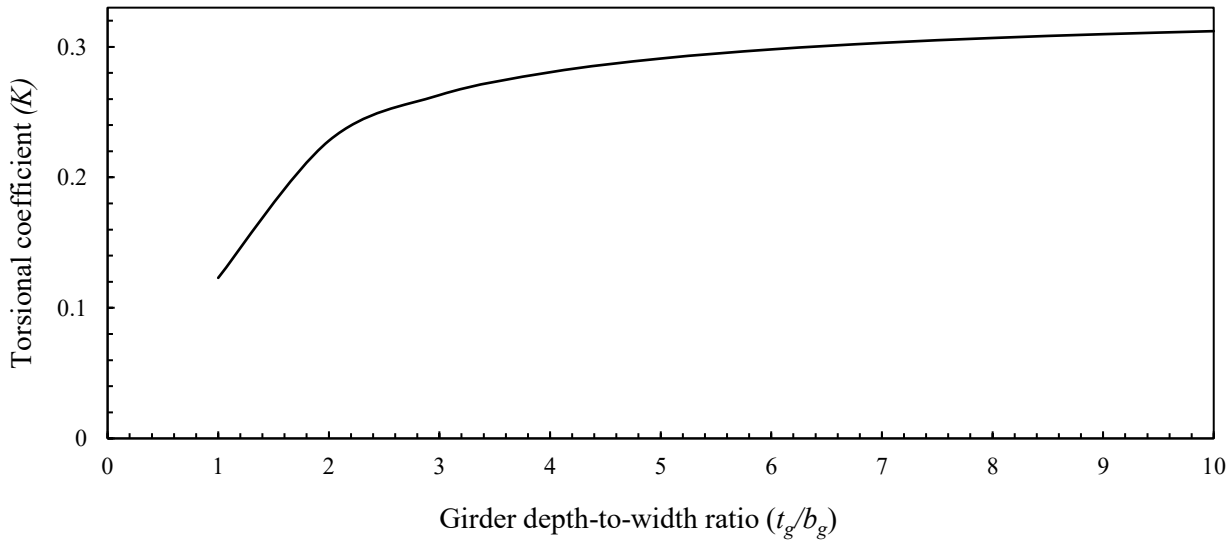

Fig. 2.5. Values of the torsional coefficient, K [reproduced from Bakht & Jager (1985)]

By substituting Eqs. (2.17) to (2.19) into Eqs. (2.12) and (2.13), the "characteristic parameters", α and θ, can be simplified to:

$$\alpha = \frac{D_{xy}}{2(D_x D_y)^{0.5}} \tag{2.20}$$

$$\theta = \frac{b}{L} \bullet \left(\frac{D_x}{D_y} \right)^{0.25} \tag{2.21}$$

After α and θ are determined, Fig 4.11 of Bakht & Jager (1985) (or the same figure that appears in the 1983 version of OHBDC) was used to determine D and C_f (the correction factor for the load distribution parameter). These parameters were then used to determine the girder design moment (M_s) as described in the following sub-Sections.

In the 1983 edition of the OHBDC, the girder moment, M_s, was determined as follows:

$$M_s = \left(\frac{S}{D_d} \right) M \tag{2.22}$$

where S and M are defined in Section 2.2.2, and D_d is the design value of the load-distribution parameter (D), taken as:

$$D_d = D\left(1 + \frac{\mu C_f}{100} \right) \tag{2.23}$$

where μ is the lane width modification factor [which relates the actual design lane width (W_e, in meters) to the basic design lane width (the SMA was created assuming a design lane width of 3.3 meters)], i.e.:

$$\mu = \frac{W_e - 3.3}{0.6} \leq 1.0 \tag{2.24}$$

For timber bridges, $C_f = 0$. Hence, the girder design moment (M_s), due to the live load in Eq. (2.22) can be reduced to:

$$M_s = \left(\frac{S}{D} \right) M \tag{2.25}$$

where M (i.e., the total moment in the section under consideration) is determined from Fig 4.7 of Bakht & Jager (1985). Fig. 4.7 (Bakht & Jager 1985) gives the maximum moment generated from one line of wheel loads or half the lane loading scenarios (this differs from CSA S6-00 and subsequent code versions, which all use two lines of wheel loads or the full lane loading scenario).

2.2.2.3. SMA in OHBDC '91

Research conducted between 1983 and 1991 showed that it was possible to simplify the OHBDC '83 SMA without a significant loss of accuracy (Bakht & Jaeger, 1992). For example, Bakht & Moses (1988) showed that for typical slab-on-girder-type bridge types, the parameter D_x and D_y can be related to span length (L) and bridge width (W_b), thus producing a predictable range of θ values according to Eq. (2.21). Similarly, the parameter α [Eq. (2.20)] was shown to fall between 0.06 and 0.2 (Bakht & Jaeger, 1985). By using the upper and lower limits of α and θ, Bakht & Jager (1985) showed that D: (a) generally fell within a narrow band for a given bridge type, (b) varied principally as a function of the number of design lanes (n) and the span length (L), and (c) could be calculated from a simple equation (without having to first determine α and θ) (Bakht & Jaeger, 1992).

Hence, in the 1991 edition of the OHBDC, the D value for the moment was determined by using equations presented in the code, which are summarized, for sawn wood girder bridges, in Table 2.1 (Bakht & Jaeger, 1991). This change from a graphical solution to a numerical one was done principally to limit discrepancies in "reading from the charts", which would sometimes result in different answers for the load effects in the same girder (Bakht & Jaeger, 1991).

Table 2.1. Moment D values, in meters, corresponding to ULS and SLS II

Type of Bridge	Class of Highway	n	External/ Internal	D		C_f(%)
				3< L ⩽10 m	L > 10 m	
Sawn Wood Girder Bridges	A or B	1	External or internal	1.8	N/A	0
		2,3,4	External or internal	1.30 + (4L/100)	N/A	0
	C	1	External or internal	1.8	N/A	0
		2,3,4	External or internal	1.40 + (4L/100)	N/A	0

The girder design moment (M_s) in OHBDC '91 was then determined, again, by using Eqs. (2.22) to (2.25).

2.2.2.4. SMA in CSA S6-88

In 1988, CSA S6-88 replaced the OHBDC, creating a coast-to-coast standard for the design of Highway Bridges (CSA, 1988). CSA S6-88 used a dis-involved version of the SMA which limited applicability of the SMA to bridges where the deck cantilever is less than 60% of the girder spacing (i.e., 0.6S) [as mentioned at the end of Clause 5.3.2.2.2 of CSA S6-88 (CSA 1988)].

The SMA provided in CSA S6-88 followed a similar procedure to those in previous OHBDCs for determining M_s; however, it took into account the effect of wider design lanes (> 3.3m) in the value of D itself (rather than through the factor μ in the parameter D_d). These values of D were given in Tables 8 and 9 of CSA S6-88 for different bridge types and roadway widths (W_c). The D values in Tables 8 and 9 of CSA S6-88 also

included a reduction factor for multi-lane loading effects. The girder design moment M_s was then calculated according to Eq. (2.26), which is the same as Eq. (2.25):

$$M_s = \left(\frac{S}{D}\right) M \tag{2.26}$$

For Eq. (2.26), the maximum moment (M) was determined using the loading conditions outlined in CSA S6-88 which are similar to those still used today, outlined in Section 4.2.

2.2.2.5. SMA in CSA S6-00

With the adoption of CSA S6-00, more stringent criteria needed to be met in order to use the SMA compared to CSA S6-88. These are the criteria that were outlined, previously, in Section 2.2.2.1. In CSA S6-00, the long-used *S/D* term [e.g., Eq. (2.26)] was replaced by a new "amplification factor", F_m, and instead of M, the maximum moment per lane used in OHBDC 83' – 91' and CSA S6-88, the "average" bending moment in each girder, $M_{s\,\text{avg}}$ was introduced, giving a new general form of the SMA equation for bending:

$$M_s = F_m M_{s\,avg} \tag{2.27}$$

where M_s is the design girder moment and $M_{s\,avg}$ is determined by sharing equally the total moment on the bridge cross-section among all girders in the cross-section [i.e., taking the total area under the curve in Fig. 2.3(c) and dividing it by N].

Where in CSA S6-88, the term (S/D) was multiplied by the maximum moment, now we have this amplification factor, F_m, multiplied by $M_{s\,avg}$, where:

$$M_{s\cdot avg} = \frac{nM_T R_L}{N} \tag{2.28}$$

where M_T is the maximum longitudinal moment in the cross-section due to CL-W loading, from Clause 3.8.3.1.1 in CSA S6:19 (CSA, 2019a) (also described in Section 4.2), at the point of the span under consideration and n determined per clause 3.8.2 of CSA S6-00 which gives the number of design lanes for a specified width, W_c (covered in more detail in Section 4.2); R_L is the modification factor for multi-lane loading following CSA S6-00 Clause 3.8.4.2 and Clause 14.8.4.2 (CSA, 2000).

While $M_{s\,avg}$ seems apparently "more involved" than the original M variable used in other versions of the SMA, all that has changed – in reality – is that, instead of the multilane loading effects being implicit in the D values used, they are now taken into account in the loading variable, $M_{s\,avg}$.

The load sharing variable, F_m in Eq. (2.27) is defined as follows:

$$F_m = \frac{SN}{F\left(1 + \frac{\mu C_f}{100}\right)} \geq 1.05 \tag{2.29}$$

where N is the number of girders or longitudinal wood girders in the bridge width (W_b); and F is the width dimension that characterizes the load distribution of a bridge. [Note that the parenthetical term in Eq. (2.29) is the same lane width correction factor used in Eq. (2.23).] The parameters F and C_f are both obtained from Table A5.7.1.2.1 of CSA S6-00 (which is reproduced in Table 2.2) for the corresponding bridge type, length, and the number of design lanes (CSA, 2000). As in previous editions of the SMA, C_f for timber bridges is 0, which simplifies Eq. (2.29) to:

$$F_m = \frac{SN}{F} \geq 1.05 \tag{2.30}$$

Table 2.2. Moment F and C_f values, corresponding to ULS and SLS II [recreated from CSA S6-00]

Bridge Type	Class of Highway	n	External/Internal Portion	F (m)		C_f
				3m< L ≤10m	L >10m	
Sawn Wood Timber	A or B for design or evaluation	1	external or internal	3.6	N/A	0
		2	external or internal	4.7+0.14L	N/A	0
		3	external or internal	6.2+0.19L	N/A	0
		4	external or internal	7.3+0.22L	N/A	0
	C or D evaluation only	1	external or internal	3.6	N/A	0
		2	external or internal	4.7+.14L	N/A	0
		3	external or internal	5.7+0.18L	N/A	0
		4	external or internal	5.7+0.18L	N/A	0

It can be seen that the amplification factor is beginning to look like the original S/D factor presented in the OHDBC, only now with the addition of N, the number of longitudinal beams within W_b. By understanding the changes made in this version of the code, Eq. (2.26) can be expanded and then simplified to show that for $(SN/F) > 1.05$:

$$M_s = \left(\frac{SN}{F}\right)\frac{nM_T R_L}{N} \tag{2.31}$$

where the number of girders, N, can be cancelled out, leaving:

$$M_s = \left(\frac{S}{F}\right)\left(nM_T R_L\right) \tag{2.32}$$

It can hence be seen that Eq. (2.32) [the CSA S6-00 SMA for the moment] resembles previous code SMA equations [e.g., Eq. (2.25)], but it incorporates n and R_L directly in the equation for M_s, rather than having them implicit in the equation for F.

2.2.2.6. SMA in CSA S6-06

CSA S6-06 saw minor changes to the overall procedure of the SMA, with the majority of the changes coming in the form of reorganizing and renaming tables, plus changes to the values of *F*. One of the tables that were renumbered is Table A5.7.1.2. from CSA S6-00 (CSA, 2000), which was changed to Table 5.3 in CSA S6-06 (CSA, 2006a). There were no changes being made to the section of the table related to timber girder bridges. The moment evaluation procedure is the same as outlined in Section 2.2.2.5 for CSA S6-00.

2.2.2.7. SMA in CSA S6-14

Between CSA S6-06 and CSA S6-14, some of the most significant changes were made to the SMA – some in the form of moving the incorporation of variables from one equation to another, and some in the form of renaming of variables, and their prescribed values. One of the biggest changes comes in the addition of a skew factor, F_s, to account for bridges that are curved in plan (in the case of bridges covered by this research, which are all straight, $F_s = 1.0$).

In CSA S6-14, the design girder moment (M_L) was determined as follows:

$$M_L = F_T F_S M_T \tag{2.33}$$

where M_L is the longitudinal moment per girder due to the CL-W loading; M_T is the longitudinal moment generated by CL-W loading; F_s is the skew factor (= 1.0, herein); and F_T is the truck load fraction used to generate the design longitudinal load effects, calculated using the following equation (for both ULS and SLS).

$$F_T = \frac{S}{D_T \gamma_C (1 + \mu\lambda)} \geq 1.05 \frac{nR_L}{N} \tag{2.34}$$

where n, R_L, and N are defined previously, below Eq. (2.28); S is the centre-to-centre spacing of girders, μ is defined previously, and calculated according to Eq. (2.24), D_T is the load sharing factor, λ is the Lane width parameter (akin to C_f) and, γ_C is the truck load modification factor. D_T, λ, γ_C are given for timber bridges in Tables 5.11, 5.5, and 5.6 of CSA S6-14 (CSA, 2014a). D_T factors relevant to this research, are shown in Table 2.3 based on the number of design lanes.

Table 2.3. D_T for wood deck on wood girder bridges for class A and B highways [recreated from CSA S6-14]

Bridge Type	*n*	Moment for Interior and Exterior
Bridges with Wood Plank Deck	1	2.4
	≥2	2.55

As noted previously, for timber bridges, the width correction factor, $\lambda = 0$. The factor γ_C, which is a truck load modification factor, is calculated using Table 5.5 in CSA S6-14 (recreated in Table 2.4), where S_c is the length of the cantilever. In Clause 5.6.6.1 of CSA S6-14 modification factors are given for differing number of design lanes, n, and whether the girder under consideration is on the exterior or interior of the section (CSA, 2014a).

Table 2.4. γ_c values for exterior girders of slab on girder bridges for moment

S_c	γ_c
$S_c \leq 0.5S$	1
$0.5S < S_c \leq 0.6S$	$1.25-0.5(S_c/S) \leq 1.0$

In most timber bridges there is no cantilever overhang; hence $\gamma_c = 1.0$, and Eq. (2.34) reduces to:

$$F_T = \frac{S}{D_T} \geq 1.05\frac{nR_L}{N} \tag{2.35}$$

2.2.2.8. SMA in CSA S6:19

Few changes were made to the use and application of the SMA between CSA S6-14 and CSA S6:19. All the same constraints were to be met, and no values changed in the given tables. The most notable change was the separation of Clause 5.6.7.5 in CSA S6-14 [the clause talks about the tables to be used for the determination of D_T and the correction factor λ for wood decks or wood girder bridges (CSA, 2014a)] into two separate clauses in CSA S6:19: Clause 5.6.7.5 for "transverse wood deck on wood girder bridges", and Clause 5.6.7.6 for "wood decks spanning longitudinally" (CSA, 2019a).

2.2.3. RECENT RESEARCH ON SMAS FOR TIMBER BRIDGES

Recently work concerning the SMA and its application to timber bridge in the province of Nova Scotia has been undertaken in the form of a Master's research program, between 2016 and 2018 (Section 2.2.3.1), and a load testing report, in 2021, on multiple timber bridges around the province (Section 2.2.3.2).

2.2.3.1. Experimental Tests by Smith (2018)

In 2018, Smith (2018) completed a test program that focused on the evolution of the SMA and its impact on the evaluation of timber bridges. The research provided an in-depth statistical analysis of the Nova Scotia "timber bridge inventory", looking at characteristics of the existing structures such as year of construction, clear span length (L), overall bridge width (W_b), girder count (N), centre-to-centre girder spacing (S), etc. . From an analysis of the timber bridge inventory, it was determined that a "representative Nova Scotia timber bridge was "a single-span, two-lane structure, approximately 50 years old, with a length of 7.5 m to 9 m and a width of 6.5 m to 8.5 m, having 14 to 16 girders sized at roughly 420 mm by 210 mm with girder spacings ranging from 500 mm to 600 mm." (Smith, 2018). This was used, by Smith (2018), for future modelling and case study work.

Lab testing (described below) was thereafter completed on a third-scale model of the aforementioned representative structure in Dalhousie's Heavy Structures Lab (see Fig. 2.6).

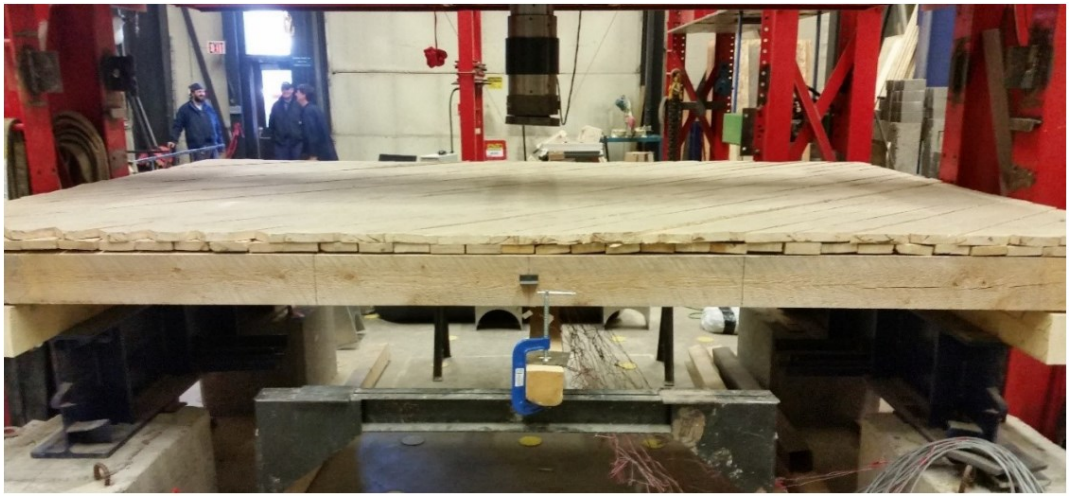

Fig. 2.6. Constructed third scale bridge tested by Smith 2018

The model was built to best represent an in-situ structure; rough-cut lumber and no fastening between the deck and stinger (to eliminate possible composite action), no deck framing (to capture the condition of a deck in service for numerous decades), and slight gaps were left between the deck planks to best account for fatigue, temperature and humidity changes after years in service. Each stinger was tested individually to collect data on their mechanical properties, and instrumented with strain gauges and linear variable displacement transducers (LVDT) at midspan (Fig. 2.7).

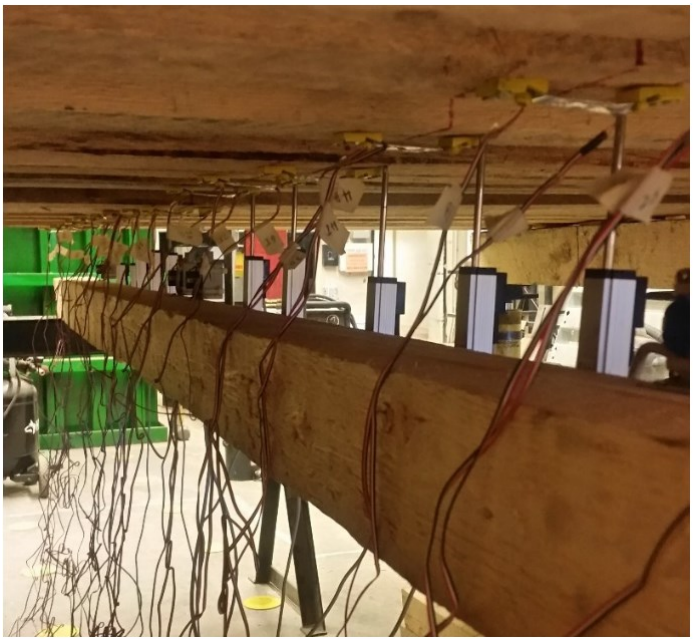

Fig. 2.7. Instrumentation of third scale bridge model (Smith 2018)

Multiple tests were done on the model, by applying a pseudo truck wheel load to the bridge deck at mid-span, in differing transverse locations (to represent the design truck being in different design lanes). This portion of the research, and the resulting data, are used to aid in the calibration and validation of the FE models in the current work (see Section 3.2).

In Smith (2018), the code-predicted values of total and stinger moment (M_T or M_L) were compared to the tests, and to predicted values obtained using the SECAN modelling program (a semi-continuum based analysis software). It was shown that the SECAN results were much more in line with the experiments, and CSA S6-06 predictions (compared to the CSA S6-14 predictions, which were very conservative). This notion is further explored in Chapters 4 and 5.

2.2.3.2. Field Tests by SHM Canada (2021)

From 2020 to 2021, six bridges around the province of Nova Scotia were load tested by SHM Canada Consulting Limited, herein referred to as SHM. Testing was completed by following a strict testing regime that is briefly outlined here, and available in more detail in *Load Testing & Development of Live Load Distribution Factors for Timber Bridges* (SHM Canada Consulting Limited, 2021).

The primary data collected during the field tests was the mid-span deflection of each girder. This data was collected using Way Con Series SX50 Draw-Wire Sensors attached to the underside of each stinger by a magnet and attached, at the other end, to a fixed datum on the ground under the bridge. The strain was also measured at the bottom of randomly selected stingers, using BDI ST 350 Strain Transducers, this data was used to verify the displacement data, and to check for any torsional effects that may be taking place. Strain data was also collected through the depth of certain girders – to get a sense of the amount of composite action between the deck and girders. The displacement at the abutments was measured for some of the six bridges, to later account for support settlement/deflection. All the data was collected using a Campbell Scientific CR1000X data logger at a speed of 3 Hz (SHM Canada Consulting Limited, 2021).

On the wearing surface of the bridges, lines were painted longitudinally and transversely as stopping points, and drive lanes. Transverse to the driving, direction lines were painted roughly every one metre, starting from the edge of the abutments. In the longitudinal direction, lines were spaced to allow a vehicle edge distance (VED) of 900 mm, and to fit between three and five “test lanes” on the road, depending on the width of the bridge. Fig. 2.8 shows some typical instrumentation and the stopping-lane layout.

(a) Bridge girder instrumentation

(b) Bridge wearing surface layout

Fig. 2.8. Instrumentation and wearing surface examples from SHM bridge load testing

The truck used to load the bridge was a three-axle dump truck weighing, on average, 25,700 kg. To load the bridge, the truck driver would begin by placing the middle axle on the test point, to their best abilities. Then, testing would begin. Data was recorded at each transverse point along each lane, at a rate of 3 Hz, for anywhere between three and five minutes (to help rule out any outliers and allow any dynamic effects to lessen). Once the static load testing was done, dynamic tests were done at slow, normal, and fast speeds to capture the dynamic behaviour of the bridge. Once all the testing was complete, the sensors were removed from the bridge and packed away, and the data saved.

Using the gathered data, an FE model and a SECAN model were constructed, validated, and calibrated by SHM. The moment effects given by different versions of the code were compared to those from SECAN and the FE models. Based on this comparison, it was concluded by SHM that the "factors determined using S6-14 and S6:19, Clause 5.6.6, are generally more conservative than those determined using S6-06. Factors from the live load tests were close to those determined using S6-06 for three of the bridges under investigation." (SHM Canada Consulting Limited, 2021). Like the lab tests, the data collected from the static tests was used in Section 3.2 to aid in the calibration and validation of the FE models in the current work.

2.3. PROPERTIES OF STRUCTURAL WOOD

As mentioned in Section 1.2.2, and Section 2.1.2 to properly evaluate timber bridges it is necessary that the properties of the timber being used are known. There is a noticeable gap in timber research concerning evaluation parameters: no values of U are provided for timber for use in the General Method, and no bias coefficients or COVs for resistance (δ_R and V_R) are given for use in the Mean Load Method. The lack of these parameters makes it difficult (or at least, confusing) to evaluate in-situ structures accurately.

Because timber is a "living" material, it can be difficult to accurately determine its structural properties. Although the timber used in a given bridge is usually all the same species and may come from the same distributor and area, due to the variability in the wood grains, knot, moisture content, etc., the structural properties can still be different from one element (e.g., girder) to another (perhaps not drastically, but enough to make a difference in overall structural resistance of the bridge).

In Canada, timber strength properties have historically been derived from testing small "clear" specimens (i.e., specimens that are free of strength reducing characteristics) in accordance with ASTM D245, *Standard Practice for Establishing Structural Grades and Related Allowable Properties for Visually Graded Lumber* (ASTM International, 2019). The strength properties derived from the methods outlined in ASTM D245 are typically based on the weakest species in a commercial species combination, and the lower fifth percentile strength properties are used. These are determined under the assumption that clear wood properties are normally distributed. The fifth-percentile strengths are further modified to account for the differences between the small clear test specimen data and the strength and stiffness of full-size members subjected to long-term loads and in-service climate conditions (CSA, 2019b) using so-called "adjustment factors".

Although many countries still use the clear specimen approach to characterize timber, due to its simplicity and historical success, in 1984, when Limit States Design (LSD) was introduced in Canada, the CSA O86/S6 Technical Committee adopted the philosophy that design properties for structural wood products be based on full-size structural tests of members, where feasible. Hence, bending design properties tabulated in CSA O86 (the Canadian timber code) (CSA, 2019), (which is referred to from CSA S6:19 Clause 14.14.1.7.3), are derived from full-size test data developed from studies completed by Madsen and Nielsen (1978c) and Bury (1981) (CSA, 2019b). Limited data is available from these programs on the strength of full-size girders in bending, which is the area/effect that this research is concerned with, but tests do show that the design properties derived from the small clear specimen approach were conservative (CSA, 2019b).

2.4. SUMMARY

As shown in the previous Chapters, while research on the evaluation of bridges has been ongoing for decades, there are still many gaps in knowledge concerning the evaluation of timber bridges. These include:

- Lack of a consistent approach of how to model a timber bridge to accurately capture real-world effects (e.g., composite action, strength/stiffness variability);
- Over-conservative statistical parameters for live load analysis (δ_{AL}, V_{AL}), for use in the Mean Load Method (these have been unchanged since CSA S6-06, despite substantial changes to the SMA since that time); and
- Following from above, the SMA in CSA S6-14/19 likely over predicts the design moment for timber bridges;
- Lack of data regarding statistical parameters of timber resistance – namely, resistance adjustment factors, bias coefficients, and COVs (U, δ_R, V_R) for use in bridge evaluation using either the General Method or the Mean Load Method;

The following Chapters address the points listed above to develop a more accurate and efficient approach for the evaluation of timber bridge infrastructure in Nova Scotia. These points are addressed through FE modelling (Chapter 3), a parametric study (Chapter 4), and experimental testing (Chapter 6). While the SMA is considered over-conservative in both the 2014 and 2019 version of CSA S6 herein only CSA S6:19 will be referred to as it is the most recent version of the code.

Chapter 3: FINITE ELEMENT MODELLING OF TIMBER BRIDGES

3.1. INTRODUCTION AND FINITE ELEMENT MODELLING OVERVIEW

The work done by SHM Canada (Section 2.2.3.2), while insightful, looked only at six bridges around the province of Nova Scotia, which has a timber bridge inventory of over 2000 bridges (Smith 2018). To broaden the scope covered by the experimental data and range of geometrical properties tested, finite element (FE) is preformed herein. While FE modelling is widely accepted and has become more mainstream in the industry, it is still prudent that the model is developed and validated properly. Calibration and validation of the model is done herein by comparing results against data collected by Smith (2018) and SHM Canada (2021).

Section 5.9 of CSA S6:19, *Refined methods of analysis for short- and medium-span bridges* (CSA, 2019a) outlines the following requirements for rigorous analysis models, including those developed using FE:

(a) The model must be representative of the expected structural system behaviour;
(b) All members must contain an adequate number of nodes to avoid any concentrated effects due to modelling;
(c) The aspect ratio of all elements must be at most two;
(d) Linear elastic properties must be used for determining structural and component responses; and
(e) The model must be validated to ensure it reproduces the expected behaviour.

3.2. FINITE ELEMENT MODELING

In accordance with the requirements listed above, FE models were constructed using the commercially available FE software package MIDAS Civil. MIDAS Civil is a bridge analysis and design-specific FE software that includes several tools that allowed the parametric study to be completed with relative ease. The FE models were constructed using linear-elastic beam, solid and/or shell elements, which utilized Timoshenko and Mindlin-Reissner element formulations built-in to MIDAS Civil. The models were used to conduct a sensitivity study which varied mesh densities, mechanical properties, and element types. The models used in the calibration, validation and sensitivity study were constructed to replicate the geometric properties of two tests from Smith (2018) and two tests from SHM Canada (2021) on straight timber bridges.

3.2.1. BRIDGE GEOMETRY MODELLING

Timber bridges in Nova Scotia are typically designed with a simple structure similar to that shown in Fig. 2.3. The benefit of their simpler construction is that only the load resisting elements needed to be modelled (e.g., girders, and deck), guard rails, sidewalks, etc. were omitted. As mentioned, multiple different sensitivity models were constructed, changing key parameters. Two different element types were used and subsequently compared to one another to evaluate their effectiveness at modelling the timber girders. Beam elements were one of the elements utilized to model the girders, chosen due to their simplicity and ability to directly return displacement, solid elements were the other, chosen due to their ability to show stress distribution through the girder during loading. Although solid elements are typically not used in bending applications, due to a phenomenon called shear locking, which makes the model stiffer, dividing the girder up into a large amount of smaller solid elements this issue can be improved upon, allowing the solid elements to capture an adequate bending response. One beam model and three different solid models were constructed, the solid models varied the number of through-thickness elements of the girder from three elements to five.

Composite action was initially considered, using the connection modelling technique shown by Choi and Crews (2012) outlined in Section 2.2.1.4 and depicted in Fig.3.1(a). Based on results from the lab (Section 2.2.3.1) and the field (Section 2.2.3.2) as well as preliminary modelling, composite action was found to be negligible. Hence, a different method was introduced, used for the models comprised of beams. Links are still used to model the connection, although instead of rigid links, connected to the top corner nodes of the solid element, only one general link (similar to rigid link although general links allow for altering the stiffness in the three principal directions) was used between each of the beam element ends and the deck. To ignore composite action but still prohibit the deck from penetrating the girders the stiffness of the general links was set to 100,000 N/mm in the Z- direction (i.e. the direction of gravity) and near 0 N/mm in all other directions. Fig. 3.1 illustrates the two different contact modelling methods.

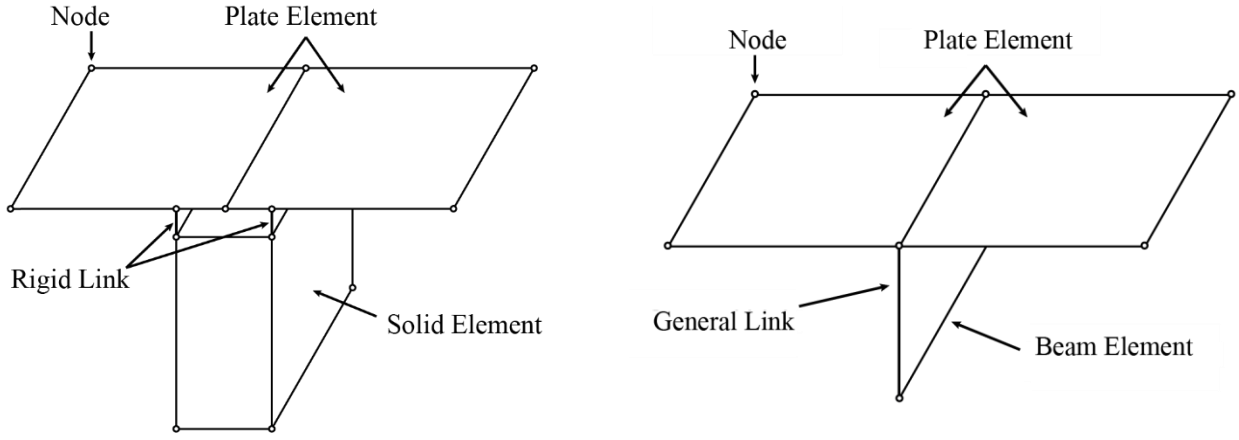

(a) Connection modelling with solid element (b) Connection modelling with beam element

Fig. 3.1. Different connection modelling procedures

All the bridges were modelled assuming simply supported girders, allowing the ends to rotate but not move vertically. While it is possible to experience abutment settlement, little data was collected on this by SHM and Smith 2018 and as such was omitted from the study; therefore, all the displacements were assumed to be relative to the abutments.

3.2.2. Model Sensitivity Study

Three major parameters (i.e., element type, girder *E,* and mesh density), covered in Sections 3.2.2.1, 3.2.2.2 and 3.2.2.3 respectively, were investigated, along with two minor parameters (i.e., deck material properties and deck thickness). All these parameters were investigated in order to develop a robust and general FE model that captured the real-world effects present in the tests by Smith (2018) and SHM Canada (2021). The primary results used to evaluate the FE models against the tests were the load distribution factors (LDFs) for each girder. The LDFs are a measure of how an applied load is distributed through the width of the bridge deck, to each girder can be, taken as:

$$\mathrm{LDF} = \frac{\Delta_i}{\Delta_{avg}} \tag{3.1}$$

where Δ_i is the maximum deflection of any girder i, and Δ_{avg} is the average of the maximum deflections of all the girders in the structure at the same longitudinal location. Note, deflection is not the only way LDF can be calculated, it can also be done with moments for example, though deflections are easily recorded in the field and lab and were therefore used as a suitable substitute.

The LDFs (ergo, deflections) were used as the primary metric as these were the most accurate available data to compare against, and for all tests the structures were assumed to be acting within the linear elastic region. The strain measurements by Smith (2018) showed large discrepancies when compared to FE data and simple hand calculations, it was therefore deemed undesirable for comparison. For the tests by Smith (2018), Test T1 involved a single point load on the east side of the third-scale bridge model by Smith (2018), and Test T2 involved two point loads applied on the west side of the third-scale bridge. The two bridges tested by SHM (2021) and used in this sensitivity study are HFX061 and HFX322. The two tests by Smith (2018) used applied point loads of 26 kN. The truck used to load the bridges tested by SHM (2021) was a single unit tandem-axel truck (3 axles) loaded close to the legal capacity (25,700 kg). From front axle to rear axle the Truck was 5.52 metres long, with 4.2 metres between the front and middle axles, and 1.32 metres between the middle and rear axles. The truck was positioned with its middle axle at midspan on the bridge for each lane.

All models used a deck thickness of 95 mm as many of the bridges tested by SHM showed a deck thickness of 95 mm. Drawings from Nova Scotia Public Works (NSPW) from 1958 and 2003 specify a deck thickness of 100 mm, though using a thickness of 95 mm can be considered a conservative approach, as a thicker deck tends to be stiffer and in turn lowers the LDF value by better distributing the load to adjacent girders. Graphs showing the effect of increasing deck thickness are available in Appendix A1.

Three different material models were considered for the deck. Initially it was assumed that the deck would behave as an isotropic material, but this needed to be verified. The three material models included: an isotropic material model, an orthotropic material model, and a "hybrid" material model. The hybrid material model was based off bridge plans supplied by NSPW. The properties of each are given in Table 3.1 below, where E_L is the modulus of elasticity in the longitudinal direction; E_T is the modulus of elasticity in the transverse direction; E_R is the modulus of elasticity in the radial direction, see Fig. 2.4; G_{LT} is the modulus of rigidity in the longitudinal-radial plane; G_{LR} is the modulus of rigidity in the longitudinal-tangential plane; and G_{TR} is the modulus of rigidity in the radial-tangential plane.

Table 3.1. Deck model material properties

Mat. Model ID	E_L (MPa)	E_T (MPa)	E_R (MPa)	G_{LT} (MPa)	G_{LR} (MPa)	G_{TR} (MPa)
A	10,000	10,000	10,000	-	-	-
B	626	10,000	626	753	753	74.2
C	10285	12588	12588	1480	1480	824

Material Model A is a model that assumes an isotropic material, with the same properties as the girders, Material Model B is an orthotropic model assuming the deck is laid perpendicular to the girders as shown in Fig.1.1 (d), Material Model C is an orthotropic model assuming transverse deck combined with an apron laid at 15º off the longitudinal. It was determined quickly that all the models provided very similar results confirming the assumption that the deck acted isotropically, hence for simplicity all models assumed isotropic deck properties. Graphs comparing these models are shown in Appendix A2.

Table 3.2 (on the following page) shows the results from the initial sensitivity study conducted on the two tests by Smith (2018) (T1 and T2), this initial study accounted for different element types and girder modulus models covered in Sections 3.2.2.1 and 3.2.2.2. Table 3.3 (also on the following page) shows the final sensitivity study results (just mesh density) for both sets of tests from Smith (2018) and SHM (2021) and it includes the mesh density models.

The Model IDs (designations) in the leftmost column of Table 3.2 and Table 3.3 pertains to various element types and mesh densities. Beam models are denoted by the letter B (in the first position of the Model ID) with a 1 in the second position. Solid models are denoted by the letter S in the first position, and the numbers 3, 4 and 5 in the second position of the Model ID correspond to the number of through-depth elements, the three different mesh densities – coarse, medium, and fine – are denoted by the letters C, M, and F, respectively (in the third position of the Model ID).

For the lab tests, two models were created to determine the effect of the girder modulus, this was done because the individual values of *E* for the girders was determined by Smith (2018) and are given in Table 3.4. One model assumed a uniform value of *E* for all the girders and the other was created using the individual *E*

values for each Girder. These models are discussed in Section 3.2.2.2 and denoted by U and I respectfully in the fourth position of the Model ID.

Table 3.2. Initial FE sensitivity study results

Test ID	Model ID	No. elem.	No. nodes	Comp. time (sec)	LDF_T	LDF_{FE}	LDF_T/LDF_{FE}
T1	B1MU	496	544	1.16	3.06	3.13	0.98
	B1MI	496	544	1.18	3.06	3.12	0.98
	S3MU	5984	3568	8.04	3.06	2.15	1.42
	S4MU	4592	7344	9.66	3.06	2.18	1.40
	S5MU	8672	13728	19.84	3.06	2.29	1.34
T2	B1MU	496	544	1.17	2.39	2.18	1.10
	B1MI	496	544	1.18	2.39	2.16	1.11
	S3MU	5984	3568	7.34	2.39	1.77	1.35
	S4MU	4592	7344	9.47	2.39	1.79	1.34
	S5MU	8672	13728	19.33	2.39	1.83	1.31

Table 3.3. Final FE sensitivity study results

Test ID	Model ID	No. elem.	No. nodes	Comp. time (sec)	LDF_T	LDF_{FE}	LDF_T/LDF_{FE}
T1	B1CU	248	288	0.88	3.06	3.14	0.97
	B1MU	496	544	1.16	3.06	3.13	0.98
	B1FU	992	1056	2.17	3.06	3.12	0.98
T2	B1CU	248	288	0.70	2.39	2.10	1.14
	B1MU	496	544	1.17	2.39	2.18	1.10
	B1FU	992	1056	1.90	2.39	2.17	1.10
HFX 061	B1CU	728	792	29.60	1.39	1.40	0.99
	B1MU	816	880	33.33	1.39	1.40	0.99
	B1FU	992	1056	43.64	1.39	1.40	0.99
HFX 322	B1CU	1376	1467	14.35	2.45	2.45	1.00
	B1MU	1536	1627	20.29	2.45	2.45	1.00
	B1FU	1856	1947	83.48	2.45	2.45	1.00

Table 3.4. Values of E for girders used in T1 & T2 [Smith (2018)]

Girder ID	E_{app} (MPa)	Girder ID	E_{app} (Mpa)	Girder ID	E_{app} (Mpa)	Girder ID	E_{app} (Mpa)
G1	9,800	G5	9,750	G9	7,600	G13	9,100
G2	12,100	G6	10,600	G10	10,500	G14	9,800
G3	7,900	G7	11,000	G11	6,000	G15	11,400
G4	8,200	G8	9,350	G12	12,050	G16	11,450
						Average	9,790
						COV	0.18

3.2.2.1. Element Type

Two types of elements were used for the girders in this initial sensitivity study: beam and solid elements. It was decided, early on, that the deck would be modelled using plate elements, as these types of elements are most typically used for modelling deck behaviour. Only one model for beam elements was created, while three different variations of the solid element models were made: with three, four, and five through-thickness elements (as shown in Fig. 3.2). The number of elements width wise depended on the size of the girder.

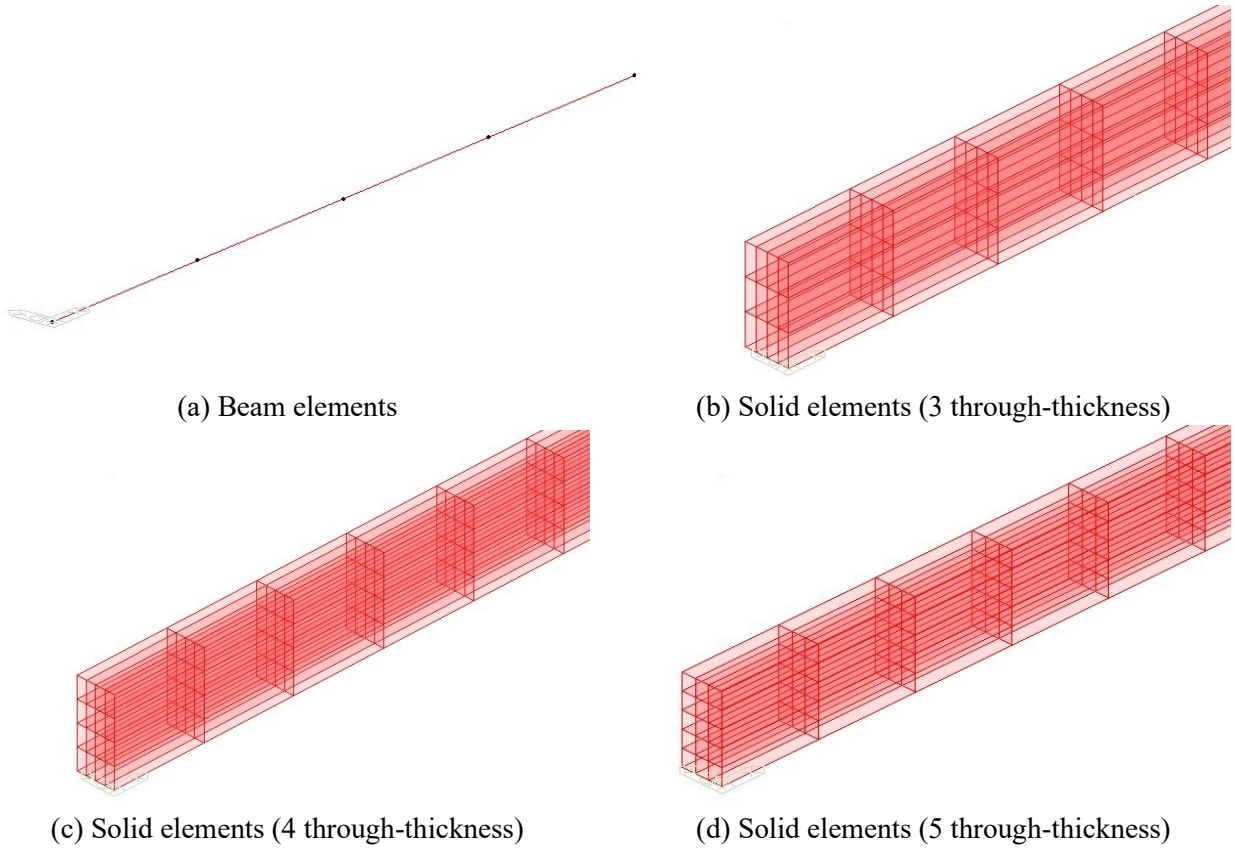

(a) Beam elements (b) Solid elements (3 through-thickness)

(c) Solid elements (4 through-thickness) (d) Solid elements (5 through-thickness)

Fig. 3.2. Different girder element models for sensitivity study

The effects on deflection and the LDFs from each of these models were compared to the results from T1 and T2. The results are shown in Fig. 3.3. It is apparent in Fig. 3.3 that, of the four different element models evaluated, the model using beam elements is a much better representation of the girder response in the two tests. The beam model is very close to the actual data from T1 and – while it is not perfect for T2 – it is the most accurate amongst the models considered. Hence, it was decided that beam elements would be used to model the girders.

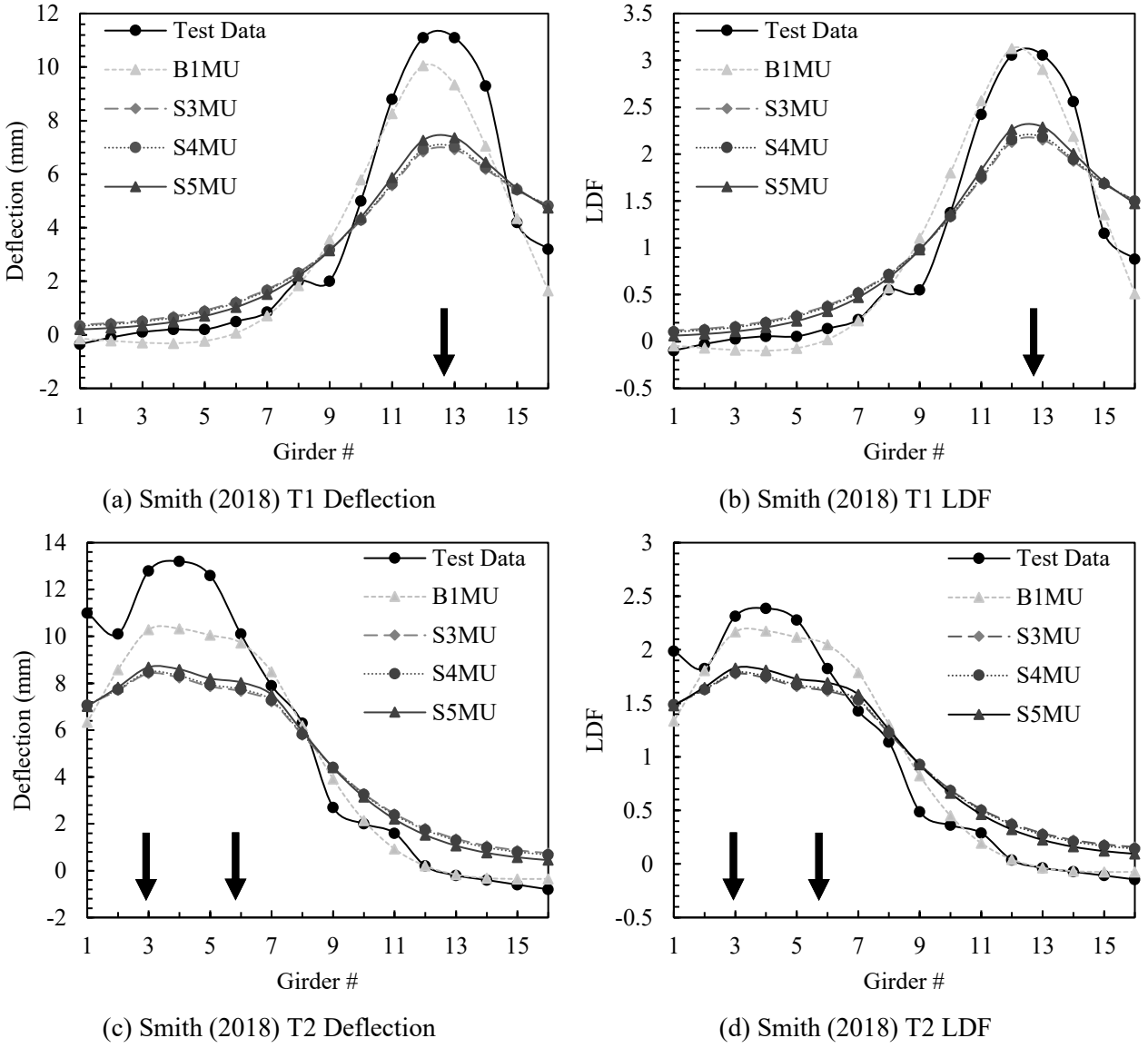

(a) Smith (2018) T1 Deflection

(b) Smith (2018) T1 LDF

(c) Smith (2018) T2 Deflection

(d) Smith (2018) T2 LDF

Fig. 3.3. Element type sensitivity study results

3.2.2.2. Girder Modulus

The other parameter examined in the initial sensitivity study was uniform vs. individual values for *E* in a bridge. As discussed, modelling timber bridges using FE methods comes with its own set of complexities due to uncertainties in material properties (due to the orthotropic nature of and no homogeneity of timber), time-dependant effects, and non-uniformity (i.e., different mechanical properties/dimensions from one girder to another within the same structure). Prior to constructing the 1/3 scale representative bridge, Smith (2018) gathered data on the individual values of *E* for each of the girders (designated as G1 - G16) used, these values were presented previously in Table 3.4.

Fig. 3.4 shows the results of using a uniform value of E across all girders, compared to using each girder's individual value of E for both deflection and LDFs. As can be seen the difference is very minor and was deemed to be negligible. Further, in the 1983 paper by Bakht, it's noted that in the analysis of a timber bridge, varying the E_L between girders has little to no effect on the LDF, and that the mean live load effects between a bridge with uniform E_L and a varying E_L correlate strongly (Bakht, 1983).

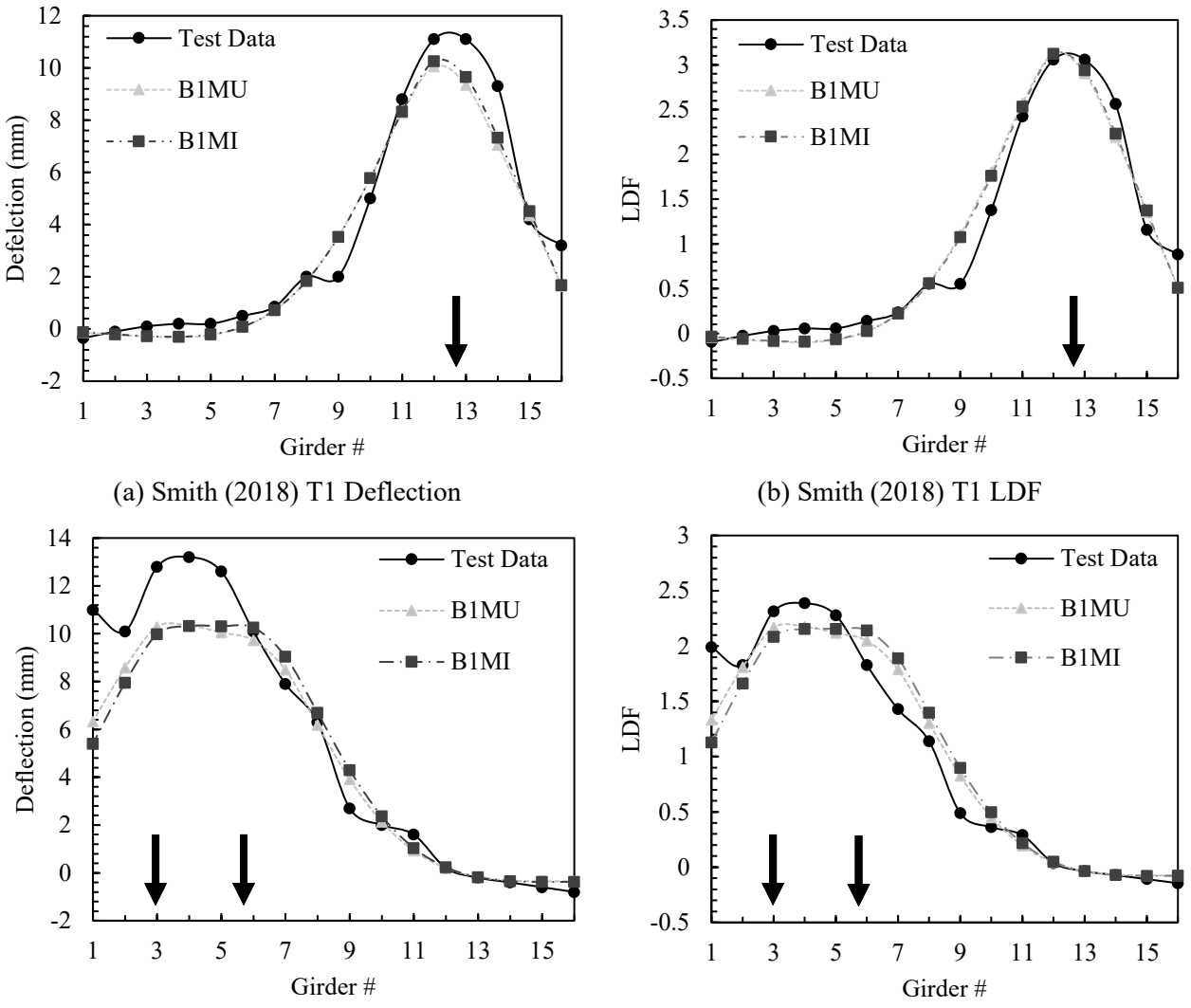

(a) Smith (2018) T1 Deflection

(b) Smith (2018) T1 LDF

(a) Smith (2018) T2 Deflection

(b) Smith (2018) T2 LDF

Fig. 3.4. Effect of using individual values for E on deflection and LDF

Once the data for the bridges tested by SHM (2021) was received, models were built assuming they were designed with the values provided by CSA S6 and CSA O86 for the E for coastal Douglas fir (11,000 MPa) (as much material for the bridges in Nova Scotia comes from British Columbia). Although, when using this value and comparing the deflection results from the FE models to the data from SHM (2021), there was a noticeable difference in deflection values, as shown in Fig. 3.5(a). While the code value for E for is 11,000 MPa, given in

CSA S6:19 Table 9.17 (CSA, 2019a), to achieve the same deflections observed by SHM (2021), the value of *E* needed to be roughly 15,000 MPa. On the other hand, when comparing the LDFs for different values of *E*, there is no difference, hence why some lines are not visible [see Fig. 3.5(b)]. This is mainly due to the fact the bridge remained (and was modelled to be) linear elastic, and hence both the individual girder and average deflection are proportional to *E*. Another reason that could explain this difference in stiffness is some amount of composite action being present, while none was considered, newer bridges may experience some degree of it.

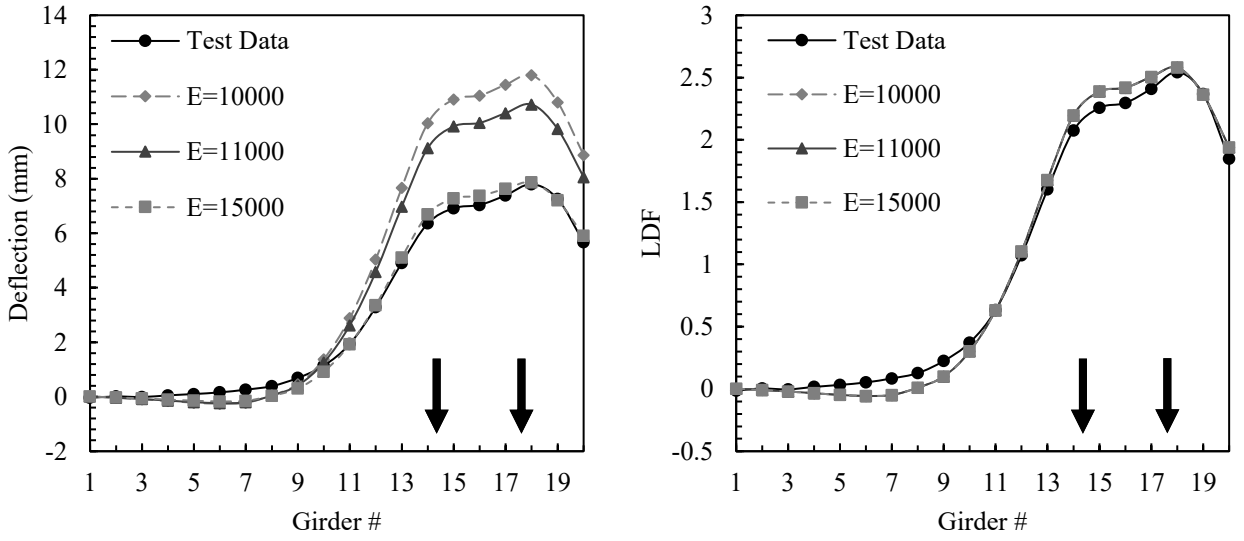

(a) SHM (2021) Deflection measurements (b) SHM (2021) LDF measurements

Fig. 3.5. Effect of changing *E* uniformly on deflection and LDF (HFX 322)

3.2.2.3. Mesh Density

Using the results from the beam-element FE models the mesh density was varied, longitudinally three different mesh densities were used; a coarse density, a medium-fine density, and a fine density, denoted by C, M, and F in the third position of the Model ID, see Fig. 3.6 for examples of each. Transversely across the deck it was decided that the density would be dependent on the girder spacing to try to keep the individual elements as close to an aspect ratio of 1.0 as possible.

Fig. 3.7 shows the effect that changing the mesh density has on the results of the FE models for both T1 and T2 from Smith (2018) as well as the two bridges, HFX061 and HFX322 from SHM (2021). While Fig. 3.7 shows relatively low sensitivity towards a changing mesh density, the increase in computation time is significant. As shown in Table 3.3, the difference in computation time between a coarse and medium mesh is relatively small compared to the increase between a medium and fine mesh, in one test this increase is nearly a factor of four, see Table 3.3 for HFX 322 between B1MU and B1FU. Based on these results, a medium-mesh (denoted M in the Model ID) was selected to continue forward with.

Note that the computation times between the lab tests by Smith (2018) and the bridges tested by SHM (2021) show a substantial increase because the former were analyzed with single-point loads whereas the bridge tests were modelled using moving loads.

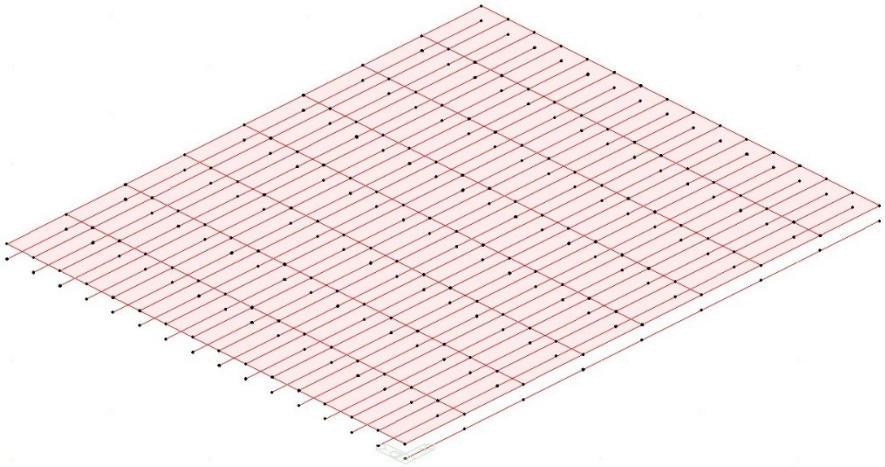

(a) Coarse mesh

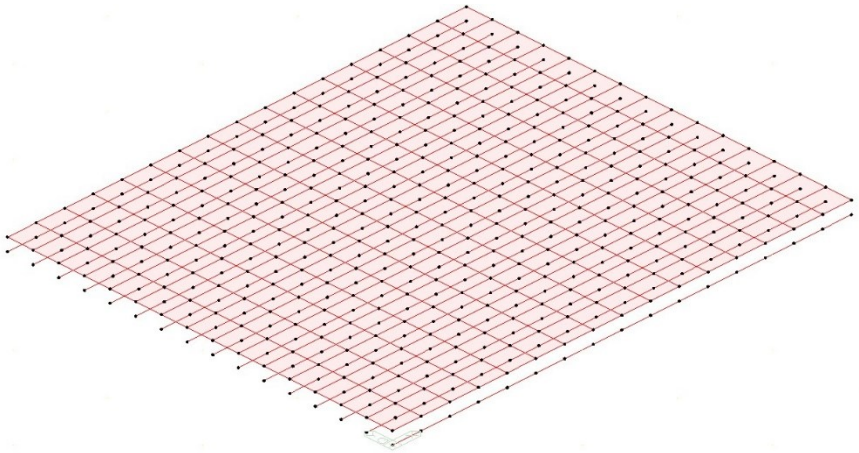

(b) Medium mesh

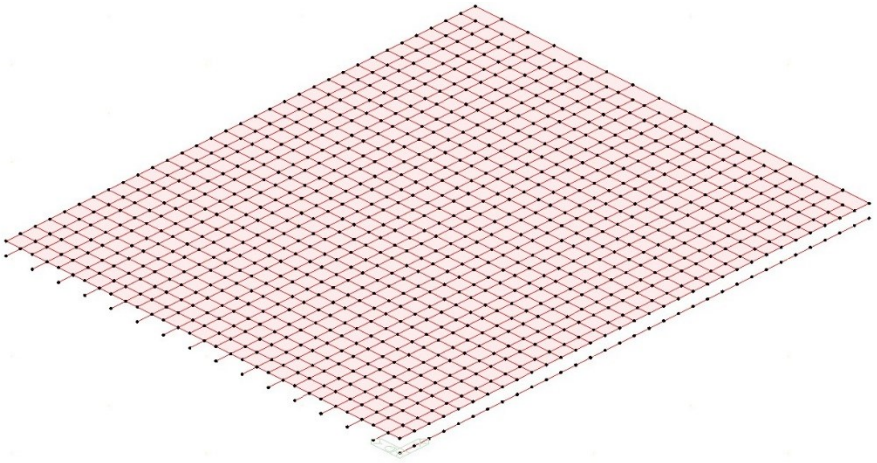

(c) Fine mesh

Fig. 3.6. Mesh sensitivity models

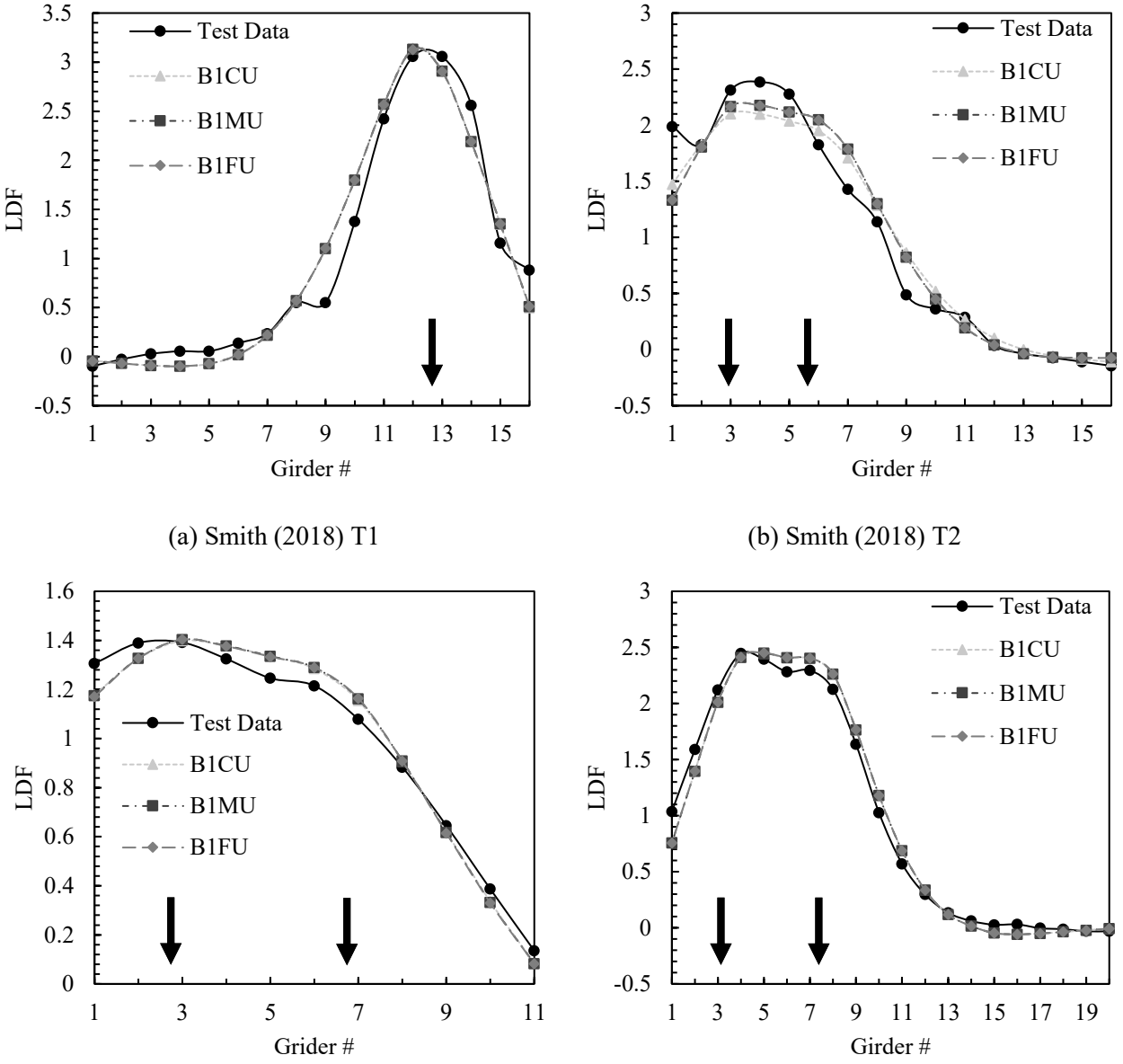

(a) Smith (2018) T1

(b) Smith (2018) T2

(c) SHM (2021) HFX061

(d) SHM (2021) HFX322

Fig. 3.7. Effect of mesh density on *LDF*

3.3. FINITE ELEMENT MODELS EVALUATED AGAINST EXPERIMENTAL RESULTS

With the sensitivity study completed, the models could be compared to the experimental results provided by Smith (2018) and SHM Canada (2021) for validation. The model was compared to ten sets of results to calibrate it efficiently: tests T1 and T2 from Smith (2018), and two bridges (note bridges, and not single tests) from SHM (2021). Fig. 3.8 presents two of the comparison plots. Additional plots are presented in Appendix A.

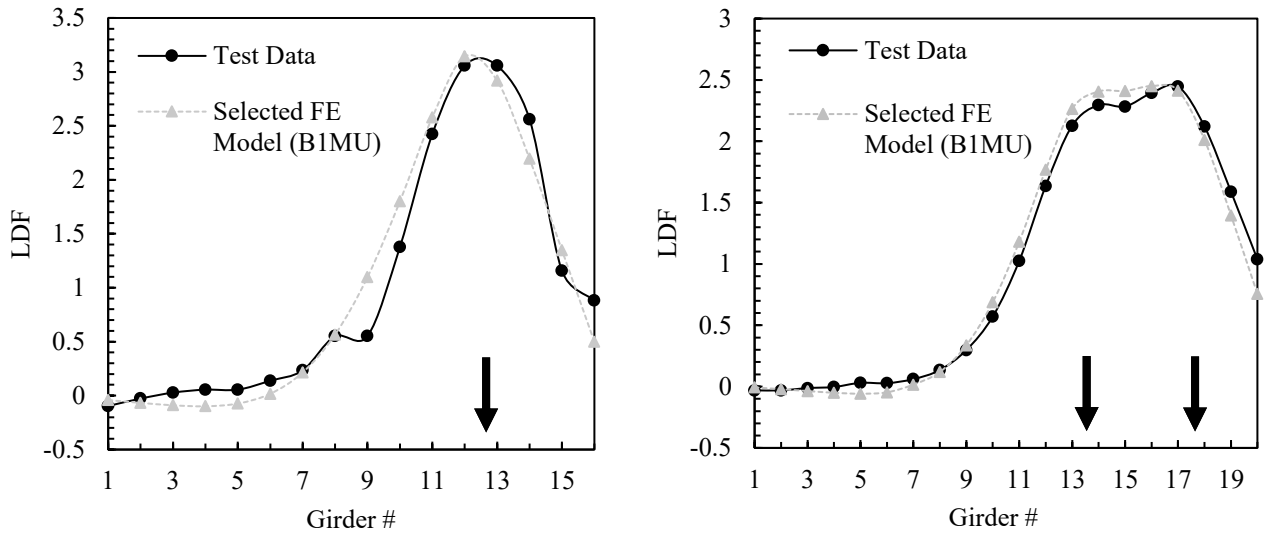

(a) Smith (2018) Test T1 (b) SHM (2021) HFX 322

Fig. 3.8. Comparison of LDFs between FE models and lab and field test data

The plots in Fig. 3.8 show that there is a good correlation between LDFs in the FE model and the experimental data provided. Table 3.5 shows values of maximum measured experimental LDF to the maximum predicted FE LDF values for all the tests considered. The bolded values in the table are the average values for the five stopping points considered based on the maximum LDF of each lane (L1, 2, 3 etc.). The FE/Measured column shows that the model generally over-predicts the LDF by a mere 3%, on average, over the 10 data sets considered.

Table 3.5. Maximum predicted LDF values

Test	Measured LDF	FE LDF	FE/Measured	COV
Smith (2018) T1	3.06	3.13	1.02	-
Smith (2018) T2	2.39	2.18	0.91	-
HFX322	**2.42**	**2.49**	**1.03**	**0.06**
L1	2.54	2.58	1.02	-
L2	2.15	2.45	1.14	-
L3	2.40	2.38	0.99	-
L4	2.45	2.45	1.00	-
L5	2.58	2.58	1.00	-
HFX061	**1.29**	**1.38**	**1.07**	**0.05**
L1	1.39	1.40	1.01	-
L2	1.22	1.33	1.10	-
L3	1.26	1.40	1.12	-
AVERAGE			**1.03**	**0.07**

3.4. SUMMARY AND RECOMMENDATIONS

FE models were constructed and compared to four LDF data sets. The completed models covered three material models, four element models, three mesh density models and multiple models to determine deck thickness trends. All results of these models were used in the course of the sensitivity study to help determine a set of model parameters that best capture the loading responses of timber bridges in the lab and field. Many different parameters were changed between each of the initial 12 model layouts, including mesh density, element types, and modulus of elasticity.

In the end, with a FE to Measured data LDF ratio of 1.03 over ten unique sets of data, a model was picked to continue forward with for the parametric study. The Model (given the ID B1MU) consisted of:

- Simply supported girders, modelled with Timoshenko beam elements
- A deck modelled using plate elements, keeping the aspect ratio close to unity
- Deck to girder connections done with rigid links, neglecting composite action
- Deck thickness of 95 mm
- Medium-fine mesh, roughly every 250 mm
- Using isotropic material properties, from CSA S6

The simply supported girders allow rotation but no deflection at the supports, if deflection at the supports is required it can be done through rigid links with stiffness set appropriately. The plate elements allow for in and out of plane responses and allows the deck to behave similarly to a real-world bridge deck. Using general links with a stiffness set very, very large in the Z-direction (direction of gravity) ensures the deck and girders displace the same amount. Also, using general links as opposed to springs allows for the incorporation of composite action, if it is present. Using a deck thickness of 95mm allows the model to transfer an appropriate amount of loading to adjacent elements while being on par with the typical deck thickness of timber bridges in

Nova Scotia. By using a medium mesh (i.e., divisions every 250 mm), the model can capture the deflection with good accuracy, while not taking a significant time to run. Furthermore, using simple isotropic properties (as opposed to orthotropic properties) can approximate the LDF with high accuracy. It is generally recommended that the *E* values found in CSA S6 be used; however, as shown in Fig. 3.5, these values may not be strictly accurate if predicting the LDF is not the desired outcome.

Chapter 4: PARAMETRIC STUDY OF LOAD DISTRIBUTION IN TIMBER BRIDGES

4.1. SCOPE

Using the validated model (Model ID: B1MU) developed in Chapter 3, a parametric study was undertaken to broaden the database of bridges used in this research. The parametric study comprised of 204 hypothetical bridges, with parameters based on the Nova Scotia timber bridge inventory analyzed by Smith (2018). The ranges of parameters included in the study are shown in Table 4.1. A full list of the 204 bridges analyzed (and their parameters) is given in Appendix B.

Table 4.1. Parameters and ranges included in parametric study

Parameter	Range
Span	$4\text{ m} \leq L \leq 13\text{ m}$
Bridge Width	$4\text{ m} \leq W_b \leq 11\text{ m}$
Girder Spacing	$350\text{ mm} \leq S \leq 650\text{ mm}$
Girder width	$4\text{ m} \leq b_g \leq 13\text{ m}$
Girder depth	$4\text{ m} \leq t_g \leq 13\text{ m}$
Number of Girders	$6 \leq N \leq 21$
Number of lanes	$1 \leq n \leq 2$

4.2. GENERAL ANALYSIS METHOD FOR NUMERICAL FE PARAMETRIC STUDY

With the bridge geometry modelled, appropriate design live loads could be applied. Moreover, the only loads considered herein for the evaluation of SMAs were the live loads. Dynamic load effects were ignored (because the analysis was being done statically). The loading considered the CL-W loading defined in CSA S6:19 Clause 3.8.3.1, which consists of using both CL-W truck and lane loading (outlined in Clauses 3.8.3.1.2 and 3.8.3.1.3 respectively). Clause 3.8.3.1.1 in CSA S6:19 states that "a loading of not less than CL-625 shall be used for the design of a national highway network that is generally used for interprovincial transportation.". While most timber bridges are not part of a national highway network, the CL-625 truck/lane loadings were used and are shown in Fig. 4.1 (recreated from CSA S6:19).

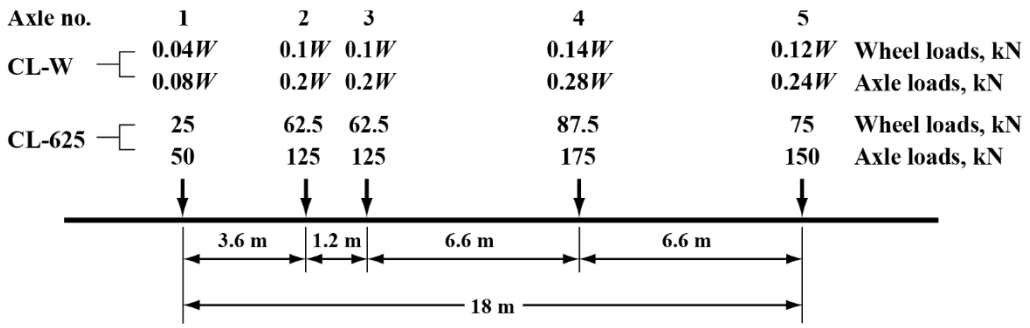

a) CL-W truck loading

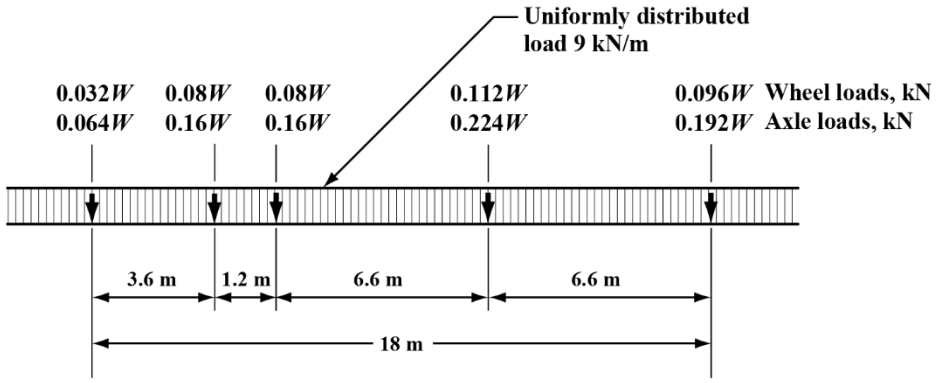

b) CL-W lane loading

Fig. 4.1. CSA S6:19 loading (CSA 2019a)

The CL-W Truck loading is an idealized five-axle truck with wheel spacing and weight distribution(s) as shown in Fig. 4.1(a). For analysis using the SMA, the truck is placed such that the "worst-case" scenario, or largest moment effect, is achieved. The CL-W lane loading uses the same CL-W truck, with each axle load reduced to 80% of the original load, superimposed with a uniformly distributed load of 9 kN/m at 3 m wide (i.e. 27kPa over a 3 m wide lane that runs the length of the bridge) (CSA, 2019a) as shown in Fig. 4.1(b). Again, for the lane loading, the truck is placed to create a "worst-case" scenario.

As mentioned in Section 4.1, the finite element (FE) parametric study, conducted herein, covers a wide range of parameters, including bridge width, W_b. Bridge width (W_b) is related to deck/roadway width (W_c) (a parameter that is more often used in bridge analysis and evaluation) defined in Eq .4.1, as well as vehicle edge distance (VED)(D_{VE}) which is defined as the distance from the centerline of the wheel load to the edge of the bridge, D_{VE} includes the width of any curbs and/or barriers on the bridge structure (D_C), and part of the clearance envelope (CE) of the truck

$$W_c = W_b - \left(2D_C\right) \tag{4.1}$$

Deck width (W_c) is defined in CSA S6:19 Section 13.3 (CSA 2019a) as being "the horizontal distance measured perpendicular to the direction of travel from face to face of the curbs or barrier walls". For the current study, a curb/barrier wall width of 0.3m has been assumed on each side of the bridge to calculate W_c (see Eq. (4.2) and Eq. (4.3))[and, hence, to determine n (the number of design lanes), in accordance with CSA S6:19 Table 3.5, W_e (the width of each design lane) = W_c/n (Eq. 4.4)]. The curb width may be wider although larger load effects are observed when the truck is located closer to an edge where the load is distributed to fewer girders.

$$W_c = W_b - 2(0.3) \tag{4.2}$$

$$W_c = W_b - 0.6 \tag{4.3}$$

For live-load analysis using the CL-W truck, the distance from the curb/barrier face to the centerline of either wheelset was taken as not less than 0.6m following the clearance envelope described by CSA S6:19 Figure 3.2 (which is recreated in Fig 4.2, below). Hence, by summing these two values (curb/barrier wall width + clearance to curb, from wheel centerline), the assumed vehicle edge distance in the analysis, D_{VE} = 0.9m, can be determined. Thus, the results of this study are applicable to timber-girder bridges with curb/barrier wall widths ≤ 0.3m.

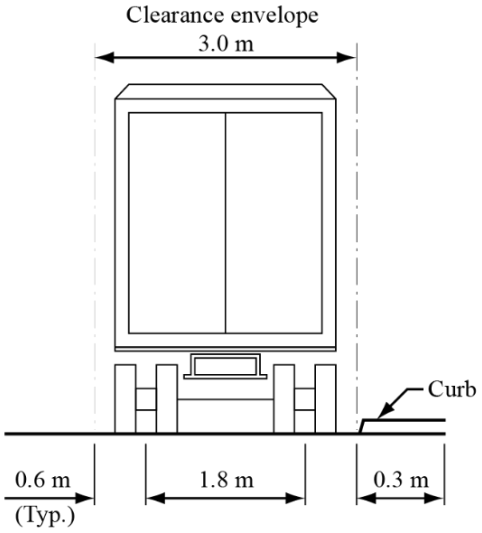

Fig. 4.2. Design truck clearance envelope

The deck width (W_c) is also directly related to the number of design lanes, n, based on Table 4.2 (which is reproduced from CSA S6:19).

Table 4.2. Number of design lanes by deck width

Deck Width, W_c, m	n
6.0 or less	1
6.0 to 10.0	2
10.0 to 13.5	2 or 3*
⋮	⋮

* Only two bridges considered within the range of parameters given in Table 4.1 fit into the three-design-lane category; hence, three-lane loading was excluded from the study.

From the table above, and the deck width (W_c), the lane width W_e can be determined as:

$$W_e = \frac{W_c}{n} \tag{4.4}$$

All bridges were modelled with a single design lane, initially, with the lane spanning the entire width of the deck, allowing the design truck to travel anywhere within the lane. Subsequently, all bridges that met the width requirement for two lanes ($W_c \geq 6.0$ m) were modelled as such. This was done to ensure that all possible lane configurations would be captured in the analysis because, while a bridge may have multiple lanes, the critical case could be either when only a single lane, both, or all lanes are loaded.

For the one-lane load case, the allowable lane width (W_e) was set to the width of the deck (W_c), calculated using Eq. (4.1) but replacing D_C with D_{VE} as MIDAS Civil does not account for a CE for one lane loading and assumes the truck is only 1.8 meters wide (width of the axles). Hence, for one lane loaded bridges W_e was defined as

$$W_e = W_b - \left(2D_{VE}\right) \tag{4.5}$$

The program would place the truck at either edge of the allowable lane width, as well as in the middle, travelling in both directions, to determine where the worst possible location for the design truck existed.

For the two-lane load case, a similar process was used – with some additional parameters needing to be defined. W_c is used here again [Eq. (4.1)], but additionally a "margin", (the distance from the centerline of the wheel load to the edge of the CE), needed to be defined for Multi lane loading in MIDAS Civil, this was set to 0.6m as per CSA S6:19. The lane width was set to a minimum of 3.3m, equal to the clearance envelope of the design truck. The program would move the lanes within the bridge, and the trucks within the lanes, checking all possible locations of truck positions travelling in both directions, keeping the Trucks a minimum of two times the margin apart (per code requirements), to determine the worst location for them to be positioned.

Once all the bridges were modelled, they could be analyzed. MIDAS moves the CL-W truck/CL-W lane loading, and the lanes automatically to generate an influence surface to determine where the CL-W loading needs to be placed to generate the maximum girder moment. Once the analysis was complete the models were each individually checked to ensure the results were as expected, and no anomalies were present. Subsequently a single beam model of the each of the different lengths of bridge was analyzed in the same way, MIDAS moves the CL-W loading along the beam assuming the wheel loads are superimposed on top of each other to

find the location that generates the maximum girder moment. With the results from both the bridge models and the single beam models the truck load fraction (F_T) was calculated by taking the largest girder moment from the bridge model and dividing it by the maximum moment from the single beam model.

Appendix B gives the values for F_T calculated in this manner, as well as in a manner using deflections (where F_T = maximum girder deflection from the bridge model/total deflection of the single beam model). While the former approach (the so-called "moment truck fraction") is technically the correct way to determine F_T, the so-called "deflection truck fraction" is often used in bridge load testing, since deflections can be directly measured/recorded in the field. A comparison of the data in Appendix B shows that while the latter approach is less accurate, it may still – in most cases - be sufficient.

Herein, the "FE moment truck fraction" (F_T) results were taken as the "actual"/true values (F_{Ta}), and the values determined by the different code versions of the SMA (CSA S6-06 and CSA S6:19) are called the "predicted" F_T values (F_{Tp}). These values are compared across all 204 bridges analyzed in Fig. 4.3, where values above the diagonal line are under-predictions (i.e., unconservative) and values below the diagonal line are over-predictions (i.e., over-conservative). Values laying on or near the diagonal line are more accurate than values away from it. Fig. 4.3 shows, in general, that CSA S6-06 is much better at predicting the actual (F_{Ta}) values, and CSA S6:19 is – in most cases – over-conservative. This generalized finding is elaborated upon in Section 5.

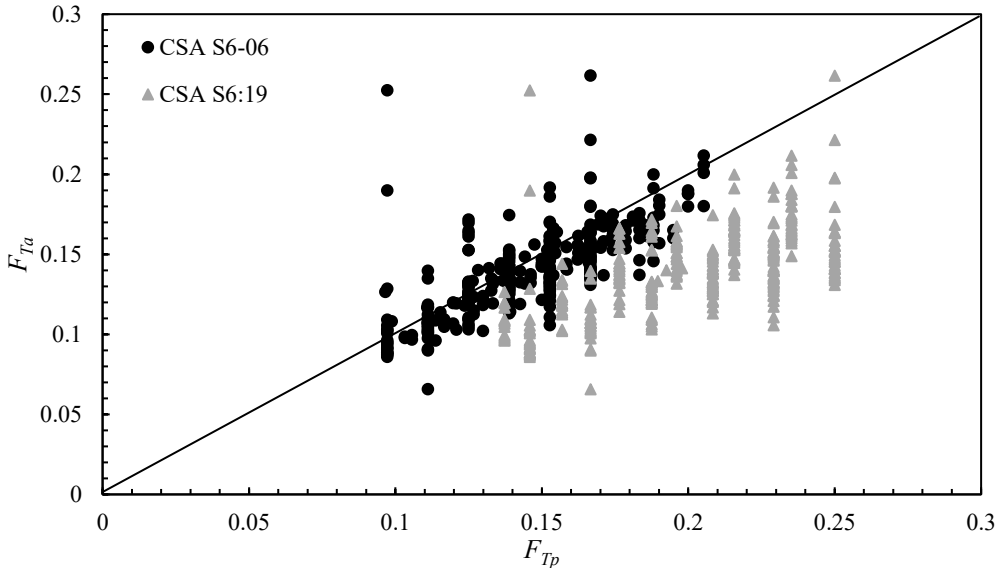

Fig. 4.3. Comparisons of actual and predicted truck fractions using CSA S6-06 and CSA S6:19

Chapter 5: EVALUATION OF SMAS

5.1. SCOPE

This Chapter looks deeper at the results presented in Fig. 4.3 by considering the effect of various parameters on the ratio of the actual-to-predicted truck fraction (F_{Ta}/F_{Tp}). The parameters considered are: span (L), girder spacing (S), and girder depth (t_g). In the figures that follow, values less than one are over-conservative (i.e., the SMA overpredicts the design moment) and values greater than one are unconservative (i.e., the SMA underpredicts the design moment).

5.2. EFFECT OF SPAN

As discussed in Chapter 2, the 2006 version of CSA S6 is very similar to the 2000 version, and both take the span length (L) into account when using the SMA. While Table 2.2 only provides equations for F (akin to F_T for the 2019 version of the code), when 3 m < L < 10 m, longer bridges were analyzed in the current study, for those bridges, F was determined using the same equation as those for L< 10m. A plot of F_{Ta}/F_{Tp} vs. L for all bridges analyzed (according to CSA S6-06) is shown in Fig. 5.1(a). While a few outliers are present, it can be seen that the majority of the F_{Ta}/F_{Tp} ratios are close to unity – for both one- and two-lane bridges.

As also discussed in Chapter 2, CSA S6:19 is very similar to CSA S6-14, and it does not take into account the span length when calculating F_T [as mentioned in Section 2.2.2.7, it also provides a single value for F_T, independent of the number of lanes on the bridge] (see Table 2.3). A plot of F_{Ta}/F_{Tp} vs. L for all bridges analyzed (according to CSA S6:19) is shown in Fig. 5.1(b). It is apparent from Fig. 5.1(b) that F_{Ta}/F_{Tp} ratios are less than those obtained using CSA S6-06 across the entire range of spans considered. Furthermore, it appears that CSA S6:19 is less accurate for the prediction of F_T for one-lane bridges than two-lane bridges.

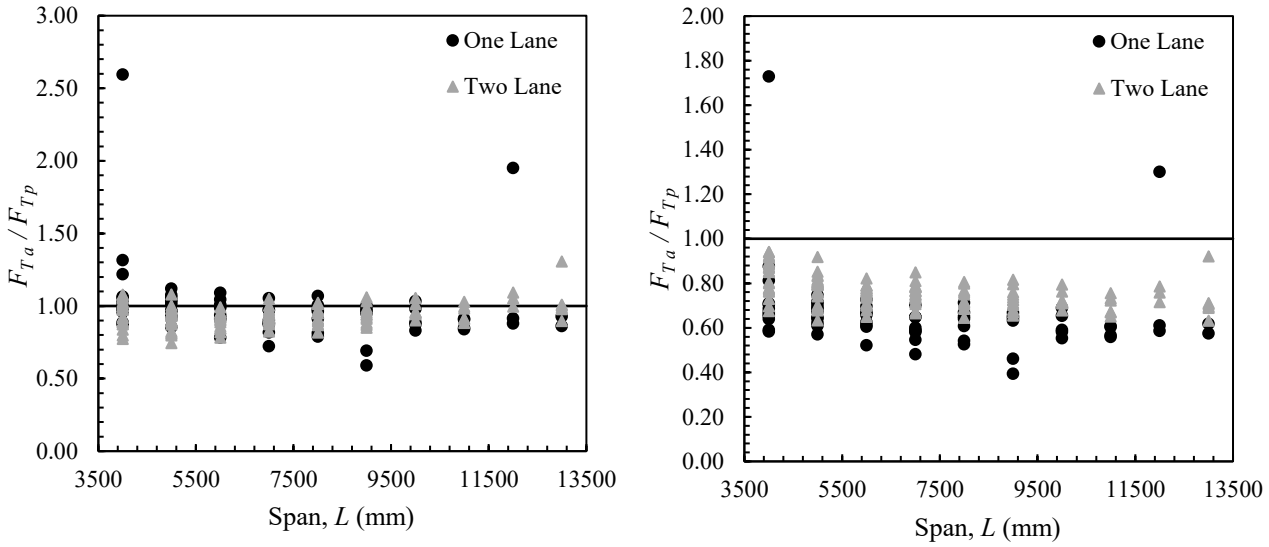

(a) CSA S6-06 (b) CSA S6:19

Fig. 5.1. Plots of F_{Ta}/F_{Tp} vs. span

5.3. EFFECT OF GIRDER SPACING

Figs. 5.2(a) and 5.2(b) show plots of F_{Ta}/F_{Tp} vs. girder spacing (S) for all bridges analyzed according to CSA S6-06 and CSA S6:19, respectively. Similar to above, the SMA in CSA S6-06 is much more accurate than CSA S6:19 at predicting the actual load fraction(s) over a wide range of S. It is also evident, again, that CSA S6:19 is less accurate for the prediction of F_T for one-lane bridges than two-lane bridges.

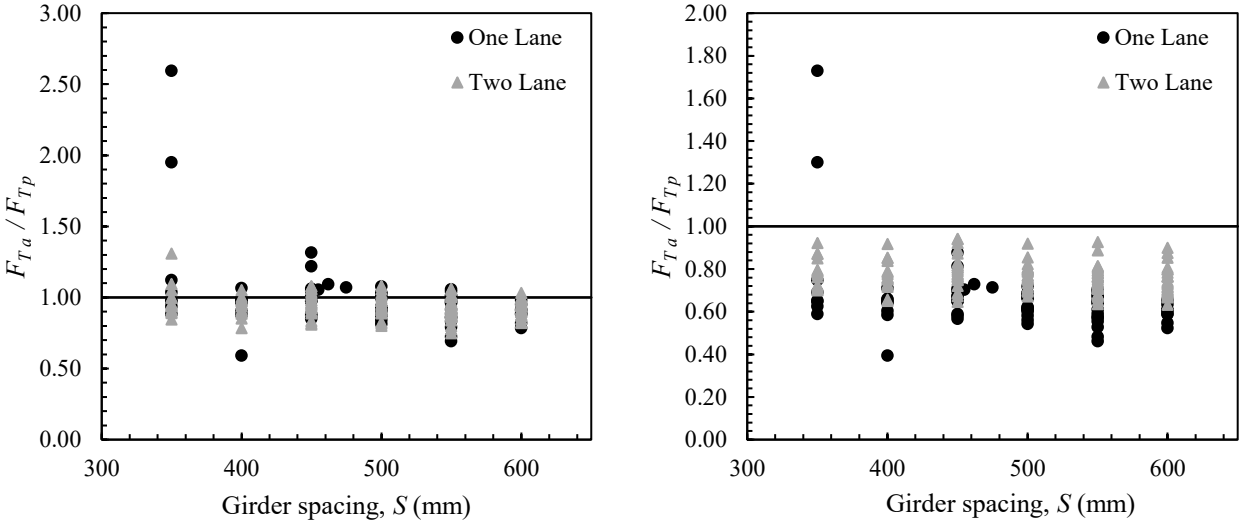

(a) CSA S6-06 (b) CSA S6:19

Fig. 5.2. Plots of F_{Ta}/F_{Tp} vs. girder spacing

5.4. EFFECT OF GIRDER DEPTH

A relatively vague trend can be seen when comparing F_{Ta}/F_{Tp} to the depth of the girder (t_g) in Figs. 5.3(a) and 5.3(b). As t_g increases, the predictions of both SMAs (CSA S6-06 and CSA S6:19) generally improve. While the predictions of CSA S6-06 are quite accurate to begin with, as the girder gets deeper, the ratio F_{Ta}/F_{Tp} trends closer to unity. Although CSA S6:19 does not adequately predict the load fraction, in general, as t_g increases, the predictions improve. Nonetheless, it is clear that CSA S6:19 grossly over-predicts F_T for both one and two-lane brides.

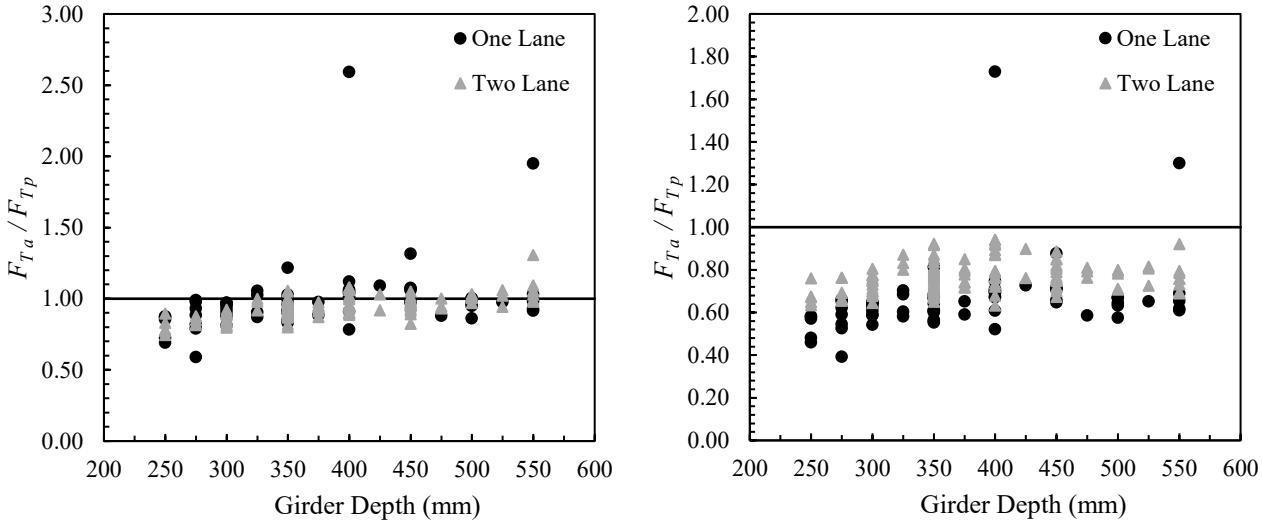

(a) CSA S6-06 (b) CSA S6:19

Fig. 5.3. Plots of F_{Ta}/F_{Tp} vs. girder depth

5.5. INHERENT BIAS FACTORS, COVS, AND SUMMARY

From the above data [i.e., the ratios of actual (FE) (F_{Ta}) to code-predicted (F_{Tp}) truck fractions for all 204 bridges considered], bias coefficients (δ) and COVs (V) were calculated for the various SMAs, for both one- and two-lane bridges, as well as all bridges considered together. The bias coefficient δ is simply taken as the mean of the F_{Ta}/F_{Tp} value(s) across the bridges considered, and the COV is determined using Eq. 5.1:

$$V = \frac{\sqrt{\dfrac{\sum_{i=1}^{j}(x_i - \delta)^2}{j-1}}}{\delta} \tag{5.1}$$

where x_i is the value of the F_{Ta}/F_{Tp} for bridge i; and j is the total number of bridges analyzed. The results are summarized, for CSA S6-06 and CSA S6:19, in Table 5.1.

Table 5.1. SMA evaluation results

Bridge Type	Variable	CSA S6-06	CSA S6:19
One-lane	δ	0.98	0.66
	V	0.19	0.19
Two-lane	δ	0.94	0.76
	V	0.08	0.12
Combined	δ	0.97	0.70
	V	0.16	0.17

Table 5.1 further validates the concerns that the current version of the SMA (CSA S6:19) vastly over-predicts the maximum anticipated girder moment (M_L). As evidenced by the combined bias factor (δ = 0.70) the magnitude of the over-prediction is 30%, on average. Note that the current values given for use in the SMA for δ and V are 0.93 and 0.12 respectively, and as mentioned in Section 2.4, so while some over-prediction is expected, as a trade-off for simplicity, CSA S6:19 is actually quite over-conservative. Table 5.1 shows that CSA S6-06 was, in fact, a far better predictor of M_L.

In summary, the SMA in CSA S6:19 often overpredicts the truck load fraction. The magnitude of this over-prediction is generally greater for one-lane bridges than it is for two-lane, and for bridges with shallower girders (lower t_g values). This, in turn, can lead to overdesign, or false recommendations for repair/retrofit, when the SMA is used for assessment.

Chapter 6: EXPERIMENTAL TESTING OF TIMBER GIRDERS

6.1. INTRODUCTION AND EXPERIMENTAL PROGRAM OVERVIEW

One of the knowledge gaps identified in Chapter 2 was concerned with having accurate input parameters for the strength and apparent modulus of elasticity (E_{app}) of in-situ timber girders. Hence, an experimental program was designed to ascertain these parameters based on the testing of timber girders supplied by Nova Scotia Public Works (NSPW). Testing entailed four-point bending, with loading to failure, and the collection of deflection data (at mid-span and under the load points, as well as at the supports) to determine E_{app}.

6.2. EXPERIMENTAL SPECIMEN DESCRIPTION

The test specimens were sampled from a large group of decommissioned timber girders at one of NSPW's yards (Fig. 6.1). The test specimens were initially selected to be 8 to 10 metres long, with a nominal cross-section of 450mm x 225mm. Prior to delivery, the specimens were cut to just over 6 metres in length, to facilitate easier transportation, storage, and disposal. Eight test specimens were selected, with the criteria being that there was no major damage or rotting of the timber.

Fig. 6.1. Decommissioned timber girders

6.3. Experimental Specimen Geometric Properties and Moisture Content

6.3.1. Geometric Properties

After delivery and prior to testing, each of the eight specimens was measured to collect their actual geometric properties for use in the calculation of their theoretical strengths, and Young's moduli, as outlined in Sections 6.5 and 6.6. Cross-sectional measurements were taken at five points along the length of each girder, one at each end, one at mid-span, and one under each load point (third points). These measurements were then averaged to determine the "actual dimensions" of the specimen. Table 6.1 shows each measurement and the final actual cross-sectional dimensions of each girder, where t_g is the depth of the girder and b_g is the width.

Table 6.1. Test specimen geometric properties

Girder #	East End		Load point 1		Midspan		Load point 2		West End		Average	
	t_g (mm)	b_g (mm)	t_g (mm)	b_g (mm)	t_g (mm)	b_g (mm)	t_g (mm)	b_g (mm)	t_g (mm)	b_g (mm)	t_g (mm)	b_g (mm)
1	444	232	450	230	452	230	448	230	452	232	449	231
2	470	246	450	228	448	226	452	228	456	230	455	232
3	450	230	446	230	448	228	444	228	440	235	446	230
4	458	238	454	232	456	232	458	234	456	230	456	233
5	442	232	440	234	446	230	442	230	454	234	445	232
6	450	228	456	230	454	232	450	228	448	226	452	229
7	462	204	468	204	462	192	460	196	460	194	462	198
8	456	234	458	230	460	228	452	226	452	236	456	231

In addition to cross-sectional measurements, measurements were taken along the length of each specimen to define the over-hang, span length (l), Shear span (shear-free span length), and the distance to load points (1 and 2) from each support. The span length, l (see Fig. 6.2, on the following page), was nominally set to six metres, with 250 mm of over-hang from the centre of the supports. Using third-point loading, the shear-free span length was nominally two metres. Table 6.2 shows the actual measurements of these dimensions for each specimen.

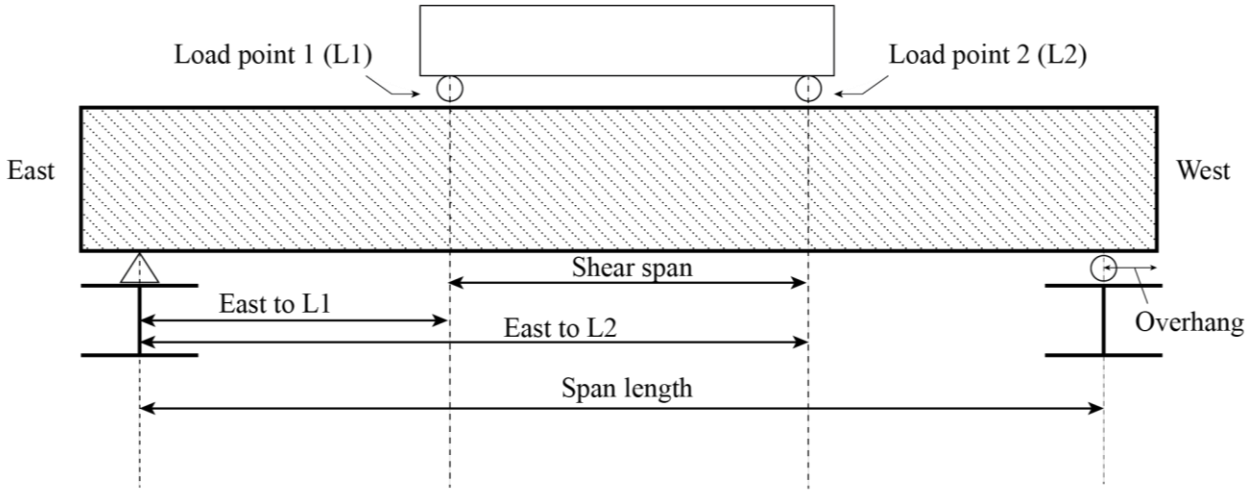

Fig. 6.2. Testing measurement definitions

Table 6.2. Measured geometric properties of test specimens

Girder #	Overhang		span length (l) (mm)	Shear span length (mm)	East to L1 (a) (mm)	East to L2 (mm)
	East end (mm)	West end (mm)				
1	215	260	6001	2005	1998	4003
2	260	285	6005	2015	1995	4010
3	280	265	5990	1995	2030	4025
4	235	210	6051	1996	2050	4046
5	225	250	5985	2005	1985	3990
6	180	260	6100	2000	2050	4050
7	260	280	5999	1997	2003	4000
8	265	250	5995	2005	1995	4000

6.3.2. MOISTURE CONTENT

ASTM D198 stipulates that if moisture content cannot be measured as per the procedures outlined in ASTM D4442 "*Test Methods for Direct Moisture Content Measurement of Wood and Wood-Based Materials*" (ASTM International, 2021) (ASTM International, 2020) then it can be measured using a calibrated moisture meter in accordance with ASTM D7438 "*Standard Practice for Field Calibration and Application of Hand-Held Moisture Meters*" (ASTM International , 2020). In this study, a Tavool Digital Pin Type Moisture Metre was employed in accordance with ASTM D7438 (ASTM International , 2020). The moisture meter was calibrated based on the manufacturer's instructions prior to each use.

While some preservatives can affect the readings of the moisture meters, creosote appears to have insignificant effects (James, 1965). Care was taken to take moisture measurements at least 500mm from the end, in the center of the face, away from knots and with the pins parallel to the wood grain as stated in ASTM D7438 (ASTM International , 2020). Five measurements were taken along the length of each specimen, in similar locations to those used in measuring the actual geometric properties, near the ends (but at least 500mm form them), at the load points and mid-span (where the failure occurred). the measurements were then averaged to determine a moisture content for the specimen. The moisture content readings are used to determine a service condition factor used in the calculation of bending resistance [i.e., the specimen can be in one of two service conditions: "dry" or "wet". "Dry" service conditions are when the average moisture content is less than 19%, and "wet" service conditions are all other conditions as per CSA O86-19 Clause 2.1 (CSA, 2019)]. The specimens and their moisture content readings are given in Table 6.2. As seen therein, all specimens were tested under "dry" service conditions.

Table 6.3. Test specimen moisture content readings

Girder #	Ambient temp. (°C)	East End	Load point 1	Mid span	Load point 2	west end	Average
1	21.7	13.50%	12.30%	14.40%	13.90%	14.60%	13.74%
2	21.4	16.80%	14.30%	13.90%	14.70%	14.50%	14.84%
3	21.5	15.90%	13.60%	14.30%	14.50%	13.10%	14.28%
4	22.1	16.00%	16.40%	17.80%	17.40%	13.40%	16.20%
5	21.5	13.90%	14.80%	15.20%	15.40%	17.20%	15.30%
6	21.9	13.00%	13.40%	13.60%	12.40%	14.40%	13.36%
7	21.2	16.00%	16.90%	14.50%	17.20%	17.80%	16.48%
8	21.3	15.70%	19.10%	16.00%	17.20%	21.20%	17.84%

6.4. INSTRUMENTATION AND TESTING PROCEDURE

Instrumentation and testing were completed in accordance with ASTM D198-21a *Standard Test Methods of Static Tests of Lumber in Structural Sizes* (ASTM International, 2021). The specimens were lifted into place using a crane and positioned on metal bearing plates to prevent damage to the specimens. The bearing plates had a width greater than the specimen width, to ensure during loading and rotation of the specimen, that uniform bearing was maintained across the entire width of the specimen. The bearing plates were fitted on rigid beams securely fastened to the floor of the heavy structures lab to limit support movement; the support set up is shown in Fig. 6.3.

Fig. 6.3. LVDT at support

Third points were marked along the length of the beam as the loading locations and sensor locations. Three string pots were connected to the specimen using small screw-in eye hooks as connection points at the third points and mid-span and attached to the lab floor using magnets. Support settlement was collected at the mid point of the rollers using linear variable displacement transducers (LVDT). The instrumentation set up is shown in Fig.6.3 and 6.4. The specimens were loaded using a 1MN MTS servo-hydraulic controlled actuator which loaded a two-metre-long spreader beam, transferring the load from the actuator to the load points equally. Loading was done at a rate of 11mm/min to achieve testing times of at least four mins (per ASTM D198-21a) and the specimens were loaded until failure as specified by ASTM D198, the deflection and load data was recorded at a sampling rate of 1 Hz.

Fig. 6.4. Testing set up

6.5. NOMINAL BENDING STRENGTH CALCULATIONS

To determine the bending strength of timber, many factors need to be considered. The equation for the moment resistance of a timber girder/beam is presented below, Eq. (6.1) (and can also be found in Clause 6.5.3.1 of CSA O86:19 *Engineering Design in Wood,* as well as Clause 9.6.1 of CSA S6:19):

$$M_r = \phi F_b S K_L K_{Zb} \tag{6.1}$$

where ϕ is the resistance factor for timber (taken as 1.0 to compute nominal bending strength, M_n); S is the section modulus of the girder, defined in Eq. (6.2) for rectangular sections; F_b is the factored strength in bending as defined in Eq. (6.3); K_L is the lateral stability factor, taken as 1.0, in this study, per Clause 6.5.3.2 of CSA O86:19; and K_{Zb} is the size factor in bending, taken as 1.0, in this study, from Table 6.13 in CSA O86:19.

$$S = \frac{b_g t_g^2}{6} \tag{6.2}$$

where b_g is the width of the girder; and t_g is the height or depth of the girder, and:

$$F_b = f_{bb}(K_D K_H K_{Sb} K_T) \tag{6.3}$$

where f_{bb} is the specified strength in bending given in Table 14.9 of CSA S6:19 for beam and stringer (same as girder) grades of timber, taken as 20 MPa (assuming No.1 Douglas Fir-Larch); K_D is the load duration factor, taken as 1.0 from Table 5.1 in CSA O86:19 (or Clause 9.5.3 in CSA S6:19) for standard term loading; K_H is

the system factor, which is generally retrieved from Table 6.12 in CSA O86:19 (see discussion below); K_{Sb} is the service condition factor for bending at the extreme fibre under dry service conditions taken as 1.0 as per Table 6.10 of CSA O86:19 (or Table 9.2 of CSA S6:19); K_T is the treatment factor of preservative-treated lumber in a dry service condition, taken as 1.0 from Table 6.11 in CSA O86:19 (or Table 9.6 in CSA S6:19).

For calculating the resistance of timber in a system, such as a bridge, K_H is replaced with K_m, the load sharing factor, which is taken from Table 9.4 in CSA S6:19. Since only a single girder was being tested herein, $K_H = K_m = 1.0$.

Using all the above-mentioned equations and modification factors, as well as the actual (measured dimensions), the theoretical nominal bending resistances (M_n) were calculated for all eight specimens. The results are summarized in Table 6.4.

Table 6.4. Test specimen section modulus and theoretical bending strength

Girder #	S (mm^3)	M_n (kN-m)	Girder #	S (mm^3)	M_n (kN-m)
1	7.76 x 10^6	171	5	7.65 x 10^6	168
2	7.99 x 10^6	176	6	7.77 x 10^6	171
3	7.61 x 10^6	168	7	7.05 x 10^6	155
4	8.09 x 10^6	178	8	7.98 x 10^6	176

6.6. EXPERIMENTAL RESULTS

Testing was performed as described in Section 6.4, and the results were analyzed to determine the actual moment resistance (M_a) and E_{app} of the eight timber girders. For the determination of M_a, failure was considered the first major "drop" in load, as depicted in the total load vs. mid-span deflection plots in Fig. 6.5 where failure is defined at the end of each line. Note that the girders in the plots are in no particular order (they were placed to allow easy viewing of each of the plots). As shown therein, the girders generally exhibited linear elastic behaviour until shortly before failure.

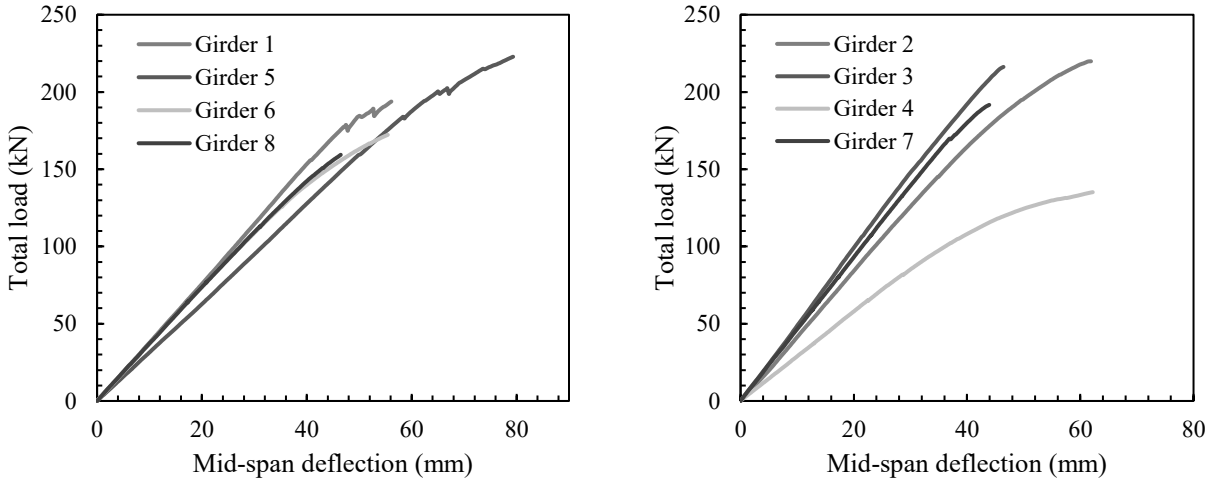

(a) Girders 1, 5, 6, 8 (b) Girders 2, 3, 4, 7

Fig. 6.5. Total load vs. mid-span deflection plots for experimental tests

Based on the results, three values were calculated for each of the eight specimens: the actual moment resistance (M_a), the modulus of rupture (S_R) (also known as the bending strength parallel to the grain, F_b), and the apparent modulus of elasticity (E_{app}).

M_a was calculated using the following beam equation for four-point loading:

$$M_a = \frac{P_{\max} a}{2} \tag{6.4}$$

where P_{max} is the maximum load borne by the specimen, loaded to failure, in kN; and a is the distance from reaction to nearest load point in mm, see Table 6.2.

To help verify these results, S_R was calculated as follows, from Table X2.1 of ASTM D198-21a (ASTM International, 2021):

$$S_R = \frac{3P_{\max} a}{b_g t_g^{\,2}} \tag{6.5}$$

where a and P_{max} are defined above; b_g is the width of the flexural specimen; and t_g is the depth of the flexural specimen.

The apparent modulus of elasticity (E_{app}) for each of the eight test girders was calculated using the equation given below, from Table X2.1 of ASTM D198-21a (ASTM International, 2021).

$$E_{app} = \frac{Pa}{4 b_g t_g^{\,3} \Delta}(3l^2 - 4a^2) \tag{6.6}$$

where P is an increment of applied load on the flexural specimen below the proportional limit in kN; Δ is the increment of deflection of the neutral axis of flexure measured at midspan corresponding to load P in mm; and l is the span of the specimen in mm. Values for l and a were taken from Table 6.2, and values for b_g and t_g were taken from Table 6.1 for each of the specimens. The ratio P/Δ was determined by taking the slope of a linear portion of the total load vs. mid-span deflection graphs given in Fig. 6.5.

Table 6.5. Test specimen experimental results

Girder #	E_{app} (MPa)	M_a (kN-m)	M_n (kN-m)	M_a/M_n	S_R (MPa)	Actual-to predicted S_R[1]
1	8438	194	171	1.13	25.0	1.14
2	8865	219	176	1.25	27.5	1.25
3	11187	216	168	1.29	28.3	1.29
4	6124	137	178	0.77	16.8	0.77
5	7158	222	168	1.32	29.0	1.32
6	8456	177	171	1.03	22.5	1.02
7	10926	190	155	1.22	26.8	1.22
8	7680	159	176	0.90	19.9	0.91
Average	8604			1.11	24.5	1.11
COV	0.20			0.18	0.18	0.18

[1] Predicted S_R value = 21.45 MPa for all specimens.

A report published in 2005 by Nowak and Eamon (2005) proposed a linear equation based on the modulus of rupture of a specimen to determine its apparent modulus of elasticity.

$$E = [0.15S_R + 0.7]1000 \tag{6.7}$$

where S_R is the modulus of rupture in psi.

Using this equation, and converting the result to SI units, an actual-to-predicted value for E of 1.01 is returned for the results in Table 6.5, which gives credence to this study's results accuracy.

6.7. INHERENT BIAS FACTOR, COVS AND DISCUSSION

The average and COV values presented in Table 6.5 are akin to the resistance bias coefficient (δ_R) and COV (V_R) used in the Mean Load Method (Section 2.1.2), in Eq. (2.2). As discussed in Chapter 2, Madsen and Nielsen (1978) performed similar tests to those described in the Chapter on a large number of new timber specimens covering a wide range of dimensions. They found δ_R and V_R to range from 1.76-2.88 and 0.23-0.33, respectively (Madsen & Nielsen, 1978c). The results of the tests completed for this study, and those completed by Madsen and Nielsen, show that the nominal strength of timber girders is generally quite underpredicted for new materials, and still slightly underpredicted for decommissioned materials of unknown age. This likely stems from the fact that Canadian codes take a lower fifth percentile for strength properties, as discussed in Section 2.3. Nonetheless, this factor (in addition to the over-conservatism in the SMAs) can lead to misleading bridge assessment results.

Chapter 7: RECOMMENDATIONS FOR IMPROVEMENT TO THE SMA AND THE EVALUATION OF TIMBER BRIDGES IN CSA S6:19

7.1. SCOPE

As shown in Chapters 4 and 5, the current version of the SMA in CSA S6:19 is over-conservative for timber bridges. Using the findings and data generated from this research program, methods to improve the accuracy of the SMA were developed. One of the methods is updating values for some key statistical parameters used in the Mean Load Method, another is keeping the current values of the aforementioned statistical parameters and introducing new equations used to calculate load fractions for bridges. A third alternative is proposed below, which circumvents the SMA, whereby the maximum girder moment is determined by using a sophisticated analysis method such as FE. Each of the methods mentioned for improving the accuracy of timber bridge evaluation has its pros and cons, which are discussed in more detail in the following sections of this chapter.

7.2. ALTERNATIVE 1: UPDATE STATISTICAL PARAMETERS

Updating the statistical parameters used in calculating the live load capacity factor (F) with the Mean Load Method for timber bridges is one of the more easily adapted recommendations made to improve the accuracy of the SMA. The change would affect the bias coefficient and COV for the live load analysis method, δ_{AL} and V_{AL} respectively, in Table C14.4 of CSA S6.1:19. This change would bring the values currently given for these parameters more in line with the observed values found from the parametric study completed in Chapter 4. The changes are shown below in Table 7.1, where the proposed values correspond to those in Table 5.1 of Chapter 5 for the current SMA. Although updating the statistical parameters of δ_{AL} and V_{AL} to those given in Table 7.1 is a relatively easy change the issue is that the new proposed values were derived based on short span timber bridges and could have adverse effects on the evaluation of bridges constructed of other materials, such as concrete or steel. For this reason, a change to statistical parameters is not the best solution without further research into its impact on other types of bridges, and hence should only be used for timber bridges.

Table 7.1. Statistical parameters for use in the Mean Load Method

	Current S6:19	Proposed S6:19
δ_{AL}	0.93	0.70
V_{AL}	0.12	0.17

7.3. ALTERNATIVE 2: REVISE SMA EQUATIONS

This change is proposing to keep the current values of δ_{AL} and V_{AL} given in Table 7.1 and updating or changing the equations used to calculate the truck load distribution width (D_T) used in Eq. (2.33). Currently, values for D_T are given in a table for timber bridges in Table 5.11 of CSA S6:19 and shown in Table 2.3 of Section 2.2.2.7. This change would revert from a single value given for D_T, to equations based on the parameters of the bridge.

7.3.1. GENERATING THE EQUATIONS

To determine these new equations, the load fraction results determined from the FE analysis for each bridge were used. To ensure the values produced by the proposed equations would be accurate with the current version of the SMA the FE results were increased by 7% to match the values given for δ_{AL} and V_{AL}. The new increased values were taken along with some parameters specific to each bridge [e.g., Span length (L), Girder Spacing (S), and Girder depth (t_g)] and inputted into a Regression software, CurveExpert, which generated a large number of possible equations based on the parameters included in the data. Many of the equations were deemed too complex and unnecessary, ultimately two sets of equations were chosen to be proposed, each with two equations, one for one-lane bridges and one for two-lane bridges.

7.3.1.1. Detailed Equations

The proposed detailed equations are linear equations accounting for all the variables mentioned above, L, S, and t_g, these three variables are used as they can directly affect the total moment on the bridge, the moment capacity of the girders, and the distribution of the load between girders. Eq. (7.1) and (7.2) are the proposed equations for one- and two-lane bridges respectively.

$$D_T = 3.16 + 0.13L + 1.66S - 3.75t_g \tag{7.1}$$

$$D_T = 3 + 0.09L + S - 2.57t_g \tag{7.2}$$

Using this set of equations and generating values for δ_{AL} and V_{AL} in the same manner as done in Chapter 5, the statistical parameter values are in close accord with those currently presented in the code (0.93 and 0.12 respectively), with a δ_{AL} and V_{AL} of 0.93 and 0.09 respectively. According to CurveExpert, they have a relatively high “correlation coefficient” of 0.75 and a “standard error” of 0.30.

7.3.1.2. Simplified Equations

An alternative set of simpler equations are proposed below. These equations account only for span length (the key parameter missing from the current CSA S6:19 formulations). This set of equations is more in line with those presented in the 2006 version of CSA S6, which makes their adoption hypothetically easier, as engineers who have been using CSA S6 for many years will be comfortable with their appearance. Eq. (7.3) and (7.4) show the proposed equations for one- and two-lane bridges respectively.

$$D_T = 2.84 + 0.08L \tag{7.3}$$

$$D_T = 2.77 + 0.05L \tag{7.4}$$

Using this set of equations and generating values for δ_{AL} and V_{AL} in the same manner as done above, they are also in close accord with the current values presented in the code, with a δ_{AL} and V_{AL} of 0.91 and 0.13 respectively; however, because these are simplified with respect to Eq. (7.1) and (7.2), they give a lower "correlation coefficient" of 0.40 and a higher "standard error" of 0.42. Nonetheless, they are simpler, and still meet the target reliability of the code, and compared to the detailed equations these simplified equations match the form of equations used in previous versions of the code.

7.4. ALTERNATIVE 3: SOPHISTICATED ANALYSIS

The final recommendation is to use a more sophisticated method of analysis, such as FE, using the proposed modelling approach for timber bridges discussed in Chapter 3 (this approach can be used directly to determine the largest anticipated girder moment). With the anticipated girder moment from the FE analysis, it is then possible to use the "sophisticated analysis method" values for δ_{AL} and V_{AL} given in Table C14.4 of CSA S6.1:19 (CSA, 2019b) in conjunction with the Mean Load Method to determine the live load capacity factor (F).

7.5. COMPARISON OF PROPOSED METHODS

To compare the new proposed equations and the sophisticated analysis method to see their effect on calculated values of F, two bridges tested by SHM were used as a case study. The girder moments for the bridges were determined using five approaches:

1. sophisticated analysis (FE);
2. the SMA in S6-06;
3. the current SMA in S6:19;
4. the SMA in S6:19 with the proposed detailed equations [Eq. (7.1) and (7.2)]; and
5. the SMA in S6:19 with the proposed simplified equations [Eq. (7.3) and (7.4)].

Note, Alternative 1: update statistical parameters, are not compared as it was determined to not be a viable option.

Table 7.2 shows the maximum anticipated girder moment based on each of the methods. As can be seen in Tables 7.2 CSA S6-06 predicted very close to the actual moment the bridge is anticipated to experience (arguably, too close), and CSA S6:19 greatly over predicted the moment by a substantial amount, being over-conservative. Both the detailed and simplified equations predict the anticipated moment within a reasonable margin of safety.

Table 7.2. Maximum anticipated girder moment comparison

Bridge	FE (kN-m)	S6-06 (kN-m)[1]	Current S6:19 (kN-m) [1]	Detailed Equations (kN-m) [1]	Simplified Equations (kN-m) [1]
HFX061	54.7	55.5 (0.99)	83.2 (0.66)	61 (0.90)	57.5 (0.95)
HFX322	43.6	47.9 (0.91)	58.1 (0.75)	49.8 (0.88)	48.1 (0.91)

[1] Value in parentheses is actual to predicted value where FE is taken as actual

Table 7.3 shows F for each of the methods, calculated using values of 1.0 and 0 as the statistical parameters for resistance, δ_R and V_R respectively since none are given in the code for timber. Again, while nothing is stated specifically for the Mean Load Method, Clause 14.14.2 of CSA S6:19 says "… Where no value of U is specified in Table 14.10, and in lieu of better information, a value of U = 1.0 may be used." (CSA, 2019a). While both bridges pass according to all of the live-load analysis methods, the 2006 version of S6, and both the detailed and simplified versions of the proposed equations provide F values that are larger, and which agree better with those obtained using a sophisticated (FE) analysis – and are hence deemed "more correct".

Table 7.3. Live load capacity factor (F) comparison

Bridge	FE	S6-06	Current S6:19	Detailed Equations	Simplified Equations
HFX061	1.90	1.70	1.21	1.54	1.64
HFX322	1.68	1.40	1.14	1.34	1.39

F calculated using δ_R=1.0 and V_R=0

Table 7.4 shows F for each of the methods, calculated using δ_R and V_R of 1.11 and 0.18, respectively. These are the values determined from the experimental testing conducted in Chapter 6. [Note that the experimental testing was done on decommissioned girders of an undetermined age and HFX322 was built in 2018; therefore, using the aforementioned values of δ_R and V_R is likely a conservative approach, as the HFX322 girders are in a much newer condition. In fact, according to SHM (2021), they received a National Bridge Inventory rating of 8 (good condition)]. Even so, all of the live-load analysis approaches provide "passing" F values with the exception of CSA S6:19 – further illustrating that it is inherently over-conservative.

Table 7.4. Live load capacity factor (F) comparison using experimental test results

Bridge	FE	S6-06	Current S6:19	Detailed Equations	Simplified Equations
HFX061	1.44	1.39	0.99	1.26	1.34
HFX322	1.21	1.09	0.90	1.05	1.09

F calculated using δ_R=1.11 and V_R=0.18

Based on the results from this comparison in Table 7.2, 7.3, and 7.4 it is recommended that the way the truck load distribution factor (D_T) is calculated should be changed from the single values currently given in CSA S6:19 bridges with transverse plank wood decking to the simplified equations [Eq. (7.3) and (7.4)] presented above.

Chapter 8: SUMMARY, CONCLUSIONS AND RECOMMENDATIONS

8.1. SUMMARY

In Canada, the design and evaluation of timber bridges is done using a simplified method of analysis (SMA) given in CSA S6. Since its addition to the code, the SMA has continuously been tweaked to be easier to use, as of the 2014 version of CSA S6 concerns have arisen from industry professionals that the SMA has become over-conservative for the evaluation and design of timber bridges.

Chapter 1 introduced timber bridges and how bridge evaluation is conducted as per CSA S6 and examined the limitations behind the methods, specifically for use with timber bridges. Chapter 2 talked about relevant research and the criteria for evaluating bridges along with looking at different methods used to analyze short span bridges, it concludes by diving into the SMA from its adoption into the Ontario Highway Bridge Design Code (OHBDC) in 1983 and examined the changes made over successive versions of the code, and identifies key areas where a knowledge gap is present. Chapter 3 introduced finite element modelling and defined a model fit for use on timber bridges based on a sensitivity study that examined the effects of material properties, mesh density, element type, deck thickness and girder modulus on the results of the model. Using the model proposed in Chapter 3 a Parametric study was hence performed and discussed in Chapter 4. Chapter 4 analyzed over 200 bridge models covering a range of parameters given in Table 4.1. Using the results produced, it appeared that the current version of the code (CSA S6:19) is much more conservative as compared to previous versions of the code (CSA S6-06) confirming the suspicions of many industry professionals. The results from Chapter 4 were further examined in Chapter 5 and broken down to look at the effect of span length (L), girder spacing (S) and girder depth (t_g), on the results of the SMA. Subsequently, the SMA from new and older versions of the code were evaluated, it was shown that the current version of CSA S6 was over predicting the truck load fraction (F_T) by 30% on average.

One of the areas of limitations for using the Mean Load Method with timber bridge structures is that there are no statistical parameters given for the resistance of timber in CSA S6. Chapter 6 outlined an experimental testing program, completed on eight decommissioned timber girders to determine their strengths and material properties, and compare the findings to other test programs completed by other researchers. From the work completed in Chapters 3-6, Chapter 7 gave recommendations to improve the accuracy of the code and compared

those recommendations to each other, as well as the current and past versions of the code to show how effective the recommendations are comparatively, and a finally a recommendation is made.

8.2. CONCLUSIONS

Based on the findings of this research study looking at the SMA, methods of evaluation for timber bridges, as well as an experimental program looking at the statistical resistance parameters of decommissioned timber girders, the following conclusions are made:

- Modelling can be done with a relatively simple FE model consisting of:
  - Simply supported girders, modelled with Timoshenko beam elements
  - A deck modelled using plate elements, keeping the aspect ratio close to unity
  - Deck to girder connections done with general links, neglecting composite action
  - Deck thickness of 95mm
  - Medium fine mesh, roughly every 250mm
  - Using isotropic material properties, from CSA S6
- Material properties such as modulus of elasticity (E) have little effect on the load distribution factor results, but will influence global phenomena such as deflection
- The resistance of timber is vastly underpredicted for new members (see Section 6.6 and 6.7) and is still slightly overpredicted for decommissioned members of an undetermined age as shown in Chapter 6

With respect to the accuracy of SMAs in the CHBDC:

- In general, CSA S6:19 overpredicts the anticipated girder moment by a significant amount (30% on average)
- CSA S6-06 was a better predictor of the anticipated girder moment and its statistical parameters are more in line with those given in the CHBDC Commentary (CSA S6.1:19)

In general, these results show there is a large gap in knowledge for short-span timber bridges, their analysis, evaluation, and the strength properties of timber as a whole. The results also show that there is a large discrepancy in the prediction of the maximum girder moment by CSA S6:19 and the actual maximum moment, as determined by FE analysis, and that this leads to unrealistic estimates and a significant amount of conservatism in the design and evaluation of timber bridges.

It is therefore recommended to exchange the current values given in CSA S6:19 used for D_T, with the following "simplified equations" for one and two-lane bridges, respectively, which were shown in Chapter 7 to be more in line with the statistical parameters given in CSA S6.1:19 and yet still fit the format of the code:

$$D_T = 2.84 + 0.08L \tag{8.1}$$

$$D_T = 2.77 + 0.05L \tag{8.2}$$

It is also worth noting that more accurate equations than those above (termed the "detailed equations") were evaluated (in Section 7.3.1.1).

8.3. Recommendations for Evaluation of Timber Bridges in Canada

The following recommendations are made concerning the evaluation of timber bridges in Canada:

- Use the Mean Load Method for evaluation. This allows designers/evaluators to account for the uncertainties in the resistance and load effects through statistical parameters, leading to more accurate results. Appendix C provides a sample calculation, which illustrates that it is relatively straightforward to apply.
- Use the above-recommended simplified D_T equations in conjunction with the CSA S6:19 SMA to determine the truck load fraction, or use a sophisticated analysis method (e.g., FE modelling using the approach presented in Chapter 3). This should be done in conjunction with the point above. Because both of these methods are calibrated to the statistical parameters presented in the CHBDC, they will yield accurate results. [As shown in Chapter 5, use of the current (CSA S6:19) SMA is over-conservative, on average, by 30%.]

8.4. Recommendations for Future Work & Research

The following recommendations are made for future work in this area:

- Conduct more experiments on new and decommissioned timber beams to determine accurate statistical parameters for use in evaluation methods. (Presently, the tabulated strength values for timber are determined from the lower fifth percentile, which can lead to conservative estimates of resistance).
- Review the statistical parameters for live load analysis using the SMA for other materials (e.g., concrete and steel) in the manner performed in Chapters 3 and 4, herein. Given that changes have been made to the various SMAs without changes to the corresponding statistical parameters for the analysis method(s), these may be out-of-date.
- A continuation of the current study focusing on shear as the governing load effect (as failure due to punching shear is a possibility in timber bridges).
- Although not discussed, a review CSA S6 to ensure clear referencing between sections (e.g., Sections 9 and 14, there seems to be a disconnect that can cause confusion when determining the strength of timber, Section 9 Clause 9.6 in CSA S6:19 does not reference the use of Table 14.9 for determining the strength of timber when evaluating existing structures.

REFERENCES

Allen, D. E. (1992). Canadian highway bridge evaluation: reliability index. *Canadain Journal of Civil Engineering*, 987-991.

ASTM International . (2020). *Standard Practice for Field Calibration and Applicaiton of Hand-Held Moisture Meters.* ASTM International.

ASTM International. (2019). *Standard Practice for Establishing Structural Grades and Related Allowable Properties for Visually Graded Lumber.* ASTM International.

ASTM International. (2020). *Standard Test Methods for Direct Moisture Content Measurement of Wood and Wood Based Materials.* ASTM International.

ASTM International. (2021). *Standard Test Methods of Static Tests of Lumber in Structural Sizes.* ASTM International.

Bakht, B. (1983). Statistical Analysis of Timber Bridges. *Journal of Structural Engineering*, 1761-1779.

Bakht, B., & Jaeger, L. G. (1985). *Bridge Analysis Simplified.* McGraw-Hill.

Bakht, B., & Jaeger, L. G. (1991). Simplified methods of bridge analysis for the third edition of OHBDC. *Canadian Journal of Civil Engineering*, 551-559.

Bakht, B., & Mufti, A. (2015). *Bridges Analysis, Design, Structural Health Monitoring, and Rehabilitation.* switzerland: Springer.

Bakht, B., Aly, A., & Smith, D. S. (1997). Semi-continuum versus grillage methods of analysis. *Canadian Journal of Civil Engineering*, 157-160.

Bury, K. V. (1981). *Statistical Analysis of NLGA Bending Tests.* Department of Mechanical Engineering, University of British Columbia.

Choi, F., & Crews, K. (2012). Calibration of a Laboratory Timber Bridge Finite Element Model using the Experimental Modal Data. *Procedia Engineeering* , 79-84.

CSA. (1988). *Design of Highway Bridges CAN/CSA-S6-88.* Toronto, Canada: Canadian Standards Association .

CSA. (2000). *Canadian Highway Bridge Design Code. CAN/CSA-S6-00.* Toronto, Canada: Canadian Standards Association.

CSA. (2006a). *Canadian Highway Bridge Design Code. CAN/CSA-S6-06.* Mississauga, Canada: Canadain Standardsd Association.

CSA. (2006b). *Commentary on CAN/CSA-S6-06, Canadain Highway Bridge Design Code. CAN/CSA-S6.1-06.* Mississauga, Ontario, Canada: Canadian Standards Association.

CSA. (2014a). *Canadian Highway Bridge Design Code. CSA S6-14.* Mississauga, Canada: Canadian Standards Association.

CSA. (2019). *Engineering Design in Wood. CAN/CSA O86:19.* Toronto, Ontario : CSA Group.

CSA. (2019a). *Canadian Highway Bridge Design Code. CAN/CSA-S6:19.* Mississauga, Ontario, Canada: Canadian Standards Association.

CSA. (2019b). *Commentary on CAN/CSA S6:19, Canadian Highway Bridge Design Code, CSA S6.1:19.* Toronto, Canada: Canadian Standards Association.

Cusens, A., & Pama, R. P. (1975). *Bridge Deck Analysis.* London; New York: Wiley.

Eamon, C., Nowak, A. S., Ritter, M. A., & Murphy, J. (2000). Reliability-Based Criteria for Load and Resistance Factor Design Code for Wood Bridges. *Transportation Research Record 1696*, 316-322.

Ekholm, K., Ekevad, M., & Kliger, I. R. (2014). Modeling Slip in Stress-Laminated Timber Bridges: Comparison of Two Finite-Element-Method Approaches and Test Values. *Journal of Bridge Engineering*, 1-8.

Hambly, E. C. (1991). *Bridge Deck Behaviour .* London, New York: E & FN Spon.

Hrennikoff, A. (1941). Solution of problems of elasticity by the framework method. *Journal of Applied Mechanics* , 169-175.

Jaeger, L. G., & Bakht, B. (1982). The Grillage Analogy in Bridge Analysis. *Canadian Journal of Civil Engineering*, 224-235.

James, W. L. (1965). *Effects of Wood Preservatives on Electric Moisture Meter Readings.* U.S. Forest Service research note .

Madsen, B., & Nielsen, P. C. (1978c). *In-Grade Testing — Bending Tests in Canada, June 1977 - May1978.* Department of Civil Engineering, University of British Columbia.

Nowak, A. S., & Eamon, C. D. (2005). Load and Resistance Factor Calibration For Wood Bridges. *Journal of Bridge Engineering*, 636-642.

SHM Canada Consulting Limited. (2021). *Load testing & Development of Live Load Distribution Factors for Timber Bridges.* Halifax, Nova Scotia, Canada: SHM Canada.

Smith, G. A. (2018). *The impact of the evolution of simplified methods of analysis in canadian highway bridge design codes on the evaluation of timber bridges.* Halifax, Nova Scotia, Canada: Dalhousie University.

Zienkiewicz, O. C., Taylor, R. L., & Zhu, J. Z. (2013). *The Finite Element Method: Its Basis and Fundamentals.* Oxford: Elsevier Science & Technology .

Appendix A: Finite Element Modelling Sensitivity Study Graphs

A.1. Effect of Deck Thickness on Deflection & LDF Values

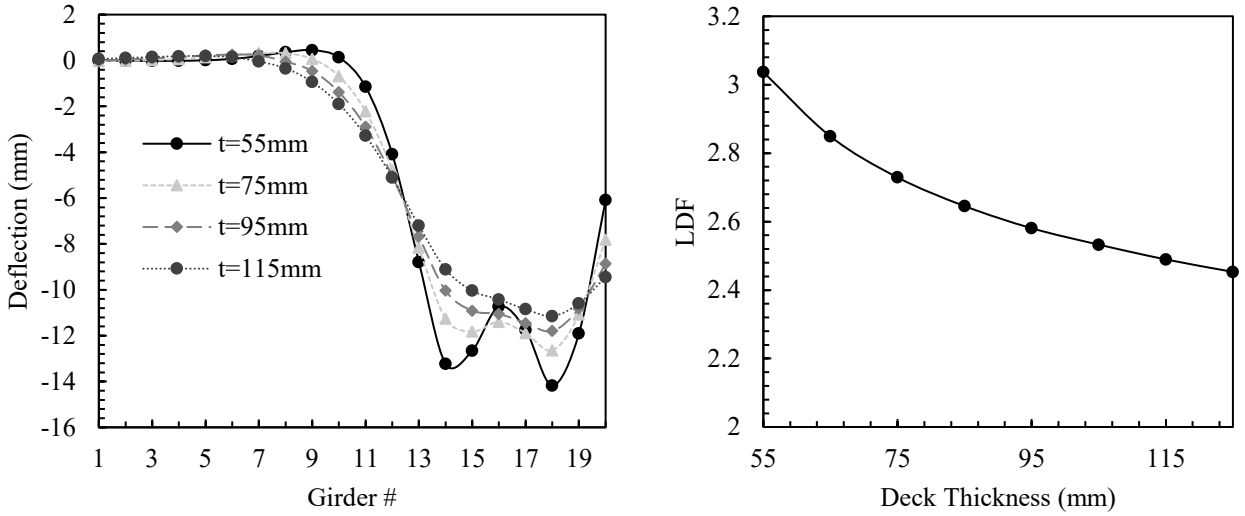

(a) Deflection (b) LDF

Fig. A.1. Effect of deck thickness

A.2. Deck Material Properties Comparison

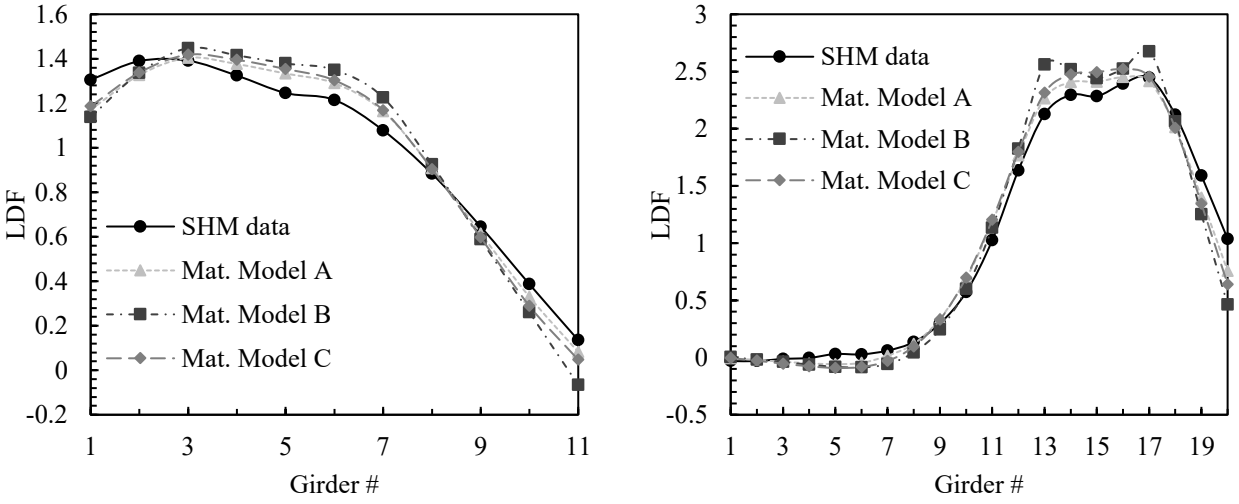

(a) HFX061 (b) HFX322

Fig. A.2. Effect of material properties models on LDF

A.3. EFFECT OF MODULUS OF ELASTICITY

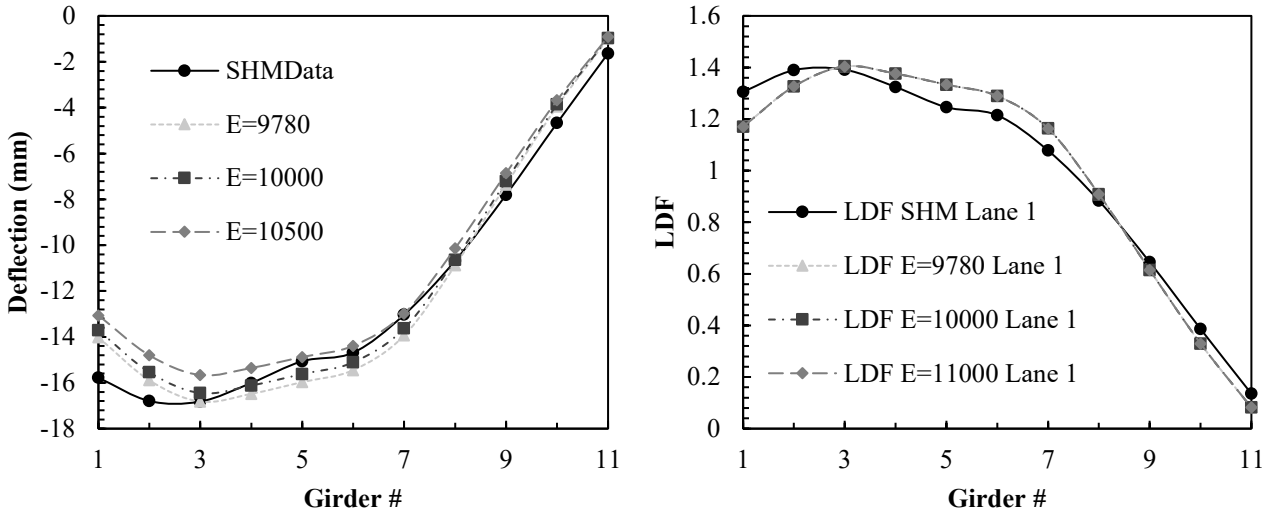

(a) Deflection (b) LDF

Fig. A.3. HFX061 Lane 1

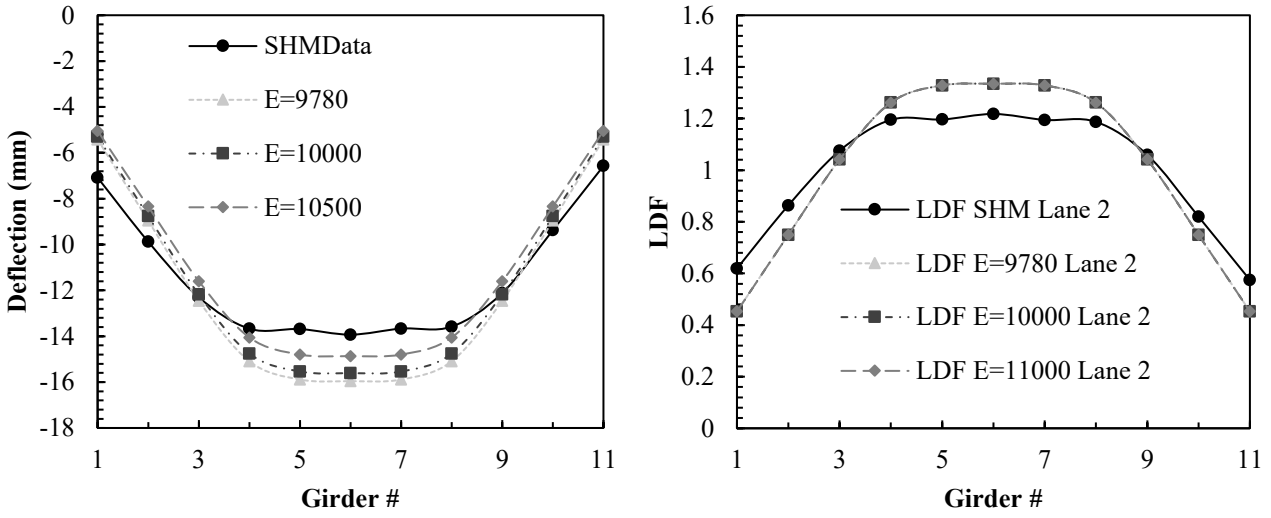

(a) Deflection (b) LDF

Fig. A.4. HFX061 Lane 2

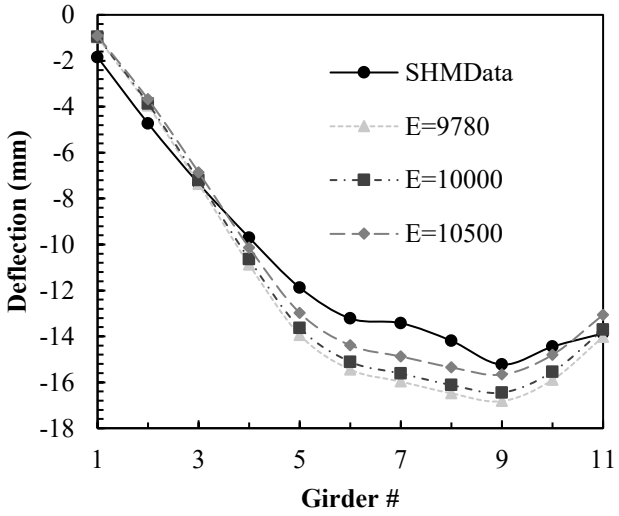

(a) Deflection

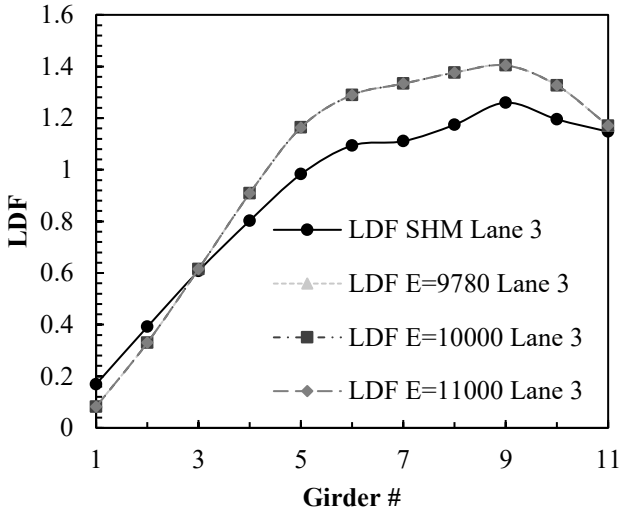

(b) LDF

Fig. A.5. HFX061 Lane 3

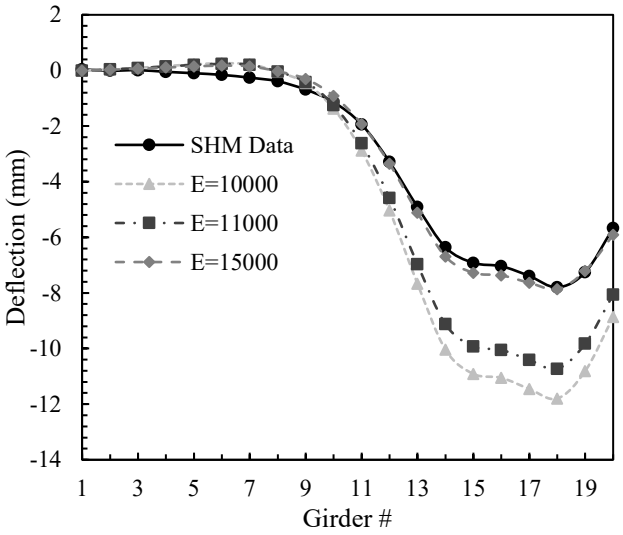

(a) Deflection

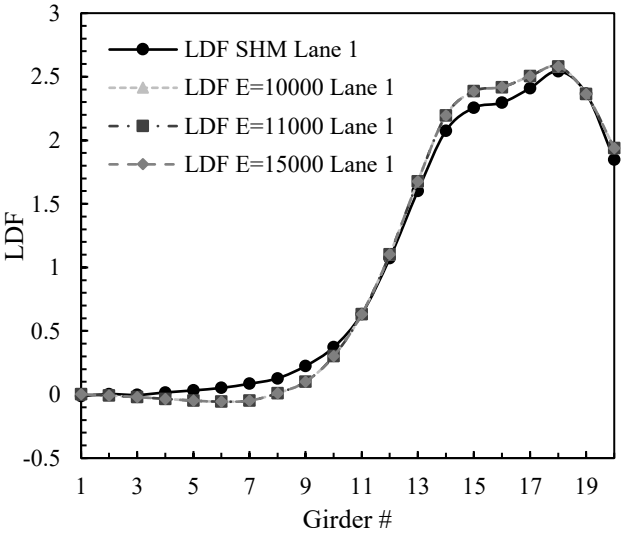

(b) LDF

Fig. A.6. HFX322 Lane 1

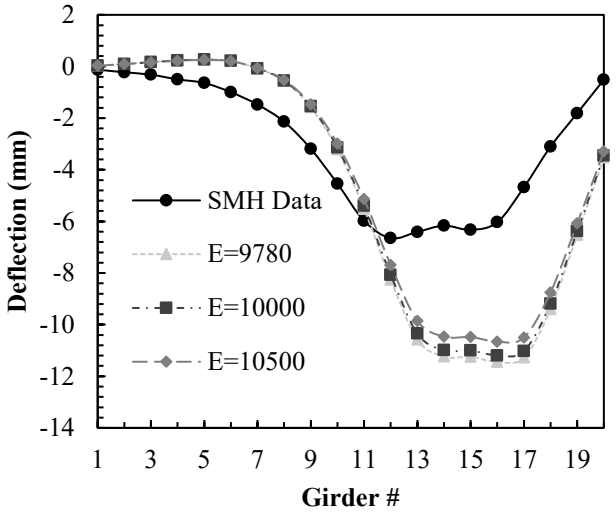

(a) Deflection

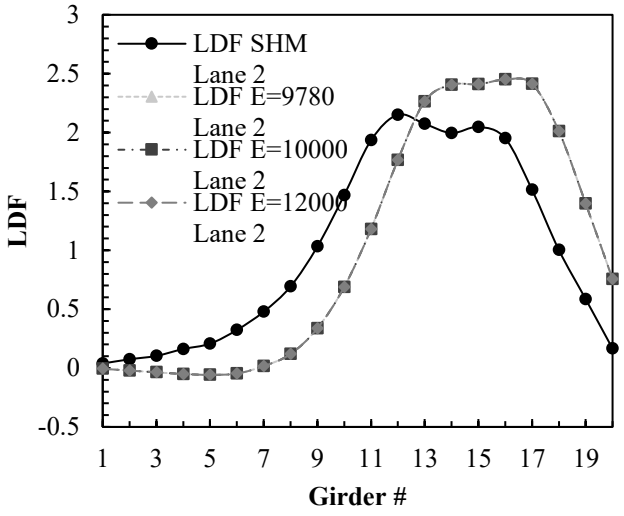

(b) LDF

Fig. A.7. HFX322 Lane 2

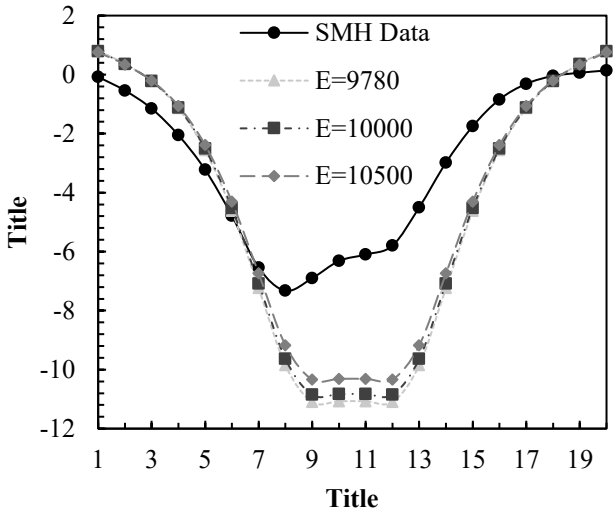

(a) Deflection

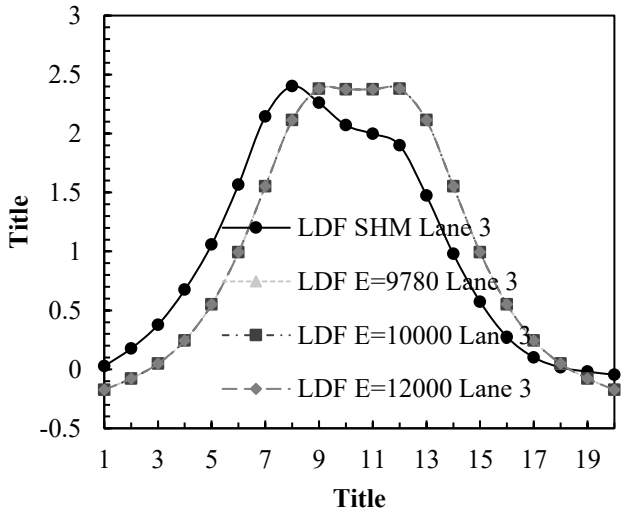

(b) LDF

Fig. A.8. HFX322 Lane 3

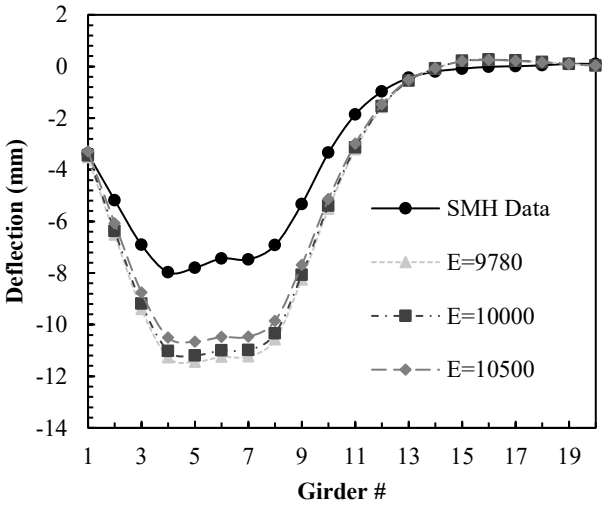

(a) Deflection

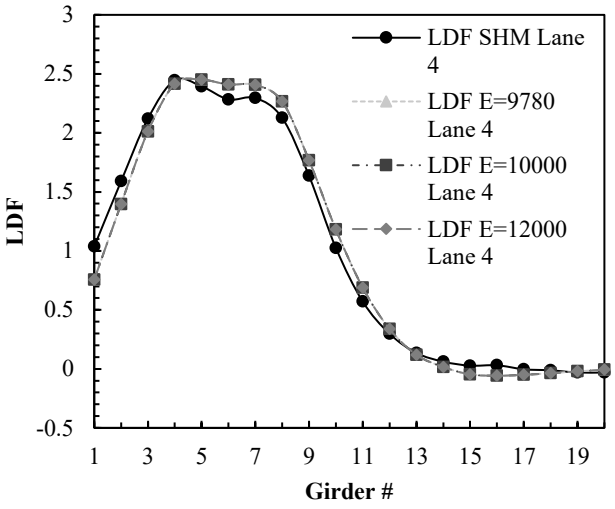

(b) LDF

Fig. A.9. HFX322 Lane 4

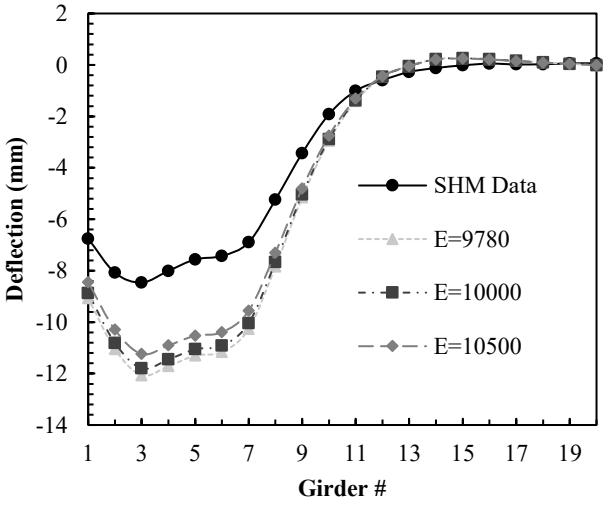

(a) Deflection

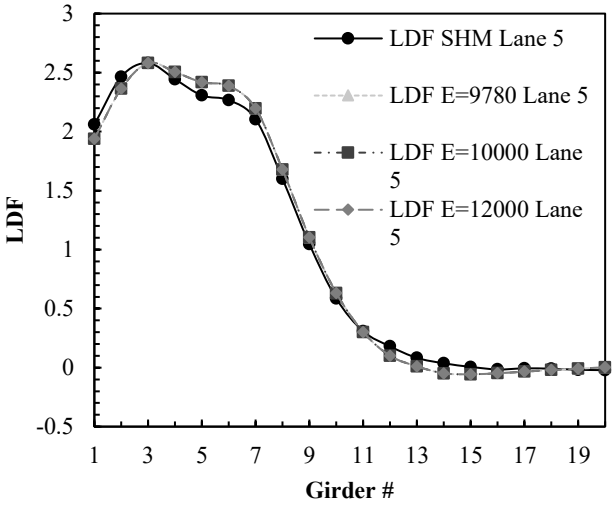

(b) LDF

Fig. A.10. HFX322 Lane 5

Appendix B: PARAMETRIC STUDY BRIDGE PARAMETERS

B.1. PARAMETRIC STUDY PARAMETER DISTRIBUTION

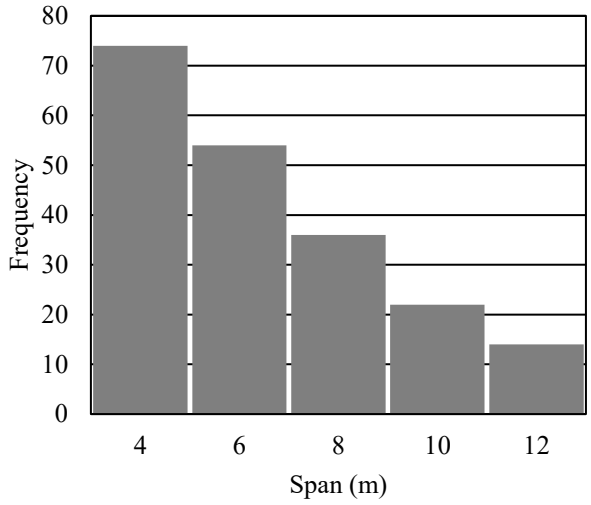

(a) Span length distribution

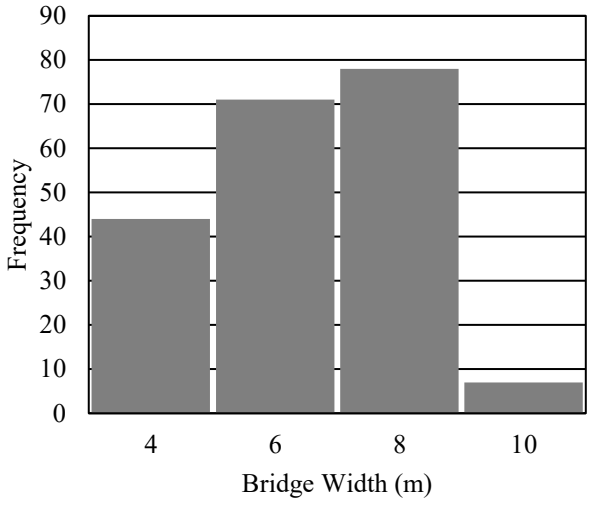

(b) Bridge width distribution

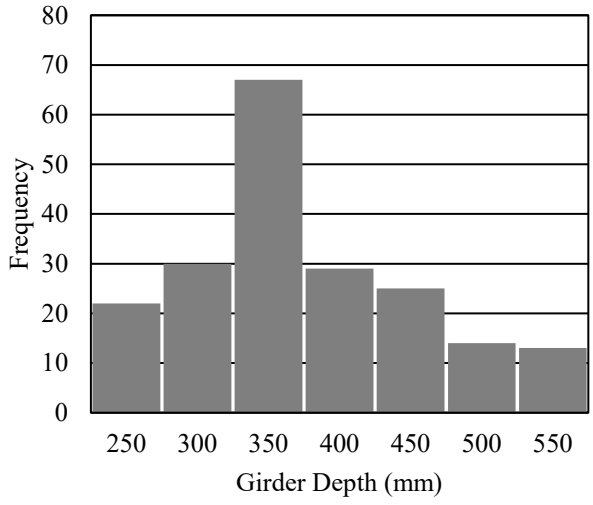

(c) Girder depth distribution

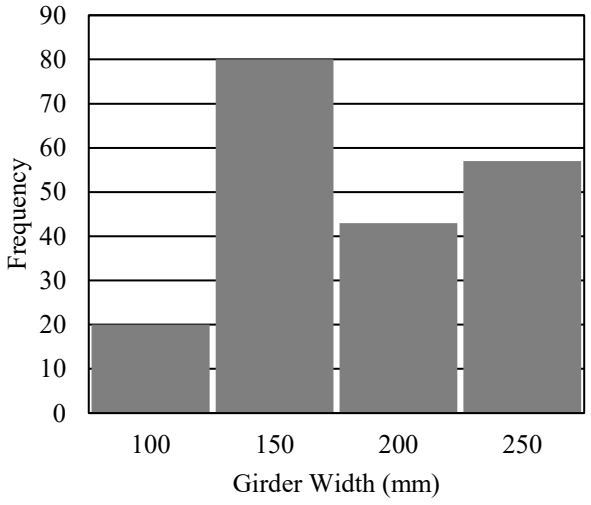

(d) Girder width distribution

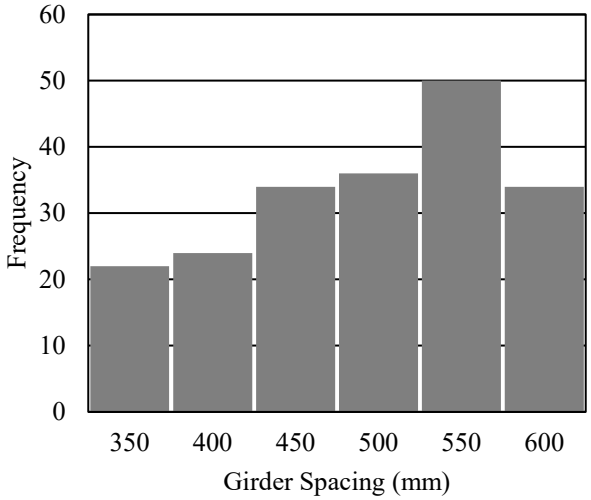

(e) Girder spacing distribution

Fig. B.1. Parametric study parameter distributions

B.2. PARAMETRIC STUDY MODEL PARAMETERS AND FE RESULTS

Table B.1. Model parameters and FE results

Model #	L (m)	W_b (m)	S (mm)	t_g (mm)	b_g (mm)	N	n	Def. fraction	Mom. fraction
1	5	7.00	500	400	230	15	2	0.153	0.180
2	6	6.01	462	425	200	14	1	0.131	0.140
3	7	5.01	455	400	230	11	1	0.125	0.133
4	8	4.28	475	450	200	9	1	0.134	0.141
5	4	4.80	400	250	100	13	1	0.108	0.097
6	4	4.95	450	350	200	12	1	0.143	0.152
7	4	4.95	550	300	175	10	1	0.151	0.147
8	4	4.95	550	275	250	10	1	0.153	0.150
9	4	5.25	350	400	150	16	1	0.115	0.252
10	4	5.40	450	450	150	13	1	0.155	0.164
11	4	5.00	500	275	200	11	1	0.144	0.138
12	4	5.00	550	325	250	11	1	0.167	0.161
13	4	6.65	350	350	125	20	2	0.114	0.120
14	4	6.00	400	400	175	16	1	0.128	0.118
15	4	6.75	450	325	250	16	2	0.142	0.154
16	4	6.00	500	325	150	13	1	0.144	0.143
17	4	6.60	550	400	250	13	2	0.205	0.200
18	4	6.05	550	350	150	12	1	0.161	0.154
19	4	6.00	600	275	200	11	1	0.167	0.148
20	4	6.60	600	450	175	12	2	0.215	0.201
21	4	7.20	400	375	250	19	2	0.127	0.133
22	4	7.20	450	400	175	17	2	0.145	0.157
23	4	7.00	500	350	175	15	2	0.138	0.137
24	4	7.15	550	275	200	14	2	0.169	0.165
25	4	7.15	550	325	175	14	2	0.172	0.173
26	4	7.00	350	400	250	21	2	0.115	0.119
27	4	8.05	350	300	125	24	2	0.101	0.106
28	4	8.10	450	350	275	19	2	0.150	0.163
29	4	8.00	500	350	150	17	2	0.165	0.167
30	4	8.25	550	450	250	16	2	0.189	0.191
31	4	8.25	550	250	150	16	2	0.159	0.146
32	4	8.40	600	275	200	15	2	0.190	0.180
33	4	8.40	600	425	200	15	2	0.215	0.212
34	4	8.10	450	400	250	19	2	0.158	0.166
35	4	9.00	450	300	100	21	2	0.141	0.137
36	4	9.20	400	350	250	24	2	0.128	0.144
37	4	9.00	500	300	175	19	2	0.162	0.158
38	4	9.35	550	300	250	18	2	0.166	0.168
39	4	9.35	550	300	150	18	2	0.162	0.158
40	4	9.00	450	400	200	21	2	0.149	0.166

Table B.2. Model parameters (continued)

Model #	L (m)	W_b (m)	S (mm)	t_g (mm)	b_g (mm)	N	n	Def. fraction	Mom. fraction
41	4	9.00	600	400	250	16	2	0.210	0.206
42	5	4.80	350	300	150	15	1	0.098	0.094
43	5	5.00	500	350	250	11	1	0.144	0.143
44	5	4.80	600	350	150	9	1	0.163	0.152
45	5	4.95	450	400	100	12	1	0.125	0.126
46	5	4.95	550	250	250	10	1	0.144	0.131
47	5	5.20	400	300	200	14	1	0.112	0.107
48	5	5.00	500	275	250	11	1	0.135	0.130
49	5	5.85	450	450	100	14	1	0.129	0.133
50	5	6.75	450	300	250	16	2	0.131	0.121
51	5	6.00	500	450	175	13	1	0.150	0.149
52	5	6.60	550	300	150	13	2	0.172	0.146
53	5	6.05	550	400	200	12	1	0.162	0.159
54	5	6.60	600	350	250	12	2	0.196	0.188
55	5	6.30	350	400	200	19	1	0.108	0.109
56	5	7.00	350	400	100	21	2	0.107	0.109
57	5	7.20	400	300	150	19	2	0.121	0.119
58	5	7.65	450	325	250	18	2	0.145	0.147
59	5	7.50	500	450	150	16	2	0.153	0.158
60	5	7.00	500	275	200	15	2	0.146	0.136
61	5	7.15	550	250	150	14	2	0.158	0.137
62	5	8.00	400	350	250	21	2	0.132	0.134
63	5	8.10	450	350	175	19	2	0.141	0.142
64	5	8.55	450	350	200	20	2	0.142	0.144
65	5	8.00	500	450	200	17	2	0.137	0.137
66	5	8.25	550	400	250	16	2	0.166	0.171
67	5	8.80	550	375	150	17	2	0.163	0.160
68	5	8.40	600	375	200	15	2	0.196	0.190
69	5	8.40	600	350	150	15	2	0.190	0.180
70	5	8.25	550	450	275	16	2	0.170	0.176
71	5	9.45	350	250	150	28	2	0.107	0.104
72	5	9.20	400	350	250	24	2	0.126	0.131
73	5	9.00	450	350	100	21	2	0.143	0.143
74	5	9.50	500	450	150	20	2	0.147	0.148
75	5	9.00	500	350	200	19	2	0.161	0.156
76	5	9.35	550	400	150	18	2	0.166	0.165
77	5	9.35	550	475	225	18	2	0.167	0.171
78	5	10.20	600	375	250	18	2	0.191	0.188
79	6	4.80	350	300	150	15	1	0.094	0.091
80	6	5.00	500	350	150	11	1	0.132	0.128
81	6	4.80	600	350	200	9	1	0.160	0.151
82	6	5.20	400	450	100	14	1	0.112	0.110

Table B.3. Model parameters (continued)

Model #	L (m)	W_b (m)	S (mm)	t_g (mm)	b_g (mm)	N	n	Def. fraction	Mom. fraction
83	6	4.95	450	400	200	12	1	0.127	0.131
84	6	4.95	550	400	250	10	1	0.155	0.154
85	6	6.80	400	300	150	18	2	0.123	0.118
86	6	6.00	500	350	275	13	1	0.138	0.138
87	6	6.60	550	300	150	13	2	0.166	0.154
88	6	6.00	600	400	200	11	1	0.168	0.131
89	6	6.60	600	300	175	12	2	0.180	0.165
90	6	7.00	350	300	100	21	2	0.101	0.096
91	6	7.20	450	300	250	17	2	0.134	0.132
92	6	7.50	500	450	150	16	2	0.158	0.155
93	6	7.00	550	375	250	14	2	0.170	0.168
94	6	7.20	400	400	175	19	2	0.123	0.124
95	6	8.40	400	250	125	22	2	0.115	0.102
96	6	8.10	450	350	200	19	2	0.139	0.137
97	6	8.00	500	350	175	17	2	0.156	0.151
98	6	8.25	550	425	175	16	2	0.166	0.164
99	6	8.80	550	400	175	17	2	0.162	0.159
100	6	9.45	350	400	200	28	2	0.104	0.109
101	6	9.20	400	350	200	24	2	0.122	0.122
102	6	9.00	450	350	150	20	2	0.150	0.135
103	6	9.00	500	450	250	19	2	0.163	0.161
104	6	9.60	600	350	150	17	2	0.170	0.160
105	7	4.80	450	300	250	12	1	0.119	0.122
106	7	4.80	550	250	150	10	1	0.129	0.111
107	7	5.00	450	300	150	12	1	0.113	0.110
108	7	5.00	500	350	150	11	1	0.128	0.125
109	7	5.40	600	275	250	10	1	0.146	0.137
110	7	5.95	350	300	125	18	1	0.089	0.086
111	7	6.30	450	450	200	15	1	0.118	0.122
112	7	6.00	500	250	250	13	1	0.125	0.121
113	7	6.60	550	475	175	13	2	0.176	0.175
114	7	6.80	400	350	200	18	2	0.125	0.123
115	7	7.20	400	350	150	19	2	0.117	0.115
116	7	7.00	500	350	250	15	2	0.146	0.144
117	7	7.15	550	350	150	14	2	0.160	0.153
118	7	7.20	600	275	250	13	2	0.169	0.157
119	7	7.65	450	250	150	18	2	0.127	0.119
120	7	8.40	350	450	175	25	2	0.114	0.117
121	7	8.10	450	350	175	19	2	0.135	0.132
122	7	8.00	500	350	250	17	2	0.156	0.154
123	7	8.25	550	450	150	16	2	0.163	0.162
124	7	8.40	600	350	200	15	2	0.188	0.184

Table B.4. Model parameters (continued)

Model #	L (m)	W_b (m)	S (mm)	t_g (mm)	b_g (mm)	N	n	Def. fraction	Mom. fraction
125	7	9.20	400	350	125	24	2	0.116	0.112
126	7	9.00	450	350	250	21	2	0.140	0.139
127	7	9.50	500	350	150	20	2	0.141	0.140
128	7	9.35	550	475	200	18	2	0.164	0.165
129	7	9.90	550	400	250	19	2	0.167	0.165
130	7	9.60	600	400	175	17	2	0.185	0.180
131	7	10.45	550	500	225	20	2	0.164	0.169
132	7	11.40	600	375	250	20	2	0.178	0.175
133	8	4.95	450	500	125	12	1	0.120	0.126
134	8	4.95	550	275	200	10	1	0.131	0.121
135	8	5.25	350	375	175	16	1	0.093	0.095
136	8	5.00	500	300	250	11	1	0.127	0.127
137	8	6.40	400	350	250	17	1	0.105	0.107
138	8	6.00	500	300	150	13	1	0.120	0.113
139	8	6.60	600	350	175	12	2	0.175	0.166
140	8	7.20	450	300	125	17	2	0.122	0.114
141	8	7.70	550	525	225	15	2	0.174	0.174
142	8	7.20	600	350	200	13	2	0.171	0.162
143	8	8.10	450	450	125	19	2	0.135	0.134
144	8	8.50	500	500	175	18	2	0.157	0.157
145	8	8.25	550	350	250	16	2	0.158	0.154
146	8	8.40	600	350	150	15	2	0.171	0.161
147	8	9.00	400	350	250	24	2	0.119	0.118
148	8	9.00	500	450	150	19	2	0.154	0.151
149	8	9.90	550	375	200	19	2	0.159	0.155
150	8	9.60	600	350	150	17	2	0.176	0.168
151	9	4.80	400	275	150	13	1	0.098	0.066
152	9	4.80	600	525	250	9	1	0.162	0.163
153	9	4.95	550	250	150	10	1	0.126	0.106
154	9	5.40	600	500	225	10	1	0.157	0.158
155	9	6.80	400	275	150	18	2	0.110	0.103
156	9	6.00	500	500	250	13	1	0.133	0.139
157	9	6.05	550	500	200	12	1	0.144	0.148
158	9	6.60	600	350	150	12	2	0.177	0.173
159	9	7.00	350	350	150	21	2	0.098	0.096
160	9	7.20	450	500	250	17	2	0.137	0.141
161	9	7.15	550	350	150	14	2	0.151	0.145
162	9	8.05	350	350	150	24	2	0.101	0.099
163	9	8.55	450	525	250	20	2	0.141	0.144
164	9	8.25	550	350	200	16	2	0.151	0.147
165	9	9.60	400	350	150	25	2	0.120	0.119
166	9	9.00	500	450	150	19	2	0.149	0.147

Table B.5. Model parameters (continued)

Model #	L (m)	W_b (m)	S (mm)	t_g (mm)	b_g (mm)	N	n	Def. fraction	Mom. fraction
167	9	9.00	550	350	225	18	2	0.156	0.154
168	9	10.20	600	525	175	18	2	0.171	0.171
169	10	4.95	450	325	175	12	1	0.111	0.109
170	10	5.25	350	550	175	16	1	0.095	0.101
171	10	5.00	550	375	250	10	1	0.135	0.135
172	10	6.00	400	550	100	16	1	0.105	0.109
173	10	6.00	550	350	200	12	1	0.132	0.127
174	10	7.35	350	350	150	22	2	0.100	0.098
175	10	7.65	450	400	250	18	2	0.136	0.135
176	10	8.40	350	375	125	25	2	0.101	0.098
177	10	8.00	500	550	175	17	2	0.158	0.156
178	10	9.45	450	400	250	22	2	0.128	0.127
179	10	9.00	550	400	150	18	2	0.151	0.146
180	10	8.80	550	450	225	17	2	0.158	0.156
181	11	4.80	400	325	250	13	1	0.101	0.101
182	11	5.00	500	350	150	11	1	0.123	0.117
183	11	6.05	550	400	275	12	1	0.137	0.140
184	11	6.30	450	350	150	15	1	0.111	0.106
185	11	7.00	500	350	250	15	2	0.140	0.131
186	11	7.20	600	550	175	13	2	0.179	0.172
187	11	8.40	400	350	200	22	2	0.118	0.114
188	11	9.00	500	550	150	19	2	0.154	0.148
189	11	9.90	550	350	250	19	2	0.149	0.140
190	11	10.20	600	450	200	18	2	0.167	0.158
191	12	5.00	500	550	125	11	1	0.125	0.127
192	12	5.40	600	475	225	10	1	0.147	0.147
193	12	6.30	350	550	150	19	1	0.092	0.190
194	12	7.15	550	550	250	14	2	0.171	0.164
195	12	8.40	600	450	200	15	2	0.178	0.169
196	12	9.10	350	550	225	27	2	0.112	0.108
197	13	4.95	550	500	125	10	1	0.136	0.132
198	13	6.00	500	550	250	13	1	0.125	0.129
199	13	7.00	600	550	150	13	2	0.176	0.164
200	13	7.35	350	550	275	22	2	0.143	0.126
201	13	8.50	500	500	175	18	2	0.149	0.139
202	13	9.35	550	500	250	18	2	0.162	0.153
203	13	10.20	600	400	225	18	2	0.162	0.149
204	13	11.40	600	550	275	20	2	0.172	0.162

Appendix C: CALCULATION PROCEDURE/EXAMPLE USING THE MEAN LOAD METHOD

This Appendix presents an example of using the proposed methods in conjunction with the Mean Load Method (shown below) to evaluate an existing timber bridge, the bridge being evaluated will be HFX061.

$$F = \frac{\overline{R}\exp\left[-\beta(V_R^2 + V_S^2)^{0.5}\right] - \sum \overline{D}}{\overline{L}}$$

C.1. STARTING OFF AND CALCULATING D_T

Gather your bridge parameters. See Table C.1 for the parameters considered herein.

Table C.1. Bridge parameters for HFX061 as measured by SHM Canada (2021)

Parameter	Value
Clear span, L (m)	7.90
Overall width, W_b (m)	4.88
No. of design lanes, n	1
No. of stringer, N	11
Stringer spacing, S (mm)	465
Stringer size (mm × mm)	450 × 225
Deck thickness (t_b)	95
Apron thickness (mm)	40
Asphalt thickness (mm)	0
Skew angle	0°

Use any allowable method to calculate M_T. In this example, it has been done using FE analysis, and M_T is determined to be 429.56 kN-m.

Use the appropriate equation from Table C.2 below to calculate D_T. As this example pertains to a single-lane bridge, the equation for $n = 1$ is used. Plug the clear span length (L) into the equation for D_T , for this example;

$D_T = 3.472$

Table C.2.. D_T equations for n lanes

n	D_T equation
1	$D_T = 2.84 + 0.08L$
2	$D_T = 2.77 + 0.05L$

C.2. CALCULATE THE TRUCK LOAD FRACTION (F_T) AND THE GIRDER MOMENT (M_L)

Use the following equation calculate the Truck load Fraction (F_T).

$$F_T = \frac{S}{D_T \gamma_C (1 + \mu\lambda)} \geq 1.05 \frac{nR_L}{N}$$

$$F_T = \frac{0.465}{(3.472)(1)(1 + \mu(0))} \geq 1.05 \frac{1(1)}{11}$$

$$F_T = 0.134$$

Calculate M_L with the F_T value calculated above, in this case F_S is 1.0 as this bridge is not skewed.

$$M_L = F_T F_S M_T$$

$$M_L = (0.134)(1.0)(429.56kN - m)$$

$$M_L = 57.5kN - m$$

C.3. CALCULATE TIMBER RESISTANCE PER MEAN LOAD METHOD

Calculate the resistance of your timber girders, for this example it is assumed the girders are No.1 Douglas fir, f_{bb} from Table 14.9 of CSA S6:19 is 20 MPa.

Using the following equation calculate F_b , the values of the modification factors can be found as follows; K_D from Clause 9.5.3 in CSA S6:19; K_{Sb} per Table 9.2 of CSA S6:19; K_T from Table 9.6 in CSA S6:19; and K_m per Clause 9.5.6 and Table 9.4 in CSA S6:19. All of which are also shown in Appendix C8.

$$F_b = f_{bb}(K_D K_{Sb} K_T K_m)$$

$$F_b = 24MPa$$

Calculate the resistance to bending using the following equation, note no resistance factor φ is included, this is because the Mean Load Method uses nominal values for resistance and load. We will use F_b from above; S the section modulus calculated as shown below; K_L is calculated using Appendix C8 or Clause 9.6.3 in CSA S6:19. In this example K_L = 0.97

$$R = F_b S K_L K_{Zb}$$

where:

$$S = \frac{bd^2}{6}$$

where b and d are the width and depth of the girder respectfully

Once R is calculated we will use δ_R = 1.11 as the bias factor (determined in Chapter 6) to determine the mean resistance using the following equation.

$$\overline{R} = \delta_R R$$

$$\overline{R} = 197.07kN - m$$

C.4. CALCULATE LOADS PER MEAN LOAD METHOD

For dead load, there are 3 categories

a) **D1:** dead load of factory-produced components and cast-in-place concrete, excluding decks;
b) **D2:** cast-in-place concrete decks (including voided decks and cementitious concrete overlays), wood, field-measured bituminous surfacing, and non-structural components; and
c) **D3:** bituminous surfacing where the nominal thickness is assumed to be 90 mm for the evaluation where their respective statistical parameters used are as follows.

Using the following equation calculate your mean dead load effect where D is D1, D2 or D3.

$$\sum \overline{D} = \sum (\delta_D \delta_{AD} D)$$

To save room the calculations are skipped over, for this example, the deck, apron, and self weight of the girders are considered all under D2.

$$\sum \overline{D} = 0.25kN - m$$

To calculate the mean live load effect the following equation is used, for the values of the statistical parameters refer to Table C14.2 and Table C14.4 in CSA S6.1:19, they are also reproduced in Appendix C.9.

$$\overline{L} = \delta_L \delta_{AL} L(1 + \delta_I I_D)$$

In this example dynamic effects were **NOT** considered, therefore, using the value of M_L (calculated in Appendix C2) as the value of L determine the mean live load effect, in this example the mean live load effect is the value below.

$$\overline{L} = 72.23kN - m$$

C.5. CALCULATE THE STD. DEV. AND COVS

To calculate the Standard deviation for the dead and live loads (S_D and S_L) use the values for the statistical parameters from the tables in Appendix C7, which reproduced from CSA S6:19 and S6.1:19 (CSA, 2019a) (CSA, 2019b)

$$S_D = \left[\Sigma \left[\left(V_D^2 + V_{AD}^2 \right) \left(\delta_D \delta_{AD} D \right)^2 \right] \right]^{0.5}$$

Because the dead load has 3 categories S_D is a sum the expanded equation is shown below.

$$S_D = \left[\Sigma \left[\left(V_{D1}^2 + V_{AD}^2 \right) \left(\delta_{D1} \delta_{AD} D1 \right)^2 + \left(V_{D2}^2 + V_{AD}^2 \right) \left(\delta_{D2} \delta_{AD} D2 \right)^2 + \left(V_{D3}^2 + V_{AD}^2 \right) \left(\delta_{D3} \delta_{AD} D3 \right)^2 \right] \right]^{0.5}$$

In this example S_D was calculated to be the value below

$$S_D = 0.025$$

To calculate S_L use the following equation, again for this example the value determined for S_L is given below.

$$S_L = \left[V_{AL}^2 + V_L^2 + \frac{(V_I \delta_I I_D)^2}{(1 + \delta_I I_D)^2} \right]^{0.5} \bar{L}$$

$$S_L = 9.029$$

Once S_D and S_L are calculated, they and the mean load effects calculated in Appendix C4 can be plugged into the equation below to calculate the Load effect COV V_s as shown.

$$V_S = \frac{(S_D^2 + S_L^2)^{0.5}}{\left(\Sigma \bar{D} + \bar{L} \right)}$$

$$V_S = \frac{(0.025^2 + 9.029^2)^{0.5}}{\left(0.25 + 72.23 \right)}$$

$V_S = 0.125$

C.6. DETERMINE THE TARGET RELIABILITY INDEX

To determine a reliability index (β) follow Clause 14.12 in CSA S6:19 (CSA, 2019a), this process is also shown below.

The value of β is determined by determining a system behaviour, element behaviour, and inspection level for the structure from below or from Clauses 14.12.2 to 14.12.4 in CSA S6:19.

System Behaviour

System behaviour shall take into consideration the effect of any existing deterioration and shall be classified into one of the following categories:

a) **Category S1**, where element failure leads to total collapse. This includes failure of main members with no benefit from continuity or multiple-load paths, e.g., a simply supported girder in a two- girder system or a two-truss system.
b) **Category S2**, where element failure probably will not lead to total collapse. This includes main load-carrying members in a multi-girder system (more than two girders) or continuous main members in bending.
c) **Category S3**, where element failure leads to local failure only. This includes deck slabs, stringers, and bearings in compression.

Element Behaviour

Element behaviour shall take into consideration the effect of any existing deterioration and shall be classified into one of the following categories:

a) **Category E1**, where the element being considered is subject to sudden loss of capacity with little or no warning. This can include failure by buckling, concrete in shear and/or torsion with less than the minimum reinforcement required by Clause 14.14.1.6.2 a), bond (pullout) failure, suspension cables, eyebars, bearing stiffeners, over-reinforced concrete beams, connections, concrete beam- column compression failure, and steel in tension at net section.
b) **Category E2**, where the element being considered is subject to sudden failure with little or no warning but will retain post-failure capacity. This can include concrete in shear and/or torsion with at least the minimum reinforcement required by Clause 14.14.1.6.2 a), and steel plates in compression with post-buckling capacity.

c) **Category E3**, where the element being considered is subject to gradual failure with warning of probable failure. This can include steel beams in bending or shear, under-reinforced concrete in bending, decks, and steel in tension at gross section.

Inspection Level

Evaluation shall not be undertaken without inspection. Inspection levels shall be classified as follows

a) **Inspection Level INSP1**, where a component cannot be inspected. This can include hidden members not accessible for inspection, e.g., interior webs of adjacent box beams.

b) **Inspection Level INSP2**, where inspection is to the satisfaction of the evaluator, with the results of each inspection recorded and available to the evaluator.

c) **Inspection Level INSP3**, where the evaluator has directed the inspection of all critical and substandard components and final evaluation calculations account for all information obtained during

For all evaluation levels the target reliability index β shall be taken from Table C.3 below or Table 14.5 in CSA S6:19 based on each of the categories determined above.

Table C.3. Target reliability index β, for normal and permit traffic [recreated from CSA S6:19]

System behaviour category	Element behaviour category	Inspection level		
		INSP1	INSP2	INSP3
S1	E1	4	3.75	3.75
	E2	3.75	3.5	3.25
	E3	3.5	3.25	3
S2	E1	3.75	3.5	3.5
	E2	3.5	3.25	3
	E3	3.25	3	2.75
S3	E1	3.5	3.25	3.25
	E2	3.25	3	2.75
	E3	3	2.75	2.5

In this example, it was determined that the System category is S2, with an element category of E2 and a INSP2 inspection level. Hence the value of $\beta = 3.25$

C.7. DETERMINE THE VALUE OF THE LIVE LOAD CAPACITY FACTOR

Finally, using all the values calculated from Appendix C.1 through C.6 they are plugged into the Mean Load Method live load capacity equation at the beginning of this appendix, also shown below. Each of the values determined in this example are given in the table below

Table C.4. Variable values used in the Mean Load Method for HFX 061

Variable	Value
$\overline{R}$	197.07 kN-m
β	3.25
VR	0.18
VS	0.12
$\sum \overline{D}$	0.25 kN-m
$\overline{L}$	72.23 kN-m

$$F = \frac{\overline{R}\exp\left[-\beta(V_R^2 + V_S^2)^{0.5}\right] - \sum \overline{D}}{\overline{L}}$$

$$F = \frac{(197.07kN-m)\exp\left[-3.25((0.18)^2 + (0.12)^2)^{0.5}\right] - 0.25kN-m}{72.23kN-m}$$

Finally, the value of the live load capacity factor of the bridge has been determined.

$$F = 1.34$$

C.8. CLAUSES AND TABLES TO CALCULATE TIMBER RESISTANCE

All of the following Clauses and Tables are recreated form CSA S6:19 and CSA S6.1:19 (CSA, 2019a) (CSA, 2019b)

Load Duration Factor (K_D) Clause 9.5.3

The value of factor K_D shall be taken as 0.65 when considering dead load alone, earth pressure alone, and dead load plus earth pressure only. For load combinations including wind and earthquake, the factor shall be taken as 1.15. For all other cases, K_D shall be taken as 1.0.

Service Condition (K_S) Clause 9.5.5

For Bending at the Extreme fiber (K_{Sb}), the value of the factor is 1.0 for dry service conditions. For wet, members with smaller dimension 89mm or less the value of the factor is 0.84, and for members where the smaller dimension is over 89mm the value of the factor is 1.0.

Treatment Factor (K_T) Clause 9.5.9

Table C.5. Treatment factor (K_T) for lumber [recreated from CSA S6:19]

Product	Dry service conditions	Wet service conditions
Untreated lumber	1.00	1.00
Preservative-treated unincised lumber	1.00	1.00
Preservative-treated incised lumber of thickness 89 mm or less		
Modulus of elasticity	0.90	0.95
Other properties	0.75	0.85

For timber treated with fire retardant or other strength reducing chemicals the assumed properties shall be based on the documented results of tests that take into account the effects of time, temperature, and moisture content.

Load Sharing Factor (K_m) Clause 9.5.6

For systems of members in flexure and shear, and for tension members at the net section, the load- sharing factor shall be obtained either directly or by linear interpolation from Table C.6 for the number of load-sharing components, N. For members in compression not spaced more than 600 mm apart, K_m shall be taken as 1.1. For all other systems, K_m shall be taken as 1.0.

For moments and shears in flexural members, N shall not be greater than the number of components within the widths D_e and $0.8D_e$, respectively, where D_e shall be as specified in Table C7.

Table C.6. Load-sharing factor for bending, shear, and tension for all species and grades [recreated from CSA S6:19]

Number of load sharing components, N	Load-sharing factor, K_m
2	1.10
3	1.20
4	1.25
5	1.25
6	1.30
10	1.35
15	1.40
20	1.40

Table C.7. Values of D_e [recreated from CSA S6:19]

Structure	D_e, m
Longitudinal nail-laminated deck	0.85
Transverse nail-laminated deck	0.40
Longitudinal stress-laminated deck	1.75
Transverse stress-laminated deck	0.75
Stringer of sawn timber stringer bridge	1.75
Longitudinal laminate of wood-concrete composite deck	1.60

Lateral Stability Factor (K_L) Clause 9.6.3

For laminated wood decks, or when the compression edge of a beam is effectively supported along its length to prevent lateral displacement and rotation, K_L shall be taken as 1.0.

Otherwise, it is determined as follows

The value of K_L shall be obtained from Table C.9, where b and d are, respectively, the width and depth of the beam, and C_B and C_K are calculated as follows:

$$C_B = \sqrt{\frac{L_e d}{b^2}}$$

$$C_K = \sqrt{\frac{0.97 E_{50} K_{SE} K_T}{F_b}}$$

where L_e is the effective length in mm, given in Table C.8; E_{50} obtained from Table 9.17 in CSA S6:19 taken as 12,000 MPa for No.1 and SS Douglas Fir-Larch; and K_{SE} the value of the factor is 1.0 for dry service conditions. For wet, members with smaller dimension 89mm or less the value of the factor is 0.94, and for members where the smaller dimension is over 89mm the value of the factor is 1.0.

a beam shall not have C_B greater than 50.0

Table C.8. Effective length (L_e) for bending members [partly recreated from CSA S6:19]

Loading condition	Lateral support at point of loading	
	Yes	No
	Single span beam	
Any loading	1.92a	1.92l_u
Uniformly distributed load	1.92a	1.92l_u
Concentrated load at centre	1.11a	1.61l_u

Note: l_u is the unsupported length, which is the distance between two points of bearing or the length of the cantilever, mm. When intermediate support is provided by purlins, diaphragms, or braces, so connected that they prevent lateral displacement of the compressive edge of the bending member, the unsupported length shall be taken as the maximum purlin, diaphragm, or brace spacing, a, mm.

Table C.9. Modification factor for lateral stability (K_L) [recreated from CSA S6:19]

d/b	C_B	K_L
≤1.0	-	1.0
>1	≤10.0	1.0
>1	>10.0 but < C_K	$1-1/3(C_B/C_K)^4$
>1	≥ C_K but ≤ 50.0	$(0.65E_{50}K_{SE}K_T)/(C_B^2F_B)$

C.9. TABLES WITH STATISTICAL PARAMETERS

These tables are recreated from CSA S6.1:19 (CSA, 2019b)

Table C.10. Statistical parameters for various dead loads [recreated from CSA S6.1:19]

Dead load type	δ_D	V_D
D1	1.03	0.08
D2	1.05	0.10
D3	1.03	0.30

Table C.11. Statistical parameters for traffic loads [recreated from CSA S6.1:19]

Load type	Span	δ_L	V_L
Normal traffic (CL-W)	All	1.35	0.035
Normal traffic (alternative loading)	All	1.35	0.035
Permit single trip (PS)	All	1.17	0.03
Permit annual (PA)	All	1.25	0.017
Permit bulk (PB)	All	1.06	0.0094
Permit controlled (PC)	All	1.002	0.039

Table C.12. Statistical parameters for lateral distribution categories for live load [recreated from CSA S6.1:19]

Lateral distribution category	δ_{AL}	V_{AL}
Statically determinate	1.00	0
Sophisticated	0.98	0.07
Simplified	0.93	0.12

Table C.13. Statistical parameters for dynamic load allowance [recreated from CSA S6.1:19]

Span		δ_I	V_I
All	1 lane loaded	0.60	0.80
	2 or more lanes loaded	0.40	0.80